AD-A158 188 MEAN CLOUDINESS OVER THE GLOBAL TROPICS FROM SATELLITE OBSERVATIONS(U) HAWAII UNIV HONOLULU DEPT OF METEOROLOGY J C SADLER ET AL. DEC 84 UHMET-84-1 1/2

UNCLASSIFIED NEPRF-CR-84-09 N00014-83-K-0496 F/G 4/2 NL

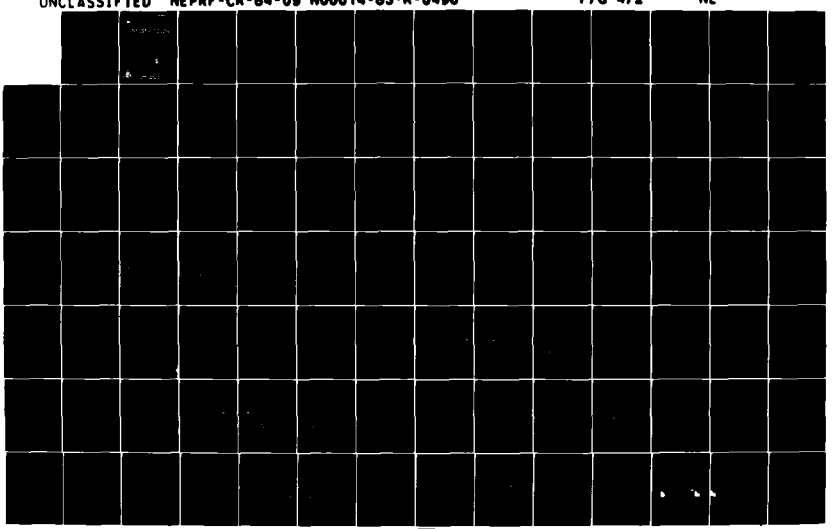

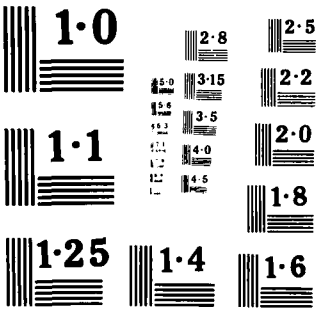
1·0
1·1
1·25
1·4
1·6
1·8
2·0
2·2
2·5
2·8
3·15
3·5
4·0
4·5
5·0
5·6
6·3

NAVENVPREDRSCHFAC
CONTRACTOR REPORT
CR 84-09

(12)

MEAN CLOUDINESS OVER THE GLOBAL TROPICS FROM SATELLITE OBSERVATIONS

Prepared By:

James C. Sadler, Bernard Kilonsky
Louis Oda, Arnold Hori
University of Hawaii
Honolulu, HI 96822

Contract No. N00014-83-K-0496

DECEMBER 1984

Prepared For:
NAVAL ENVIRONMENTAL PREDICTION RESEARCH FACILITY
MONTEREY, CALIFORNIA 93943-5106

UNCLASSIFIED

SECURITY CLASSIFICATION OF THIS PAGE

REPORT DOCUMENTATION PAGE

1a REPORT SECURITY CLASSIFICATION UNCLASSIFIED	1b RESTRICTIVE MARKINGS
2a SECURITY CLASSIFICATION AUTHORITY	3 DISTRIBUTION / AVAILABILITY OF REPORT Approved for public release; distribution is unlimited
2b DECLASSIFICATION / DOWNGRADING SCHEDULE	
4 PERFORMING ORGANIZATION REPORT NUMBER(S) UHMET 84-1	5 MONITORING ORGANIZATION REPORT NUMBER(S) CR 84-09
6a NAME OF PERFORMING ORGANIZATION Department of Meteorology University of Hawaii 6b OFFICE SYMBOL (If applicable)	7a NAME OF MONITORING ORGANIZATION Naval Environmental Prediction Research Facility
6c ADDRESS (City, State, and ZIP Code) 2525 Correa Road Honolulu, HI 96822	7b ADDRESS (City, State, and ZIP Code) Monterey, CA 93943-5106
8a NAME OF FUNDING / SPONSORING ORGANIZATION Naval Air Systems Command 8b OFFICE SYMBOL (If applicable) (AIR-330)	9 PROCUREMENT INSTRUMENT IDENTIFICATION NUMBER N00014-83-K-0496
8c ADDRESS (City, State, and ZIP Code) Department of the Navy Washington, DC 20361	10 SOURCE OF FUNDING NUMBERS PROGRAM ELEMENT NO: 62759N; PROJECT NO: WF59-553; TASK NO: ; WORK UNIT ACCESSION NO: DN793605

11 TITLE (Include Security Classification)

Mean Cloudiness Over The Global Tropics From Satellite Observations

12 PERSONAL AUTHOR(S) Sadler, James C.; Kilonsky, Bernard; Oda, Louis; Hori, Arnold

13a TYPE OF REPORT	13b TIME COVERED	14 DATE OF REPORT (Year, Month, Day)	15 PAGE COUNT
Final	FROM 6/15/83 TO 12/14/84	1984, December	55

16 SUPPLEMENTARY NOTATION

17 COSATI CODES		
FIELD	GROUP	SUB-GROUP
04	02	

18 SUBJECT TERMS (Continue on reverse if necessary and identify by block number)
Global tropical cloudiness, Satellite meteorology, Mean cloudiness, Nephanalysis, Cloud distribution, Tropics.

19 ABSTRACT (Continue on reverse if necessary and identify by block number)

Charts of mean monthly cloudiness over the global tropics, based on satellite observations during the period February 1965 through July 1973, are provided. Estimates of cloud amounts are based on daily nephanalyses for the eight-year period, assessing cloud cover in 2.5 degree latitude-longitude intervals.

Time-latitude sections are included for selected representative longitudes, to aid in summarizing seasonal variations of mean cloudiness.

Mean cloudiness is particularly useful in describing the seasonal variability of cloud systems. Both mesoscale and synoptic features of clear and cloudy areas are revealed by these analyses, including windward-leeward cloudiness changes resulting from island barrier effects.

This realistic assessment of cloud amount variability in the tropics will be useful in regional climatologies and in studies involving air-sea interaction.

20 DISTRIBUTION / AVAILABILITY OF ABSTRACT	21 ABSTRACT SECURITY CLASSIFICATION
☒ UNCLASSIFIED/UNLIMITED ☐ SAME AS RPT ☐ DTIC USERS	UNCLASSIFIED
22a NAME OF RESPONSIBLE INDIVIDUAL Fett, Robert W. (contract monitor)	22b TELEPHONE (Include Area Code) (408) 646-2823 22c OFFICE SYMBOL NEPRF WU 6.2-9

DD FORM 1473, 84 MAR 83 APR edition may be used until exhausted
All other editions are obsolete

SECURITY CLASSIFICATION OF THIS PAGE

UNCLASSIFIED

CONTENTS

1. INTRODUCTION

Cloud climatology studies using satellite observations began early in the meteorological satellite era. Clapp (1964) determined seasonal averages of total cloud amount at each 5-degree latitude-longitude intersection between 60N and 60S from March 1962 through February 1963. He used operational nephanalyses* prepared from observations made by TIROS IV, V, and VI. Sadler (1965) calculated average monthly cloudiness over 2.5-degree latitude-longitude squares from the operational nephanalyses prepared from observations made by TIROS V, VI, VII, and VIII over the Indian Ocean during 1963 and 1964. The analyses are reproduced in Volume 1 of the International Indian Ocean Expedition Meteorological Atlas (Ramage et al., 1972). Due to the inclined orbits of these early satellites and the variable nadir angle of their camera systems, the data distribution varied greatly in time and space. As a result, most areas had fewer than ten observations for any month.

On 1 February 1965, TIROS IX initiated the era of polar orbiting meteorological satellites and daily nephanalyses were available for most of the earth. The polar orbiting TIROS series was followed by the ESSA, ITOS, and NOAA series and daily nephanalyses were continued until the end of July 1973. Sadler used these nephanalyses to determine the monthly cloudiness over the global tropics between 30N and 30S. The averages for 1965 and 1966 and the two-year average (1965-1966) were published in Sadler (1968). The three-year average (1965-1967) was published in Atkinson and Sadler (1970). This Atlas is for the period 1 February 1965 through July 1973.

Computerized rectification and mapping of the satellite photographs was initiated in 1967. Subsequently the archive of daily brightness values from the visual channel reflected light was used to obtain automated climatological

*A mapped analysis of the cloud distribution.

averages of brightness. Taylor and Winston (1968) produced monthly and seasonal mean brightness for the globe for the period February 1967-February 1968. Miller and Feddes (1971) used four years (1967-1970) of brightness data to compile a global atlas of monthly and seasonal relative cloud cover. The rectified photographic mosaics were used directly and multiexposed to produce monthly and seasonal means of brightness during 1967 by Kornfield et al. (1967). Deviations from the true brightness scene of the cloud-ocean-earth are produced by the satellite-ground station system. Sources of these errors: Variability of signal within a sensor system; changes of response from one system to another; weakness in the cross-track normalization technique; changes in sensor calibration; degradation in sensor response due to aging; etc., have been discussed by Gray (1971) and Taylor and Winston (1968). Miller and Feddes concluded that their four-year averaging decreased the effect of these variations sufficiently to give a good representation of the average relative cloudiness. However, Taylor and Winston contend that the brightness variations are sufficient to preclude the automated production of meaningful anomalies. Sadler et al. (1976) demonstrated that brightness changes had no effect on the human analyst's ability to interpret total cloudiness from satellite pictures and excellent monthly anomalies were produced from the manual nephanalyses.

2. DATA

2.1. Source and Coding

Operational nephanalyses prepared by the Data Processing and Analysis Division of the National Environmental Satellite Service (NESS) of NOAA were used in deriving the averages. The nephanalyses were handdrawn from interpretations of photographs from the vidicon cameras of TIROS IX and X; ESSA 1, 3, 5, and 7; ITOS I; NOAA 1; and the visual channel scanning-radiometer of

NOAA 2. The transit times of all satellites prior to NOAA 2 were near 1400 local time. NOAA 2 was launched in November 1972 and had a transit time near 0900 local time.

Table 1

Suggested Relationship between "Neph" Categories and Cloudiness

"Neph" Category (Symbol)	Range of Cloudiness (per cent)	Assigned Value	Approximate Cloudiness (Octas)
Open (O)	< 20	1	0-1
		2	2
Mostly open (MOP)	20-50	3	3
		4	4
Mostly covered (MCO)	50-80	5	5
		6	6
Covered (C)	> 80	7	7
		8	8
Heavily covered (+C)		9	8

The categories of cloudiness depicted on the nephanalyses are listed in column 1 of Table 1. The range of cloudiness assigned to each category and utilized by the Satellite Center photo interpreter is shown in column 2. For this study, each category of cloudiness was assigned an odd numerical value ranging from 1 to 9 as shown in column 3.

2.2. Extraction and Averaging

Transparent maps, gridded on 2.5-degree latitude-longitude intervals, were prepared to the scale of the nephanalysis charts (1:15,000,000). Each nephanalysis was placed at the proper geographic position under the transparent map and the appropriate numerical value of cloudiness entered in each grid

square, the determination was straightforward. If more than one category was included in a grid square, the numerical value was obtained by subjective areal averaging (Fig. 1). Averaging can lead to the even numbers listed in column 3 of Table 1. For each grid square the daily values were totaled, and the monthly average was then obtained by dividing the total by the number of observations.

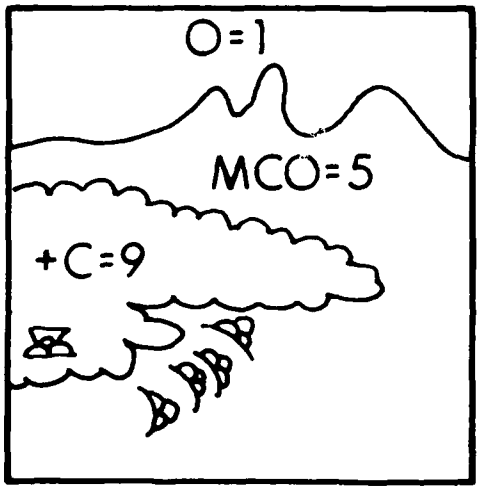

$$\frac{9+(2\times5)+1}{4}=5$$

Figure 1. Example of averaging for a grid square containing 3 "neph" categories.

2.3. Data Distribution

There were gaps in the data during some months of 1965 and 1966. They were due to a combination of satellite and ground station malfunction and occurred mainly over the central and western Pacific. In addition, the neph-analysis charts contained small date-time legend boxes on the poleward borders which blanked some data. Otherwise the data were uniformly distributed with essentially daily global coverage.

2.4. Relationship to "True" Cloud Amount

The nephanalysis averages, which will be used throughout in all figures and discussions, are assumed to be roughly equivalent to the standard World Meteorological Organization oktas of cloudiness. We will refer to the satellite derived cloudiness as octas to distinguish between the two (column 4 of Table 1). How can one relate the averages to the true cloudiness? There is no satisfactory "ground truth" for comparison. Miller et al. (1970) found that the relative cloud cover prepared from brightness values was consistently smaller than that from concurrent surface observations. Young (1967) found a significant variability between analysts in estimating total cloudiness from satellite pictures and all overestimated total cloudiness in a "torn paper" test. The mean error was 1 octa and the overestimation was greatest when the total cloudiness was less than 4 octas and the pattern resembled a cumulus population typical of the tropics and trade wind regions. There should be a similar, but perhaps larger, overestimation of cloudiness by ground observers due to the viewing angle whereby the "apparent" cloudiness increases with increasing angle from the zenith. This error is also greatest with cumulus clouds.

Using the same four-year data base, we have compared our estimate of cloudiness over the Pacific Ocean with that of Miller and Feddes (1971). The pattern of cloudiness and the positions of the maximum and minimum areas or zones of cloudiness are essentially identical. However, our estimates of total cloudiness are consistently higher than theirs. The average difference is about 1 octa. The maximum difference of more than 1 octa in the near-equatorial minimum zones reduces to about 1 octa in the cloud minimum zone south of the subtropical ridges and to less than an octa in the maximum cloud areas. The differences may be attributed to one or a combination of factors such as: An overestimation of cloudiness by the nephanalysts similar to the results of

Young; our choice of assigned values to the neph categories (column 3 versus column 1 of Table 1); our choice of equating assigned values to octas (column 3 versus column 4 of Table 1); Miller and Feddes' choice of weighting factors relating brightness ranges and relative cloud amount. In any event, the best relationship between "true" and satellite derived cloudiness cannot be determined since, as stated earlier, there is no satisfactory ground truth for comparison. However, our data base is internally consistent and the cloud patterns and gradients are preserved.

3. MEAN TROPICAL CLOUDINESS

The major tropical cloud systems--including minimum as well as maximum cloudiness--are related to the atmospheric circulation and most of the annual variation in cloudiness can be related to the annual variation in the atmospheric circulation and its interaction with the underlying surface, be it land or sea. Therefore, the discussions assume a familiarity with geography, the mean monthly atmospheric circulations and sea surface temperatures. (Atlases of the global tropics mean monthly circulations at the lower-tropospheric gradient and upper-tropospheric 200 mb levels are available in Atkinson and Sadler (1970) and Sadler (1975a), respectively.)

The very large scale tropical circulation is dominated by the monsoon and trade wind systems and each has a distinctive associated cloud distribution. The easterly trade winds are divergent in the mean and the typical cloudiness varies westward from low stratus over the cold eastern oceans to stratocumulus and then trade wind cumulus as the air passes over warmer waters and the trade wind inversion rises. The trade winds are persistent throughout the year over the central North Pacific, central and east South Pacific, South Atlantic and central and west North Atlantic; therefore, the cloudiness patterns over these

areas are persistent and quasi-anchored and the largest annual variation is in the amount of stratus over the cold eastern oceans where the maximum occurs simultaneously in the S.H. and N.H. during July-September. The tropical monsoon westerlies are convergent in the mean and the typical cloudiness is deep cumulus mixed with dependent middle and high cloud layers. The N.H. summer monsoons of Africa and Asia extend into the eastern Atlantic (to 35E) and western Pacific (to 150E), respectively, and a summer monsoon exists in the eastern North Pacific from 130W to the central American coast. The S.H. summer monsoon circulation extends from Africa across the South Indian Ocean and Australia to 170E. The South Atlantic and the eastern South Pacific have no monsoon circulations. The monsoon areas, by definition, experience a large seasonal change in the wind field. A comparable large change is observed in the cloudiness from a maximum in summer to a minimum in winter.

Over the tropical oceans there exists, in the mean, east-west oriented zones of deep convection produced by convergence of the low-level winds. One major component of this global pattern is the convection associated with the convergent low-level westerlies of the summer monsoons as mentioned earlier. The other major component is the deep convection associated with convergence between trade wind systems; the classic "clash of the trades." The zones will be noted as CZ's, implying both convergence and convective cloudiness in the zones. The satellite observations have revealed, among many things, that the CZ's do not migrate across the equator with seasons. The monsoon component of the CZ pattern builds and decays in the respective summer hemisphere and the seasonal latitudinal migration is restricted to that hemisphere. The "clash of the trades" component of the CZ pattern remains in the N.H. throughout the year.

To aid in summarizing the seasonal variations of the mean cloudiness, time-latitude sections are included for selected representative longitudes. The month to month change in mean cloudiness is particularly useful in describing the seasonal variability of the cloud systems.

3.1. Continental Land Masses

The large continental land masses have two simple and distinct cloud regimes. The subequatorial central deserts of Northern Africa, Arabian Peninsula, Iran, Pakistan, northwest India, central Australia and Southern Africa have little annual variability in cloud amount but experience a large expansion (winter) and contraction (summer) of the area with little cloudiness.

The near equatorial regions of Africa, South America and Australia have a strong annual cycle in cloud amount varying from greater than five octas in summer to less than three octas in winter. The cross section through central Africa (20E-25E) well illustrates this simple regime. The cross section of month to month change in cloudiness illustrates that the increase and decrease patterns are symmetrical about the equator and out of phase between hemispheres such that increasing (decreasing) clouds in N.H. occur with decreasing (increasing) clouds in S.H. The large change patterns are restricted to each hemisphere and do not cross the equator as would happen if the CZ migrated with seasons across the equator.

The cloud regime in S.H. of central South America (cross section 55W-60W) is very similar to that of central South Africa.

3.2. Pacific Ocean

A. Maximum Cloud Areas

_____, 1968: Average cloudiness in the tropics from satellite observations. International Indian Ocean Expedition Meteorological Monograph No. 2, East-West Center Press, Honolulu, Hawaii, 22 pp. plus 24 plates.

_____, 1975a: The upper tropospheric circulation over the global tropics. University of Hawaii, UHMET 75-05.

_____, 1975b: The monsoon cloudiness and circulation over the GATE area. Mon. Wea. Rev., 103, 369-387.

_____, 1976: Tropical cyclone initiation by the tropical upper tropospheric trough. Naval Environmental Prediction Research Facility, Monterey, Calif., Technical Paper No. 2-76 and Meteor. Dept., University of Hawaii UHMET 75-02.

_____, L. Oda, and B. J. Kilonsky, 1976: Pacific Ocean cloudiness from satellite observations. Univ. of Hawaii, Dept. of Meteor. Report UHMET 76-01, 137 pp.

Taylor, V. R., and J. S. Winston, 1968: Monthly and seasonal mean global charts of brightness from ESSA 3 and 5 digitized pictures, Feb. 1967-Feb. 1968. Technical Report No. 46, National Environmental Satellite Center, Washington, D. C.

_____, 1973: An atlas of Pacific islands rainfall. Hawaii Institute of Geophysics, University of Hawaii, HIG 73-9.

Young, M. J., 1967: Variability in estimating total cloud cover from satellite pictures. J. Appl. Meteor., 6, 573-579.

REFERENCES

Atkinson, G. D., and J. C. Sadler, 1970: Mean cloudiness and gradient-level wind charts over the tropics. Technical Rept. No. 215. Air Force Air Weather Service, Scott AFB, Illinois.

Clapp, P. F., 1964: Global cloud cover for seasons using TIROS nephanalyses. Mon. Wea. Rev., 92, 495-507.

Gray, T. I., 1971: Advanced vidicon camera systems data quality. Manuscript, National Environmental Satellite Service, Suitland, Maryland.

Kornfield, J., A. F. Hasler, K. J. Hanson, and V. E. Juomi, 1967: Photographic cloud climatology from ESSA III and V computer produced mosaics. Bull., A.M.S., 48, 878-883.

Miller, D. B., R. D. McCollum, and P. J. O'Reilly, 1970: Satellite versus surface estimates of total cloud cover. U.S. Air Force Environmental Technical Applications Center, Washington, D. C.

_____, and R. G. Feddes, 1971: Global atlas of relative cloud cover 1967-1970. National Environmental Satellite Service and U.S. Air Force Environmental Technical Applications Center, Washington, D.C.

Ramage, C. S., 1970: Meteorology of the South Pacific tropical and middle latitudes. Scientific Exploration of the South Pacific, W. S. Wooster, Ed., Nat. Acad. Sci., 16-29.

_____, F. R. Miller, and C. Jefferies, 1972: Meteorological atlas of the International Indian Ocean Expedition Vol. I: The surface climate of 1963 and 1964. U.S. Government Printing Office, Washington, D.C.

Sadler, J. C., 1963: TIROS observations of the summer circulation and weather patterns of the eastern North Pacific. Proc. of Symp. on Tropical Meteorology, Rotorua, New Zealand, 553-571.

_____, 1965: Satellite meteorology in the International Indian Ocean Expedition. Proc. of Symp. on Meteorological Results of the International Indian Ocean Expedition, Bombay, India, July 1965. India Meteorological Dept., New Delhi, India, 269-284.

_____, 1967: The tropical upper tropospheric trough as a secondary source of typhoons and a primary source of trade wind disturbances. Hawaii Institute of Geophysics, University of Hawaii, HIG 67-12.

Acknowledgments

The data were extracted by many students over many years under numerous contracts and grants from the Air Force, Navy, and National Science Foundation.

Special thanks to the National Environmental Satellite Service for furnishing the nephanalyses and to Mrs. S. Arita for typing the manuscript.

area of Arabia and Pakistan expands eastward and southward and cloudiness of less than 3 octas covers the North Indian Ocean poleward of 10N from November through April.

(2) West Indian Ocean

This region is globally unique for it is a minimum cloud area throughout the year in both hemispheres (see also cross section 50E-55E). Cloudiness exceeds 4 octas only in the narrow CZ of S.H. summer from December-February.

(3) Eastern South Indian Ocean

The influence of the Australian desert extends northwestward over the oceans as a minimum cloud area for distances varying from some 2000 km in winter to a 1000 km in summer.

May to June (see also cross section 70E-75E), exceeds 5 octas from June-August and decreases rapidly from August to September.

(ii) Bay of Bengal

The CZ moves northward from near 5N in April to near 20N in August. The cloudiness is orographically enhanced along the Burma coast to a maximum of greater than 6 octas in July and August. The pattern is also distorted by the orographically induced minimum cloudiness in the southwest section of the Bay. The cloud amount decreases rapidly from August and the CZ loses its identity by October (see also cross section 90E-95E).

(b) South Indian Ocean

The summer monsoon trough is anchored on the west and east by Africa and Australia, respectively, at approximately 20S and arcs equatorward to near 10S in the central Indian Ocean. The CZ is embedded in the westerlies equatorward of the trough. It is an oceanwide feature from December through March but best defined in February when the cloud amount exceeds 4.5 octas except for a short segment in the extreme west.

(c) Equatorial eastern Indian Ocean

Surface westerlies cover the equator east of 70E throughout the year; therefore, in addition to the principal summer trough there exists a secondary trough in the opposite hemisphere. During the transition seasons the two troughs are close to and near equidistant from the equator. As a result, a secondary relatively maximum cloud zone exists very near the equator and is most pronounced during N.H. summer and the fall transition season (see also the cross sections 70E-75E and 90E-95E).

B. Minimum Cloud Areas

(1) North Indian Ocean

With the onset of the northeast monsoon in early winter the desert

3.4 Indian Ocean

The low-level atmospheric circulation over the Indian Ocean is as complex as the circulation over the Atlantic is simple and the cloudiness distribution attests to the difference and the complexity. The North Indian Ocean, unlike the Pacific and Atlantic, is bordered on the north by land masses at relatively low latitudes of 20 to 30N; therefore, the circulation is strong monsoonal and the cloudiness varies from a minimum in winter (easterly flow) to a maximum in summer (westerly flow). The South Indian Ocean, although not land-bound to the south, also has a monsoonal atmospheric circulation but it is relatively weak and the annual cycle of cloudiness is much weaker over the south as compared to the north. Also in contrast to the central Pacific and Atlantic Oceans there are no equatorial easterlies over the Indian Ocean and, therefore, no equatorial minimum cloud zones.

A. Maximum Cloud Areas

(1) Near-equatorial maximum cloud zones (CZ)

(a) North Indian Ocean

The term CZ is used rather loosely in the North Indian Ocean for, within the latitudinally broad summer monsoon westerlies, the extensive cloudiness exists more as a large area phenomena rather than a zone of clouds; however, within the cloud area there is usually a maximum core which tends to be oriented east-west. The term "near equatorial" may also be misleading for the core is located between 15 and 20N during July and August.

(i) Arabian Sea

Significant cloudiness is restricted to the eastern portion of the Arabian Sea east of 65E. The CZ is a feature only from May through August. It moves from near 5N in May to about 20N in August, then dissipates rapidly and loses identity by October. The cloud amount increases rapidly from

a clash of the trade wind systems. The CZ cloudiness is rather uniform throughout the year, varying less than 1 octa between the minimum in April and the maximum in December.

On its western end the CZ enters South America and there is no CZ in the western North Atlantic, Caribbean Sea or Gulf of Mexico.

B. Minimum Cloud Areas

(1) The trade wind minimum over the western North Atlantic, Caribbean Sea and Gulf of Mexico

The persistent trade winds of these areas have little annual variability. This results in essentially no annual change in the cloudiness which remains below 4.0 octas overall and less than 3.5 octas between 10N and 20N (see also cross section 55W-60W).

(2) The equatorial minimum and South Atlantic trade wind minimum

In phase with the annual cycle of cold equatorial waters, a distinct minimum of cloudiness occurs along the equator from June through October. A minimum core of less than 3 octas develops near 15W in June, spreads westward to cover the entire central Atlantic in July and August (see also cross section 30W-35W), migrates to the South American coast at 45W by September, remains near the coast in October and moves just south of the equator in November before losing its identify as an equatorial feature.

The trade wind cloud minimum, downwind from the stratus maximum over the eastern South Atlantic, has a value of less than 4 octas throughout the year from the central South Atlantic to the South American coast. It merges with the equatorial minimum from June to November and is centered near 10S, 25W during April when the equatorial cloudiness increases to just over 4 octas.

3.3 Atlantic Ocean

The relatively simple mean low-level circulation over the Atlantic produces a correspondingly simple mean cloud distribution. The South Atlantic has a persistent trade wind regime throughout the year as does the central and western North Atlantic including the Caribbean Sea and Gulf of Mexico. The western end of the North African summer monsoon trough extends into the eastern North Atlantic and produces low-level monsoon westerlies to 35W during July-September (Sadler, 1975b).

A. Maximum Cloud Areas

(1) Stratus and stratocumulus of the eastern North Atlantic

The very dry air from the adjacent Sahara Desert reduces the amount and areal extent of the stratus within the northeast trades over the cold waters off North Africa. It is a significant feature only from June-August and the July maximum in less than 5 octas (cross section for 25W-30W). Because of the desert the stratus does not exist near the coast as in the eastern North Pacific and eastern North and South Atlantic.

(2) Stratus and stratocumulus of the eastern South Pacific

The maximum occurs in S.H. winter with amounts exceeding 6 octas over a large area from June-October. During this time it spreads equatorward and merges with the coastal stratus of equatorial west Africa. The stratus shrinks to a February minimum in area and the amount drops below 5 octas from January-May.

(3) Near-equatorial maximum cloud zone (CZ)

In the central equatorial Atlantic (see cross section 25°W-30°W) the CZ is sharply defined and remains in the N.H. throughout the year. It migrates from near 3N in April to near 8N in July and August and recedes more slowly to near 5N in December. During July-September the CZ is of the monsoon type and embedded in low-level westerlies. During the other nine months it results from

The equatorial minimum merges with the trade wind minimum of the eastern South Pacific and the boundary between them is indistinct except during March and April when the weak CZ near 5S separates the two.

(4) The Trade Wind Minimum of the North Pacific

A large minimum (less than 4 octas) cloudiness area dominates the Pacific trade wind region west of Hawaii. The area moves north and south and latitudinally expands and contracts in rhythm with the annual movement of the subtropical ridge. In the Central Pacific the northern 4 octa isoneph is near, and moves with, the surface subtropical ridgeline while the Southern 4 octa isoneph remains near 10N. The minimum axis moves from near 15N in winter to 25N in summer.

In the western Pacific the position and latitudinal extent of the minimum cloudiness area are more variable than in the central Pacific in response to the greater synoptic variability associated with the summer and winter monsoons. In addition the minimum axis moves from 25N in July to 30N in August.

The greatest minimum (less than 3.5 octas) undergoes marked longitudinal shifts. From October-May it is west of 180°. In July it is centered about 180° and during August-September it is in the longitudes of the Hawaiian Islands.

(5) Orographically Induced or Enhanced Minima

Good examples of the orographic lee effect in forming or enhancing minimum cloudiness areas are found over the South China Sea. During the southwest monsoon (June-September) a minimum exists off the Vietnam coast. In winter it shifts to the lee of the Philippines and the larger scale minimum is enhanced to less than 3 octas from February-April.

B. Minimum Cloud Areas

Like the maximum cloudiness areas the major minimum cloudiness areas are persistent. All experience annual expansion and contraction usually in opposition to the contraction or expansion of the adjoining maximum cloudiness areas. Some are anchored by orography or SST patterns while others have annual migrations associated with the low-level circulation systems.

(1) Coastal Eastern North Pacific

The area of minimum cloudiness along and off the west coast of North and Central America is largest in winter. An absolute minimum of less than 2 octas occurs off the Central American coast between 10N and 15N in February. In summer, expansion of stratus to the California coast and northward movement of the CZ contracts the area of scattered cloudiness and shifts the absolute minimum to the Mexican coastal waters north of 20N.

(2) Coastal Eastern South Pacific

The area of minimum cloudiness along and off the South American coast is largest from December through April and most pronounced in February. During this season it merges with the equatorial minimum. Beginning in May the stratus expands eastward and northward and the minimum cloudiness area shrinks by June to only a very thin strip along the coast.

(3) The Equatorial Minimum and the Trade Wind Minimum of the Eastern South Pacific

The equatorial minimum is centered at about 2S between 130W and 160W. The absolute minimum in this region occurs in February or just two months prior to the absolute maximum (within the minimum zone) in April. The minimum zone penetrates farthest west during the late northern summer and, if defined as less than 4 octas, extends to about 140E during August-October. Eastward, the minimum zone reaches the South American coast from January-May.

It is more intense in March than its counterpart in the Northern Hemisphere. It decreases slightly from March to April and disappears by May.

(4) Smaller Regional Maxima

Besides large-scale cloudy areas there are many smaller features. Some are due to orography and fluctuate annually in response to the low-level flow. The windward-leeward effect of islands is well demonstrated by the Philippines and Japan and is even apparent in the smaller island chains such as the Hawaiian Islands although the lee side minima tend to overshadow the windward maxima.

An interesting maximum cloudiness feature occurs in September in the eastern North Pacific north of 10N between 100W and the southern coasts of Mexico and Guatamala in response to the low-level flow. Easterly winds (an extension of the Atlantic Ocean and Gulf of Mexico trade winds) cover this small area during July and August and there is a zone of relative minimum cloudiness along and off the coast. In September the easterlies recede and the monsoon southwesterlies spread over the region and reach the coast, resulting in a small isolated (from the CZ) area of maximum cloudiness. A pronounced September rainfall maximum is restricted to this coastal strip (Taylor, 1973).

A maximum cloudiness area develops in the central North Pacific in summer between 15S and 30N in response to the upper tropospheric circulation. Intense cyclonic cells in the tropical upper tropospheric trough (TUTT) initiate deep convective cloud systems within the trade wind zone (Sadler, 1967, 1976). The upper cells move west-southwest opposite to a large gradient of sea surface temperature. Thus in August the induced cloudiness increases westward to a maximum between 170E and 180°. The isolated area of greater than 4 octas lies within the minimum cloudiness of the trade wind regime.

throughout the year. Between 120W and 180 it is anchored between 5N and 10N with an annual variation of only about 2° of latitude (between 6N and 8N). The intensity varies annually and longitudinally. There is a definite early winter (October-December) maximum and a secondary May-June maximum in contrast to the strong summer maximum of the eastern Pacific (compare cross sections of 100W-105W and 165W-170W). Mean cloudiness in the strip between 125W and 140W exceeds 5 octas during every month except April. In fact, the annual cloudiness exceeds that of any other oceanic convective cloud region of the global tropics and is rivaled only by the cloudiness of central New Guinea and portions of equatorial Africa and South America. On either end the central Pacific CZ merges into the CZ's of the eastern and western North Pacific. In early summer (June) as the western Pacific CZ forms and the eastern Pacific CZ moves northward, there exists a continuous Pacific-wide zone of maximum cloudiness between 5N and 10N.

(b) South Pacific

(i) Western South Pacific (see also cross section for 135E-140E). A maximum cloudiness zone (CZ) extends east-southeast from New Guinea through the Solomon Islands throughout the year. It is most intense and extends farthest east during the Southern summer (December-February) in association with the summer monsoon. Although it tends to merge with an area of increased cloudiness extending northwestward from a midlatitude maximum just east of 180° the two are definitely separated during most months. More importantly, there is a difference in the character of the cloudiness. The tropical CZ is typically convective while the maximum cloudiness south of about 15S is predominantly stratiform and associated with migrating midlatitude troughs which tend to stagnate in this region (Ramage, 1970).

(ii) Eastern South Pacific (see also cross sections for 100W-105W). A CZ develops in late February east of 120W near 5S. It intensifies to a maximum of greater than 4 octas in March and extends westward to about 140W.

1975b); therefore, we prefer to highlight this distinction by referring to the near equatorial zones of deep convective cloudiness as convective cloud zones (CZ).

(a) North Pacific

The North Pacific CZ has a marked longitudinal variability which is related to annual changes in the low level circulation. The eastern and western North Pacific are monsoonal in contrast to the persistent easterly flow of the central North Pacific.

(i) The Eastern North Pacific east of 120W (see also the 100-105W cross section). A CZ persists in the eastern North Pacific throughout the year shifting from just south of 5N during December-March to just south of 10N during June-August. It experiences a considerable intensity change from a minimum in March to a maximum in July and August. The maximum positive month to month cloudiness changes occur from April to June, coinciding with onset and northward movement of the low-level monsoon westerlies (Sadler, 1963). The maximum decrease in cloudiness occurs from October to Decembe. as the monsoon retreats southward and decays.

(ii) The Western North Pacific west of 150E (see also the 135E-140E cross section.) The CZ in the extreme western North Pacific is a summer feature lasting from June through October. The low-level flow during this period is an extension of the Asiatic summer monsoon and the CZ migrates north and south in rhythm with the monsoon advance and retreat. From a narrow zone between 5N and 10N in June it expands to a rather broad zone in July and August, moves to its northern limit in August, and then retreats to between 5N to 10N by October.

(iii) The Central North Pacific between 150E and 120W (see also the cross section for 165W-170W). The CZ is a persistent feature

(1) Stratus and Stratocumulus of the Eastern North Pacific

Persistent stratus and stratocumulus dominate the eastern North Pacific between about 15N and 35N from 115W and 140W. The extent and intensity vary annually from a maximum in July to a minimum in October. The stratus and the near equatorial CZ maximum are always distinctly separated. The eastern edge which is very near the California coast from May through August recedes farthest from the coast in October and April.

(2) Stratus and Stratocumulus of the Eastern South Pacific

Stratus and stratocumulus cloudiness off the west coast of South America reaches maximum intensity and extent during the Southern Hemisphere winter (July-September). Beginning in June it spreads northward to the equatorial region and merges with stratocumulus on the southern periphery of the deeper convective cloud zone between 5N and 10N; from July through October the coverage is 5 octas or greater along the equator between the Gallapagos Islands and South America. The clouds begin retreating from the equatorial and Peruvian coastal regions in November and reach their minimum extent and intensity in February.

(3) Near Equatorial Maximum Cloud Zones (CZ)

Areas of deep convective cloudiness are features of the near equatorial region throughout the year over some portion of the Pacific. This cloudiness is generally organized in rather narrow east-west zones. Since the beginning of the satellite era these zones have been equated, by many, to the much older term of intertropical convergence zone (ITCZ). However, prior to satellite observations the ITCZ was usually defined as a feature of the pressure and/or wind field with the assumption that the pressure trough, the line of "clash of the trades" and the maximum cloudiness zone coincided. Satellite data have proven this assumption to be in error over much of the tropics (Sadler,

DISTRIBUTION

COMMANDER IN CHIEF
U.S. ATLANTIC FLEET
ATTN: FLT METEOROLOGIST
NORFOLK, VA 23511

COMMANDER IN CHIEF
U.S. ATLANTIC FLEET
ATTN: NSAP SCIENCE ADVISOR
NORFOLK, VA 23511

COMMANDER IN CHIEF
U.S. PACIFIC FLEET
CODE 02M
PEARL HARBOR, HI 96860-7000

COMMANDER IN CHIEF
U.S. NAVAL FORCES, EUROPE
ATTN: METEOROLOGICAL OFFICER
FPO NEW YORK 09510

CINCUSNAVEUR
ATTN: NSAP SCIENCE ADVISOR
BOX 100
FPO NEW YORK 09501

COMMANDER SECOND FLEET
ATTN: METEOROLOGICAL OFFICER
FPO NEW YORK 09501-6000

COMSECONDFLT
ATTN: NSAP SCIENCE ADVISOR
FPO NEW YORK 09501-6000

COMTHIRDFLT
ATTN: FLT METEOROLOGIST
PEARL HARBOR, HI 96860

COMSEVENTHFLT
ATTN: FLT METEOROLOGIST
FPO SAN FRANCISCO 96601-6003

COMTHIRDFLT
ATTN: NSAP SCIENCE ADVISOR
PEARL HARBOR, HI 96860

COMSEVENTHFLT
ATTN: NSAP SCIENCE ADVISOR
BOX 167
FPO SEATTLE 98762

COMSIXTHFLT
ATTN: FLT METEOROLOGIST
FPO NEW YORK 09501-6002

COMSIXTHFLT/COMFAIRMED
ATTN: NSAP SCIENCE ADVISOR
FPO NEW YORK 09501-6002

COMMANDER NAVAL AIR FORCE
U.S. ATLANTIC FLEET
ATTN: NSAP SCIENCE ADVISOR
NORFOLK, VA 23511-5188

COMNAVAIRPAC
ATTN: NSAP SCIENCE ADVISOR
NAS, NORTH ISLAND
SAN DIEGO, CA 92135

COMNAVSURFLANT
ATTN: NSAP SCIENCE ADVISOR
NORFOLK, VA 23511

COMNAVSURFPAC
(005/N6N)
ATTN: NSAP SCIENCE ADVISOR
SAN DIEGO, CA 92155

COMSUBFORLANT
ATTN: NSAP SCI. ADV. (013)
NORFOLK, VA 23511

COMMANDER
AMPHIBIOUS GROUP 2
ATTN: METEOROLOGICAL OFFICER
FPO NEW YORK 09501

COMMANDER
AMPHIBIOUS GROUP 1
ATTN: METEOROLOGICAL OFFICER
FPO SAN FRANCISCO 96601

COMMANDER
OPTEVFOR
ATTN: NSAP SCIENCE ADVISOR
NORFOLK, VA 23511

COMMANDING OFFICER
USS AMERICA (CV-66)
ATTN: MET. OFFICER, OA DIV.
FPO NEW YORK 09531-2790

COMMANDING OFFICER
USS CORAL SEA (CV-43)
ATTN: MET. OFFICER, OA DIV.
FPO NEW YORK 09550-2720

COMMANDING OFFICER
USS D. D. EISENHOWER (CVN-69)
ATTN: MET. OFFICER, OA DIV.
FPO NEW YORK 09532-2830

COMMANDING OFFICER
USS FORRESTAL (CV-59)
ATTN: MET. OFFICER, OA DIV.
FPO MIAMI 34080-2730

COMMANDING OFFICER
USS INDEPENDENCE (CV-62)
ATTN: MET. OFFICER, OA DIV.
FPO NEW YORK 09537-2760

COMMANDING OFFICER
USS J. F. KENNEDY (CV-67)
ATTN: MET. OFFICER, OA DIV.
FPO NEW YORK 09538-2800

COMMANDING OFFICER
USS NIMITZ (CVN-68)
ATTN: MET. OFFICER, OA DIV.
FPO NEW YORK 09542-2820

COMMANDING OFFICER
USS SARATOGA (CV-60)
ATTN: MET. OFFICER, OA DIV
FPO MIAMI 34078-2740

COMMANDING OFFICER
USS CONSTELLATION (CV-64)
ATTN: MET. OFFICER, OA DIV
FPO SAN FRANCISCO 96635-2780

COMMANDING OFFICER
USS ENTERPRISE (CVN-65)
ATTN: MET. OFFICER, OA DIV.
FPO SAN FRANCISCO 96636-2810

COMMANDING OFFICER
USS KITTY HAWK (CV-63)
ATTN: MET. OFFICER, OA DIV.
FPO SAN FRANCISCO 96634-2770

COMMANDING OFFICER
USS MIDWAY (CV-41)
ATTN: MET. OFFICER, OA DIV.
FPO SAN FRANCISCO 96631-2710

COMMANDING OFFICER
USS RANGER (CV-61)
ATTN: MET. OFFICER, OA DIV.
FPO SAN FRANCISCO 96633-2750

COMMANDING OFFICER
USS CARL VINSON (CVN-70)
ATTN: MET. OFFICER, OA DIV.
FPO SAN FRANCISCO 96629-2840

COMMANDING OFFICER
USS IOWA (BB-61)
ATTN: MET. OFFICER, OA DIV.
FPO NEW YORK 09546-1100

COMMANDING OFFICER
USS NEW JERSEY (BB-62)
ATTN: MET. OFFICER, OA DIV.
FPO SAN FRANCISCO 96688-1110

COMMANDING OFFICER
USS MOUNT WHITNEY (LCC-20)
ATTN: MET. OFFICER
FPO NEW YORK 09517-3310

COMMANDING OFFICER
USS BLUERIDGE (LCC-19)
ATTN: MET. OFFICER
FPO SAN FRANCISCO 96628-3300

COMMANDING OFFICER
USS GUADALCANAL (LPH-7)
ATTN: MET. OFFICER
FPO NEW YORK 09562-1635

COMMANDING OFFICER
USS GUAM (LPH-9)
ATTN: MET. OFFICER
FPO NEW YORK 09563-1640

COMMANDING OFFICER
USS INCHON (LPH-12)
ATTN: MET. OFFICER
FPO NEW YORK 09529-1655

COMMANDING OFFICER
USS IWO JIMA (LPH-2)
ATTN: MET. OFFICER
FPO NEW YORK 09561-1625

COMMANDING OFFICER
USS NASSAU (LHA-4)
ATTN: MET. OFFICER
FPO NEW YORK 09557-1615

COMMANDING OFFICER
USS SAIPAN (LHA-2)
ATTN: MET. OFFICER
FPO NEW YORK 09549-1605

COMMANDING OFFICER
USS BELLEAU WOOD (LHA-3)
ATTN: METEOROLOGICAL OFFICER
FPO SAN FRANCISCO 96623-1610

COMMANDING OFFICER
USS NEW ORLEANS (LPH-11)
ATTN: MET. OFFICER
FPO SAN FRANCISCO 96627-1650

COMMANDING OFFICER
USS OKINAWA (LPH-3)
ATTN: MET. OFFICER
FPO SAN FRANCISCO 96625-1630

COMMANDING OFFICER
USS PELELIU (LHA-5)
ATTN: MET. OFFICER
FPO SAN FRANCISCO 96624-1620

COMMANDING OFFICER
USS TARAWA (LHA-1)
ATTN: MET. OFFICER
FPO SAN FRANCISCO 96622-1600

COMMANDING OFFICER
USS TRIPOLI (LPH-10)
ATTN: METEOROLOGICAL OFFICER
FPO SAN FRANCISCO 96626-1645

COMMANDING OFFICER
USS PUGET SOUND (AD-38)
ATTN: METEOROLOGICAL OFFICER
FPO NEW YORK 09544-2520

COMMANDING OFFICER
USS LASALLE (AGF-3)
ATTN: METEOROLOGICAL OFFICER
FPO NEW YORK 09577-3320

COMMANDING OFFICER
USS LEXINGTON (AVT-16)
FPO MIAMI 34088-2700

COMMANDING OFFICER
USS POINT LOMA (AGDS-2)
ATTN: METEOROLOGICAL OFFICER
FPO SAN FRANCISCO 96675-3406

COMFLTAIR, MEDITERRANEAN
ATTN: NSAP SCIENCE ADVISOR
CODE 03A
FPO NEW YORK 09521

COMMANDING GENERAL (G4)
FLEET MARINE FORCE, ATLANTIC
ATTN: NSAP SCIENCE ADVISOR
NORFOLK, VA 23511

COMMANDER IN CHIEF
U.S. CENTRAL COMMAND
ATTN: CCJ2-T
MACDILL AFB, FL 33608

ASST. FOR ENV. SCIENCES
ASST. SEC. OF THE NAVY (R&D)
ROOM 5E731, THE PENTAGON
WASHINGTON, DC 20350

CHIEF OF NAVAL RESEARCH (2)
LIBRARY SERVICES, CODE 784
BALLSTON TOWER #1
800 QUINCY ST.
ARLINGTON, VA 22217-5000

OFFICE OF NAVAL RESEARCH
CODE 422AT
ARLINGTON, VA 22217-5000

OFFICE OF NAVAL RESEARCH
CODE 422 CS
ARLINGTON, VA 22217-5000

OFFICE OF NAVAL RESEARCH
CODE 422 PO
ARLINGTON, VA 22217-5000

CHIEF OF NAVAL OPERATIONS
(OP-952)
U.S. NAVAL OBSERVATORY
WASHINGTON, DC 20390

CHIEF OF NAVAL OPERATIONS
NAVY DEPT. OP-986G
WASHINGTON, DC 20350

CHIEF OF NAVAL OPERATIONS
U.S. NAVAL OBSERVATORY
DR. R. W. JAMES, OP-952D1
34TH & MASS. AVE., NW
WASHINGTON, DC 20390

CHIEF OF NAVAL OPERATIONS
U.S. NAVAL OBSERVATORY
DR. RECHNITZER, OP-952F
34TH & MASS AVE.
WASHINGTON, DC 20390

CHIEF OF NAVAL OPERATIONS
OP-952D
U.S. NAVAL OBSERVATORY
WASHINGTON, DC 20390

CHIEF OF NAVAL OPERATIONS
OP-953
NAVY DEPARTMENT
WASHINGTON, DC 20350

DIRECTOR
NATIONAL SECURITY AGENCY
ATTN: LIBRARY (2C029)
FT. MEADE, MD 20755

OFFICER IN CHARGE
NAVOCEANCOMDET
BOX 81
U.S. NAVAL AIR STATION
FPO SAN FRANCISCO 96637-2900

OFFICER IN CHARGE
NAVOCEANCOMDET
U.S. NAVAL AIR FACILITY
FPO SEATTLE 98767-2903

COMMANDING OFFICER
OFFICE OF NAVAL RESEARCH
1030 E. GREEN ST.
PASADENA, CA 91101

COMMANDING OFFICER
NORDA
NSTL, MS 39529

COMMANDING OFFICER
FLEET INTELLIGENCE CENTER
(EUROPE & ATLANTIC)
NORFOLK, VA 23511

COMMANDING OFFICER
FLEET INTELLIGENCE CENTER
(PACIFIC)
PEARL HARBOR, HI 96860

COMMANDER
NAVAL OCEANOGRAPHY COMMAND
NSTL, MS 39529-5000

COMMANDING OFFICER
FLENUMOCEANCEN
MONTEREY, CA 93943-5105

COMMANDING OFFICER
NAVPOLAROCEANCEN
NAVY DEPT.
4301 SUITLAND RD.
WASHINGTON, DC 20390

COMMANDING OFFICER
U.S. NAVOCEANCOMCEN
BOX 12, COMNAVMARIANAS
FPO SAN FRANCISCO 96630-2926

COMMANDING OFFICER
U.S. NAVOCEANCOMCEN
BOX 31 (ROTA)
FPO NEW YORK 09540

COMMANDING OFFICER
NAVOCEANCOMFAC
NAS, NORTH ISLAND
SAN DIEGO, CA 92135

DIRECTOR OF RESEARCH
U.S. NAVAL ACADEMY
ANNAPOLIS, MD 21402

NAVAL POSTGRADUATE SCHOOL
METEOROLOGY DEPT.
MONTEREY, CA 93943

NAVAL POSTGRADUATE SCHOOL
OCEANOGRAPHY DEPT.
MONTEREY, CA 93943

LIBRARY
NAVAL POSTGRADUATE SCHOOL
MONTEREY, CA 93943-5100

PRESIDENT
NAVAL WAR COLLEGE
GEOPHYS. OFFICER, NAVOPS DEPT.
NEWPORT, RI 02841

COMMANDER (2)
NAVAIRSYSCOM
ATTN: LIBRARY (AIR-723D)
WASHINGTON, DC 20361-0001

COMMANDER
NAVAIRSYSCOM (AIR-330)
WASHINGTON, DC 20361-0001

COMMANDER
NAVAIRSYSCOM (AIR-07)
WASHINGTON, DC 20361-0001

COMMANDER
NAVELEXSYSCOM (PME-106)
ATTN: CDR D. MCCONATHY
WASHINGTON, DC 20363-5100

COMMANDER
NAVAL SEA SYSTEMS COMMAND
ATTN: LCDR S. GRIGSBY
PMS-405/PM-22
WASHINGTON, DC 20362-5101

COMMANDER
NAVOCEANSYSCEN
DR. J. RICHTER, CODE 54
SAN DIEGO, CA 92152-5000

COMMANDER
NAVAL WEAPONS CENTER
DR. A. SHLANTA, CODE 3918
CHINA LAKE, CA 93555-6001

COMMANDER
NAVAL SURFACE WEAPONS CENTER
DAHLGREN,VA 22448-5000

COMMANDER
NAVSURFWEACEN, CODE R42
DR. B. KATZ, WHITE OAKS LAB
SILVER SPRING, MD 20910

DIRECTOR
NAVSURFWEACEN, WHITE OAKS
NAVY SCIENCE ASSIST. PROGRAM
SILVER SPRING, MD 20910

NAVAL SPACE SYSTEMS ACTIVITY
CODE 60
P.O. BOX 92960
WORLDWAY POSTAL CENTER
LOS ANGELES, CA 90009

COMMANDER
AWS/DN
SCOTT AFB, IL 62225

USAFETAC/TS
SCOTT AFB, IL 62225

AFGWC/DAPL
OFFUTT AFB, NE 68113

AFGL/LY
HANSCOM AFB, MA 01731

OFFICE OF STAFF METEOROLOGY
WESTERN SPACE & MISSILE
CENTER (WE)
VANDENBERG AFB, CA 93437

OFFICER IN CHARGE
SERVICE SCHOOL COMMAND
DET. CHANUTE/STOP 62
CHANUTE AFB, IL 61868

HQ 1ST WEATHER WING/DN
HICKAM AFB, HI 96853

DIRECTOR (12)
DEFENSE TECH. INFORMATION
CENTER, CAMERON STATION
ALEXANDRIA, VA 22314

NOAA-NESDIS LIAISON
ATTN: CODE SC2
NASA-JOHNSON SPACE CENTER
HOUSTON, TX 77058

DIRECTOR
NATIONAL EARTH SAT. SERV/SEL
FB-4, S321B
SUITLAND, MD 20233

FEDERAL COORD. FOR METEORO.
SERVS. & SUP. RSCH. (OFCM)
11426 ROCKVILLE PIKE
SUITE 300
ROCKVILLE, MD 20852

DIRECTOR
NATIONAL HURRICANE CENTER
NOAA, GABLES ONE TOWER
1320 S. DIXIE HWY
CORAL GABLES, FL 33146

NATIONAL WEATHER SERVICE
WORLD WEATHER BLDG., RM 307
5200 AUTH ROAD
CAMP SPRINGS, MD 20023

CHIEF, SCIENTIFIC SERVICES
NWS/NOAA, SOUTHERN REGION
ROOM 10E09
819 TAYLOR ST.
FT. WORTH, TX 76102

CHIEF, SCIENTIFIC SERVICES
NWS, PACIFIC REGION
P.O. BOX 50027
HONOLULU, HI 96850

COLORADO STATE UNIVERSITY
ATMOSPHERIC SCIENCES DEPT.
ATTN: DR. WILLIAM GRAY
FORT COLLINS, CO 80523

CHAIRMAN
INSTITUTE OF ATMOS. PHYSICS
UNIV. OF ARIZONA
TUSCON, AZ 85721

ATMOSPHERIC SCIENCES DEPT.
UCLA
405 HILGARD AVE.
LOS ANGELES, CA 90024

CHAIRMAN, METEOROLOGY DEPT.
UNIVERSITY OF OKLAHOMA
NORMAN, OK 73069

CHAIRMAN, METEOROLOGY DEPT.
CALIFORNIA STATE UNIVERSITY
SAN JOSE, CA 95192

COLORADO STATE UNIVERSITY
ATMOSPHERIC SCIENCES DEPT.
ATTN: LIBRARIAN
FT. COLLINS, CO 80523

UNIVERSITY OF WASHINGTON
ATMOSPHERIC SCIENCES DEPT.
SEATTLE, WA 98195

CHAIRMAN, METEOROLOGY DEPT.
PENNSYLVANIA STATE UNIV.
503 DEIKE BLDG.
UNIVERSITY PARK, PA 16802

FLORIDA STATE UNIVERSITY
ENVIRONMENTAL SCIENCES DEPT.
TALLAHASSEE, FL 32306

UNIVERSITY OF HAWAII
METEOROLOGY DEPT.
2525 CORREA ROAD
HONOLULU, HI 96822

DIRECTOR
COASTAL STUDIES INSTITUTE
LOUISIANA STATE UNIVERSITY
ATTN: O. HUH
BATON ROUGE, LA 70803

ATMOSPHERIC SCIENCES DEPT.
OREGON STATE UNIVERSITY
CORVALLIS, OR 97331

UNIVERSITY OF MARYLAND
METEOROLOGY DEPT.
COLLEGE PARK, MD 20742

CHAIRMAN
ATMOS. SCIENCES DEPT.
UNIVERSITY OF VIRGINIA
CHARLOTTESVILLE, VA 22903

CHAIRMAN
METEOROLOGY DEPT.
MASSACHUSETTS INSTITUTE OF TECHNOLOGY
CAMBRIDGE, MA 02139

CHAIRMAN, METEOROLOGY DEPT.
UNIVERSITY OF UTAH
SALT LAKE CITY, UT 84112

CHAIRMAN
METEOROLOGY & OCEANO. DEPT.
UNIVERSITY OF MICHIGAN
4072 E. ENGINEERING BLDG.
ANN ARBOR, MI 48104

TEXAS A&M UNIVERSITY
METEOROLOGY DEPT.
COLLEGE STATION, TX 77843

ATMOSPHERIC SCIENCES CENTER
DESERT RESEARCH INSTITUTE
P.O. BOX 60220
RENO, NV 89506

ATMOSPHERIC SCI. RSCH. CENTER
NEW YORK STATE UNIV.
1400 WASHINGTON AVE.
ALBANY, NY 12222

INSTITUTE FOR STORM RESEARCH
UNIVERSITY OF ST. THOMAS
3600 MT. VERNON
HOUSTON, TX 77006

DR. CLIFFORD MASS
DEPT. OF ATMOSPHERIC SCIENCES
UNIVERSITY OF WASHINGTON
SEATTLE, WA 98195

THE EXECUTIVE DIRECTOR
AMERICAN METEORO. SOCIETY
45 BEACON ST.
BOSTON, MA 02108

MR. W. G. SCHRAMM/WWW
WORLD METEOROLOGICAL ORGANIZATION
CASE POSTALE #5, CH-1211
GENEVA, SWITZERLAND

DIRECTOR, JTWC
BOX 17
FPO SAN FRANCISCO 96630

LIBRARY ACQUISITIONS
NATIONAL CENTER FOR ATMOSPHERIC RESEARCH
P.O. BOX 3000
BOULDER, CO 80307

CHARTS OF MEAN MONTHLY CLOUDINESS
AND
TIME-LATITUDE SECTIONS

Charts -- for period 1965-73, calendar year sequence January through December. (12 charts)

Sections -- for period 1965-73, for selected representative longitudes, mean cloudiness in octas. Center panel is geographical position of section. Right panel is change in mean cloudiness from month to month. Left panel is long-term mean cloud cover for longitudinal section. (10 sections)

Note: Charts and sections printed one-side for more convenient handling by reader. Blank backs accounted for in pagination, thus numbered pages are in odd-number sequence (31, 33, 35 ...).

GPO 589-742 / 38217

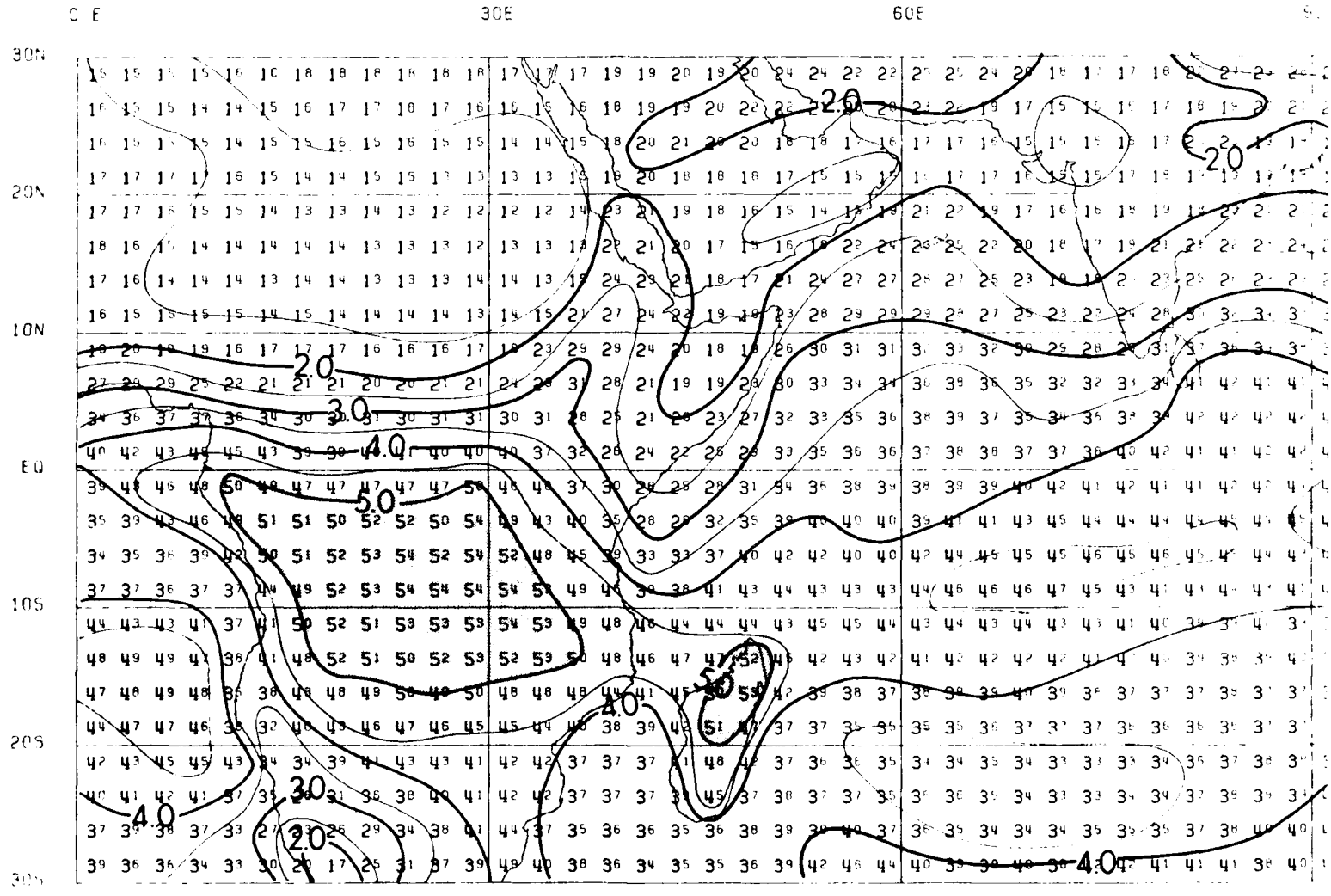

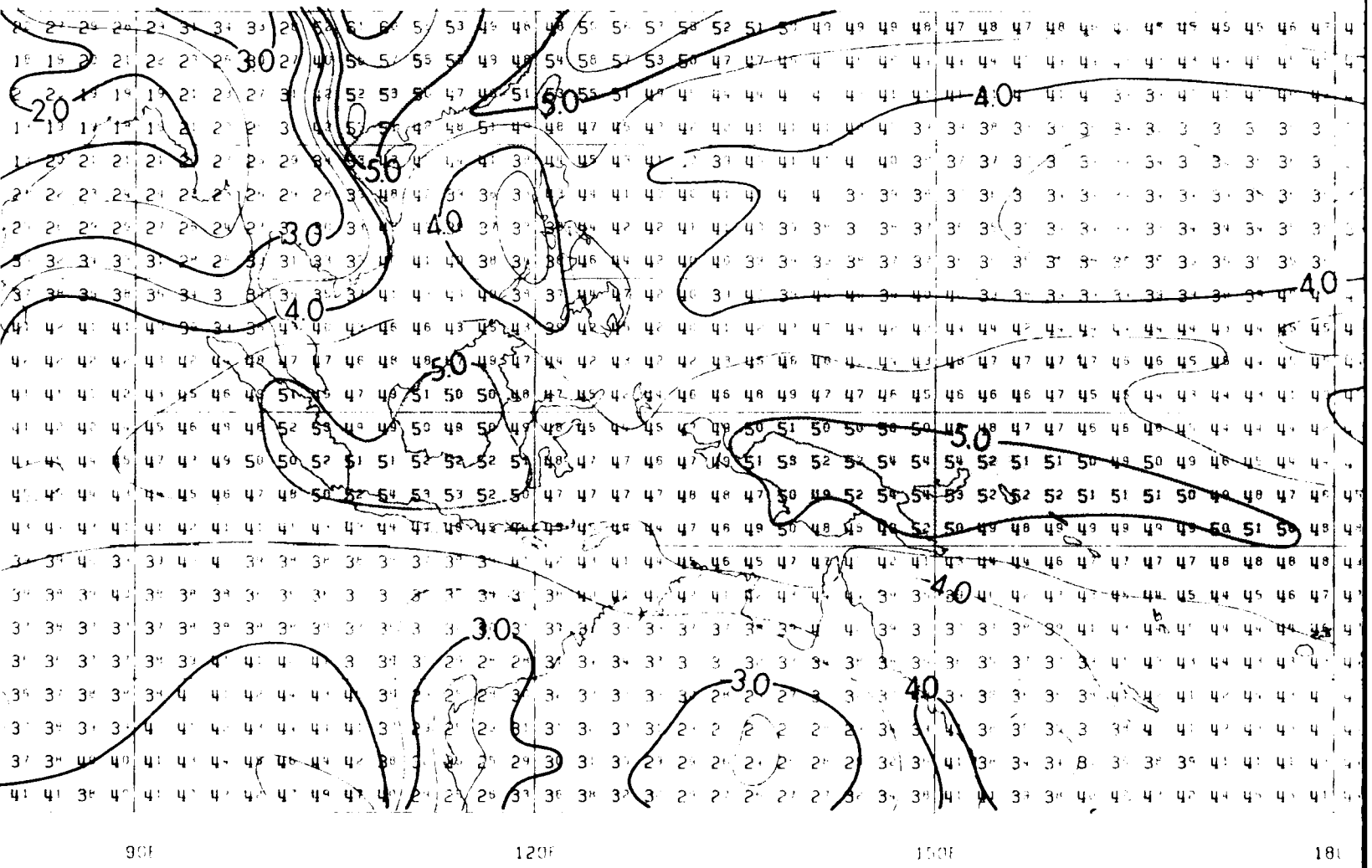
90E
120E
150E
180
90E
120E
150E
180

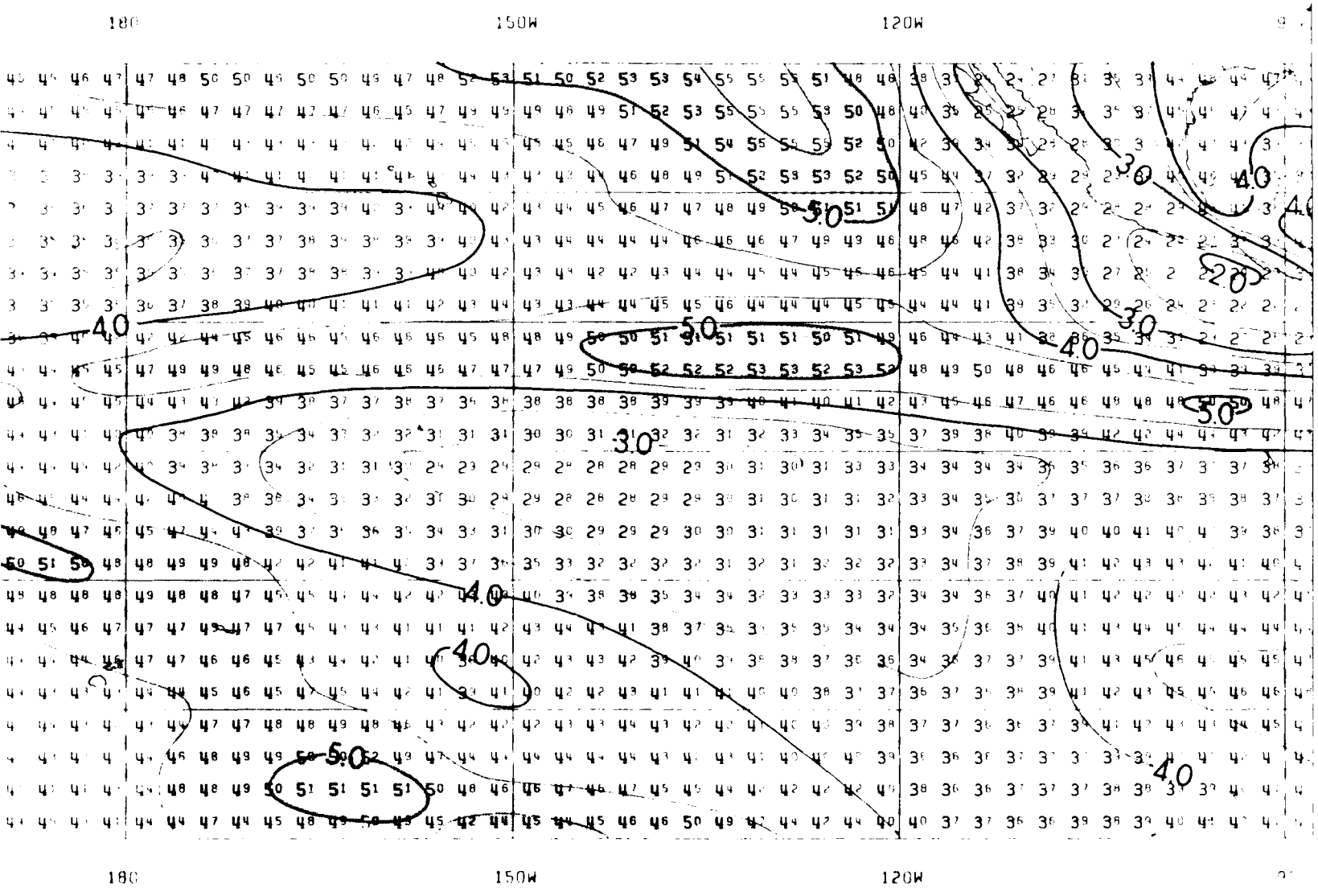
180
150W
120W
5.0
4.0
3.0
2.0
4.0
3.0
5.0
3.0
4.0
4.0
5.0
4.0
180
150W
120W

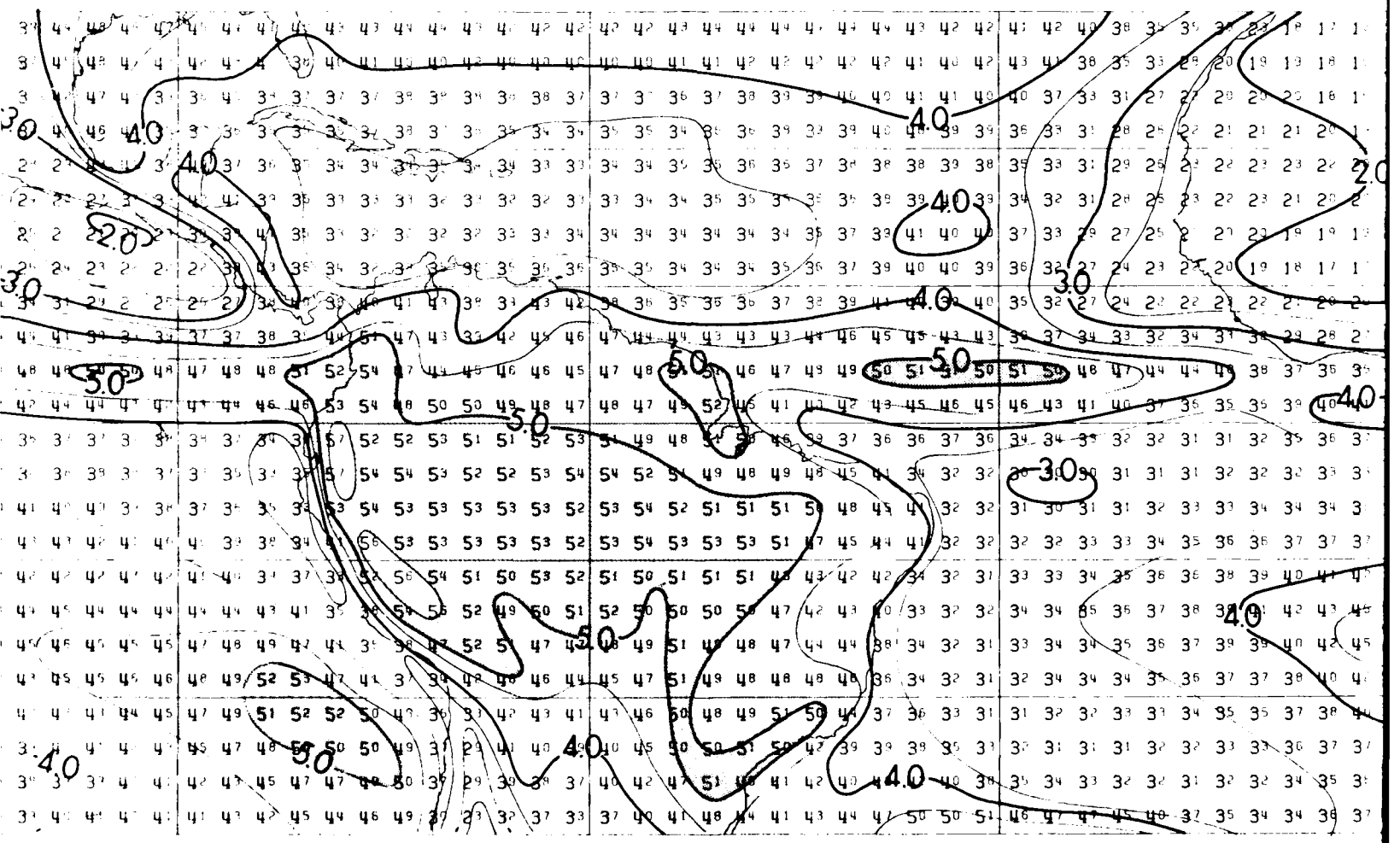

January

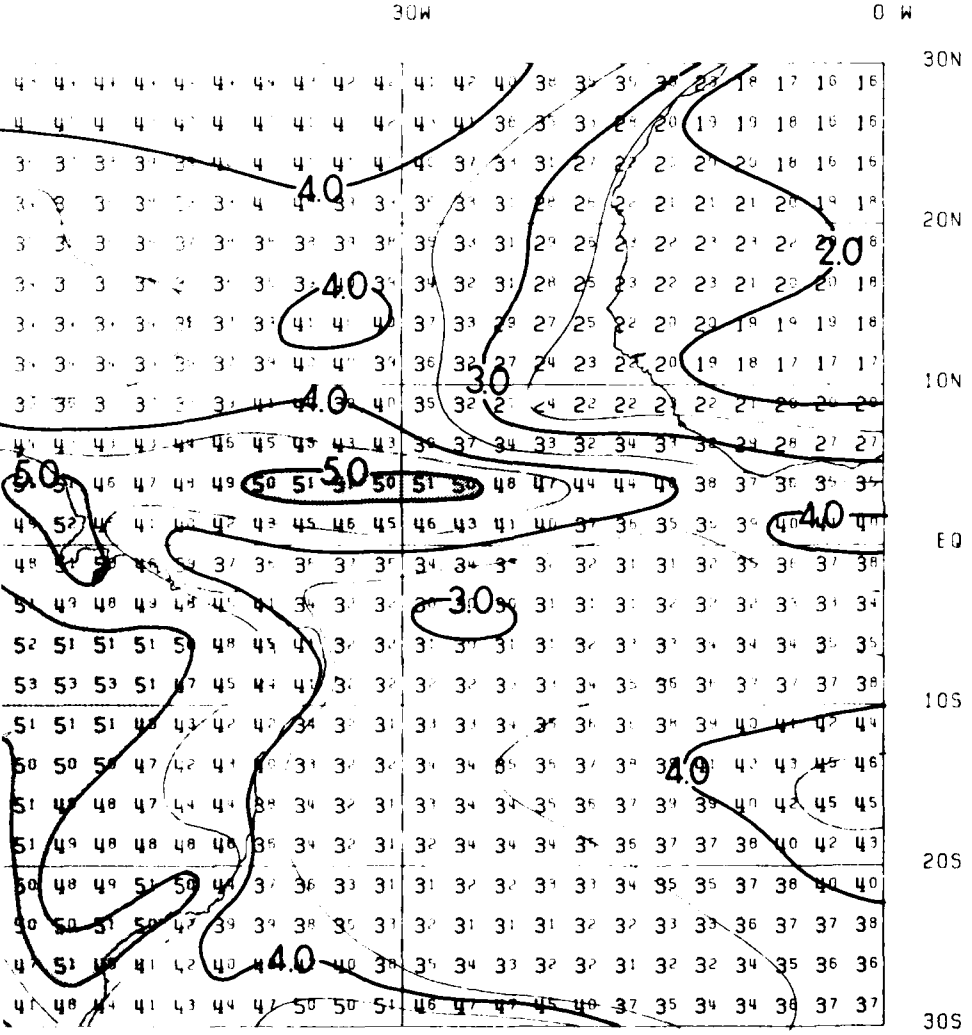

January

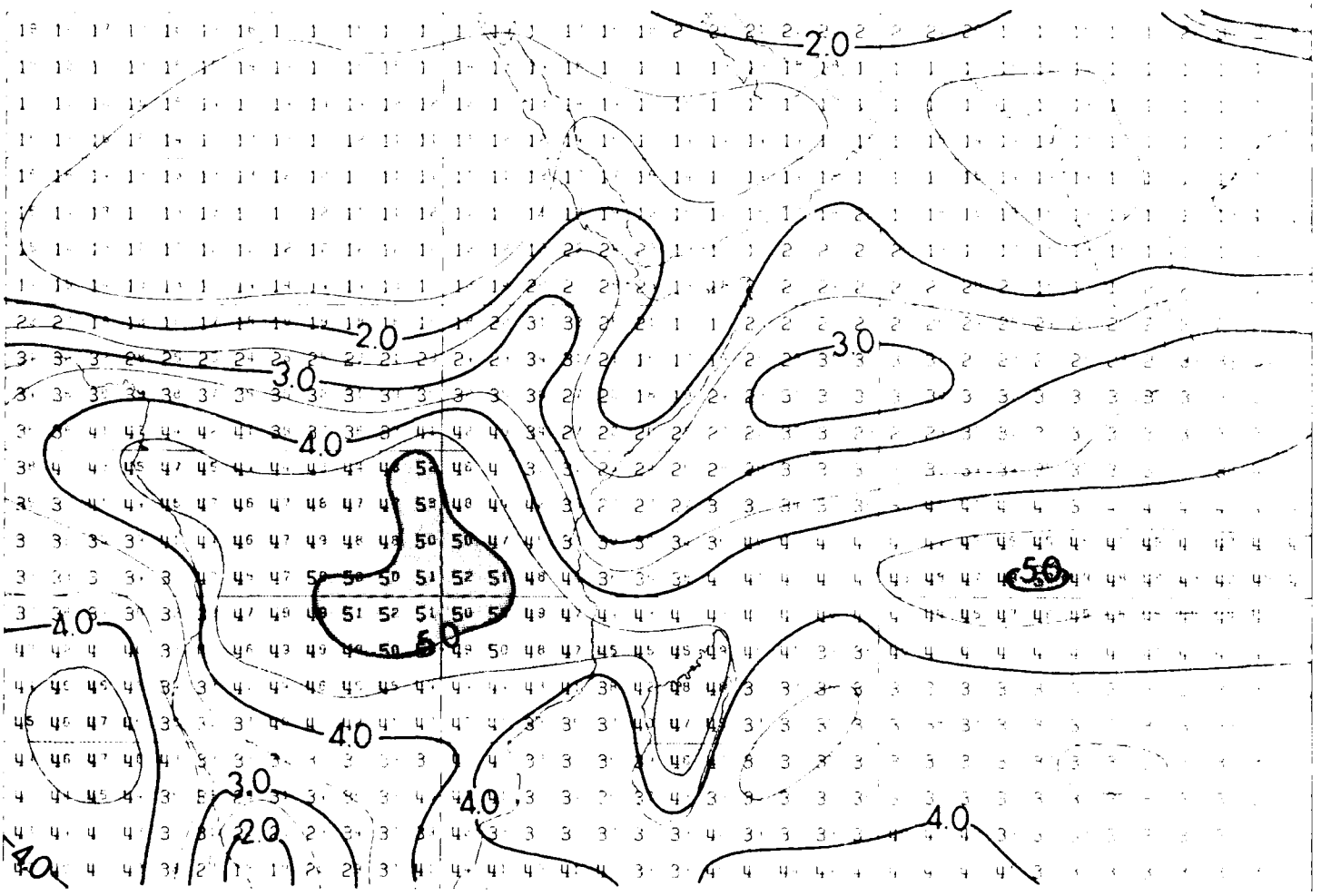

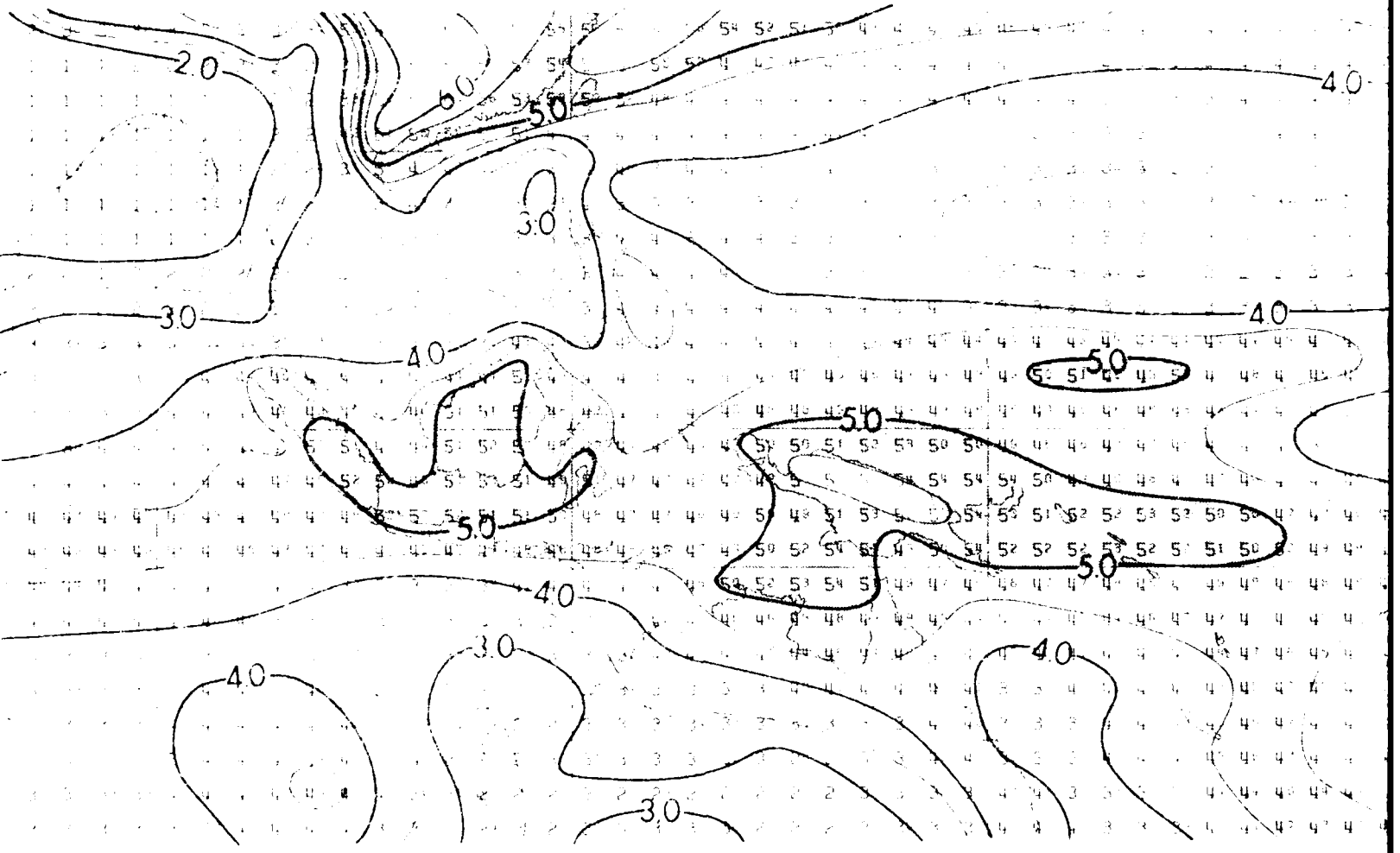
2.0
6.0
5.0
3.0
4.0
3.0
4.0
5.0
5.0
5.0
4.0
4.0
3.0
4.0
3.0

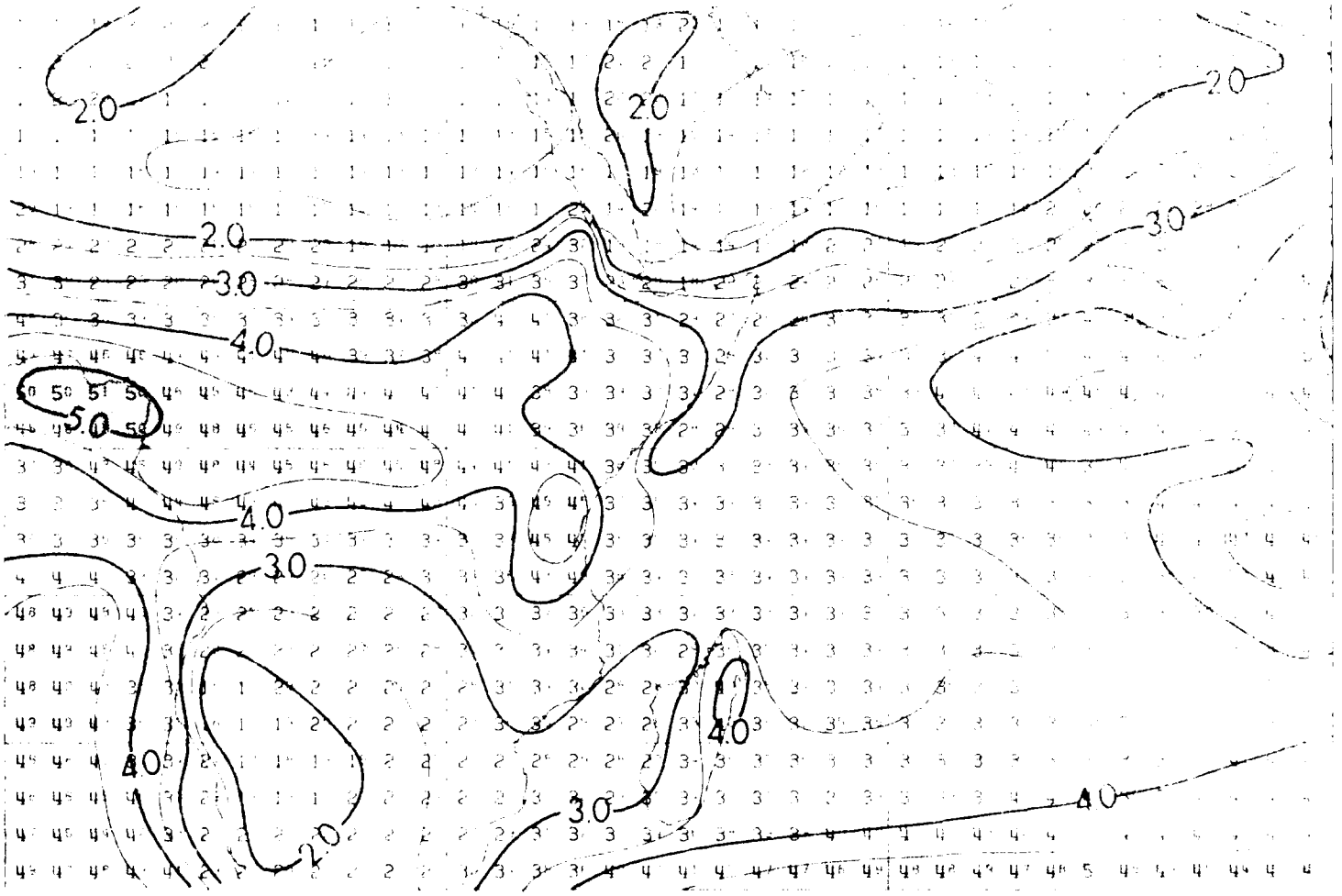

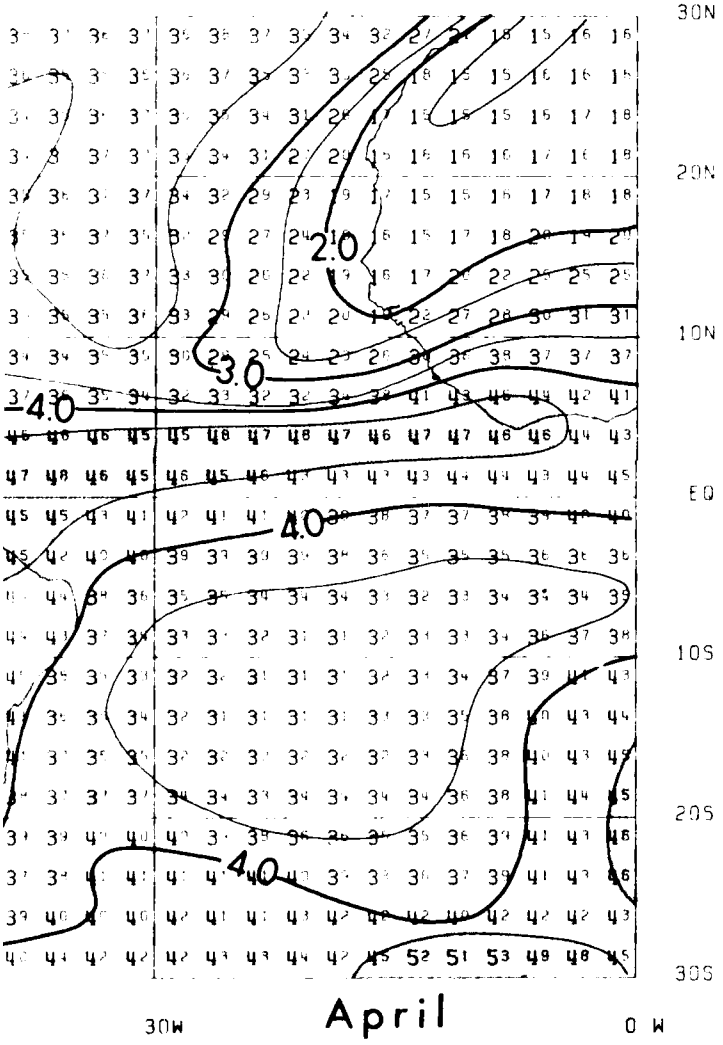

April

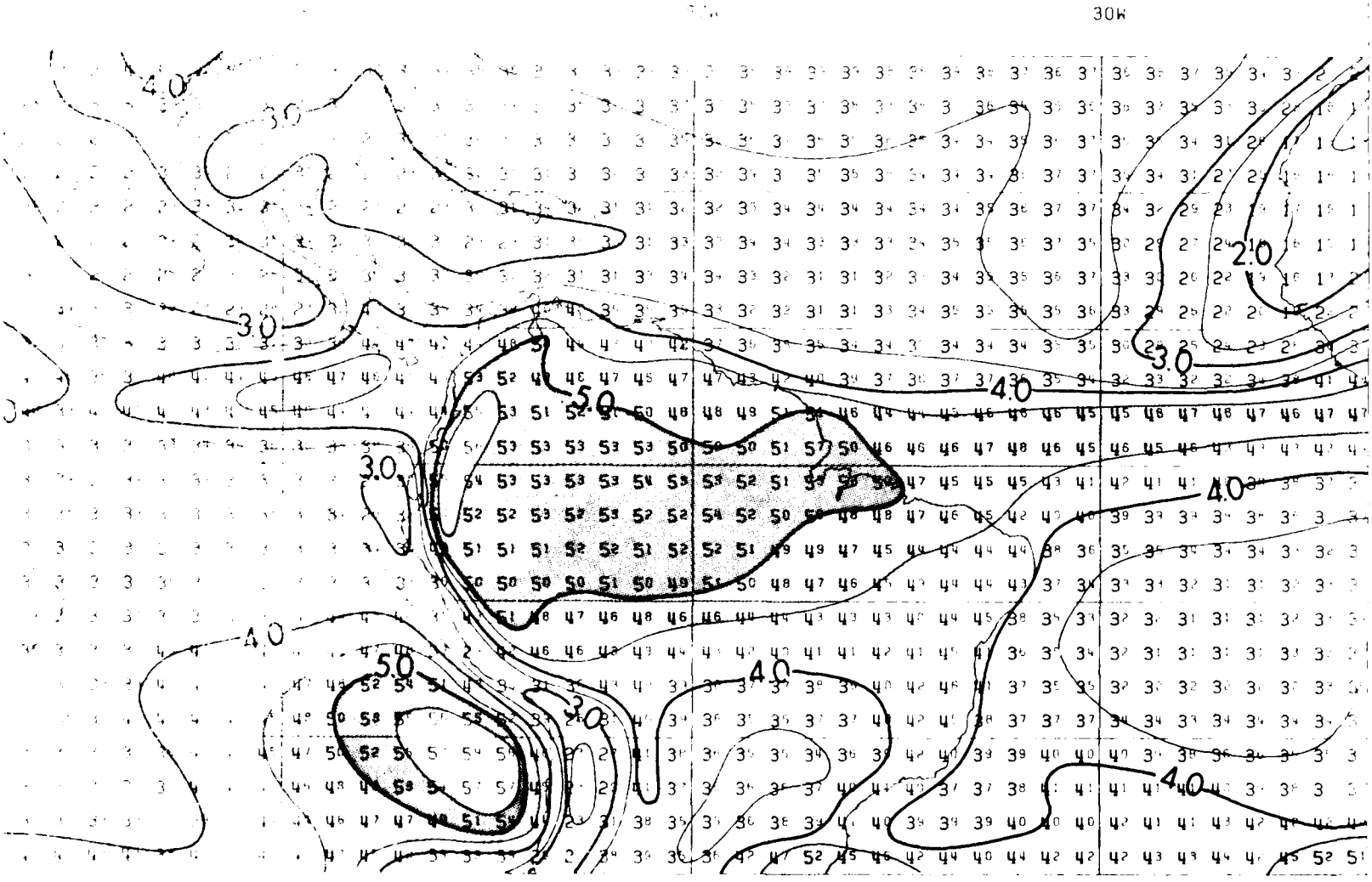

April

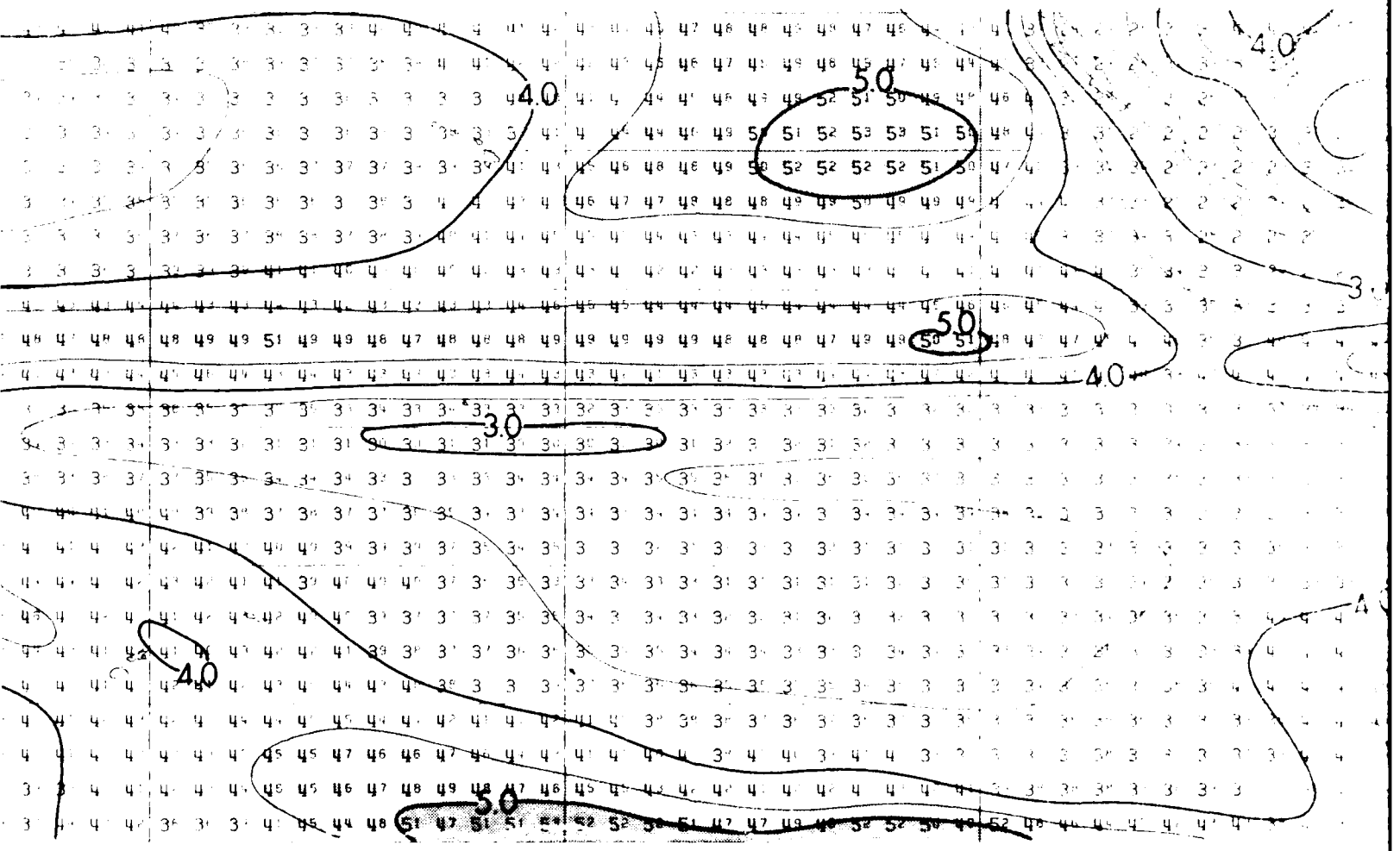
4.0
5.0
4.0
3.0
5.0
4.0
4.0
5.0

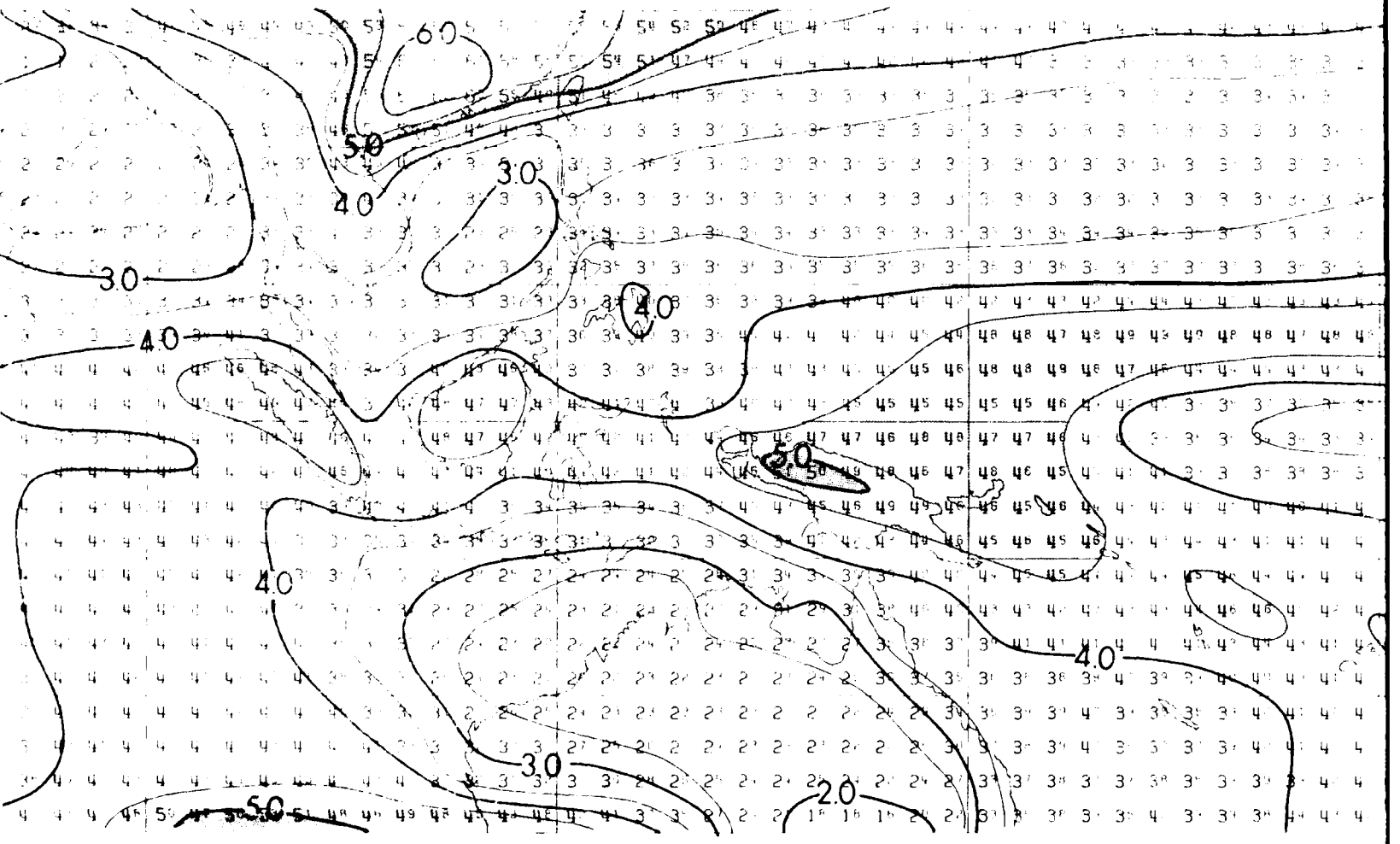
6.0
5.0
4.0
3.0
4.0
3.0
4.0
5.0
4.0
3.0
2.0
4.0
5.0

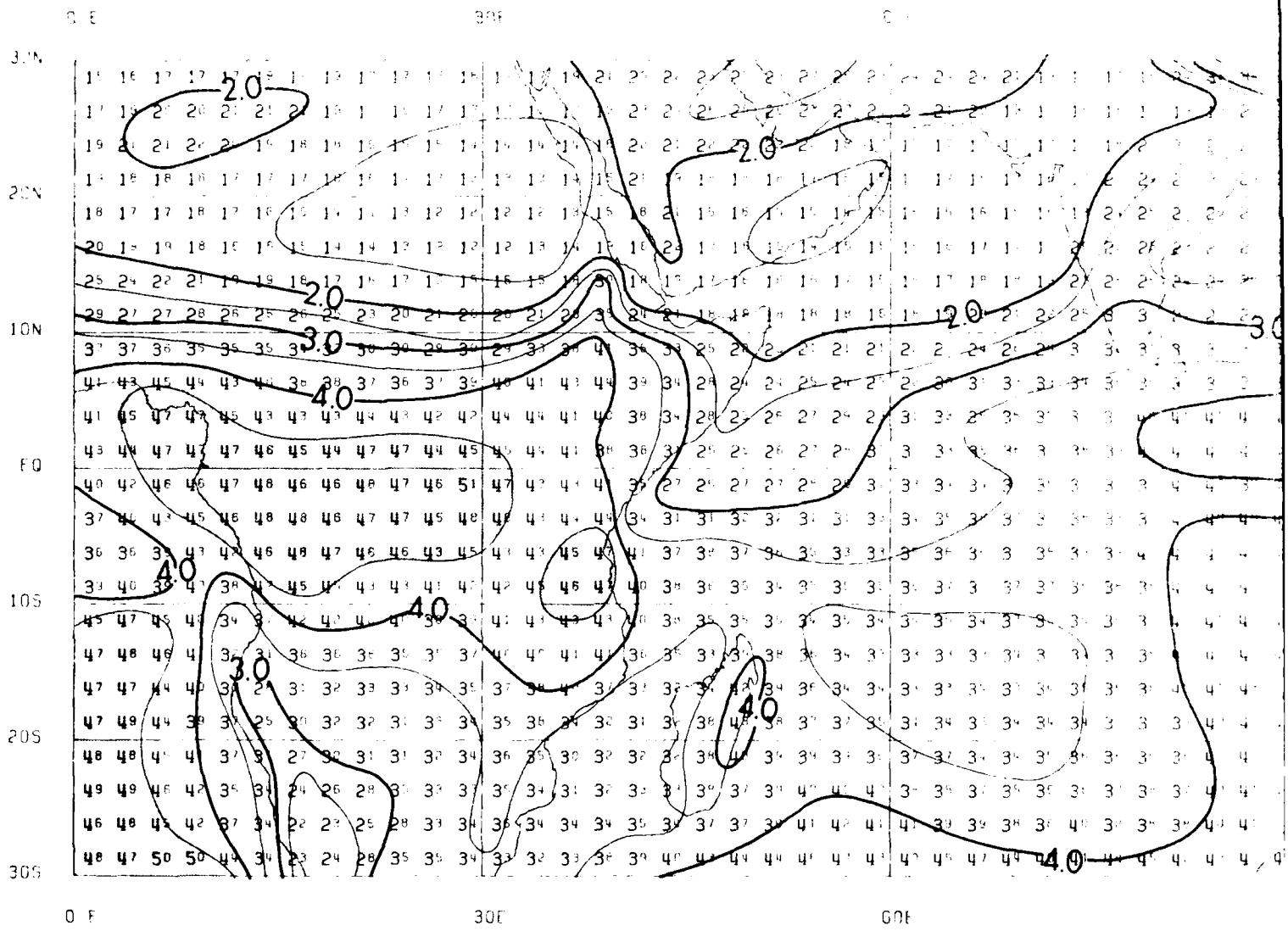

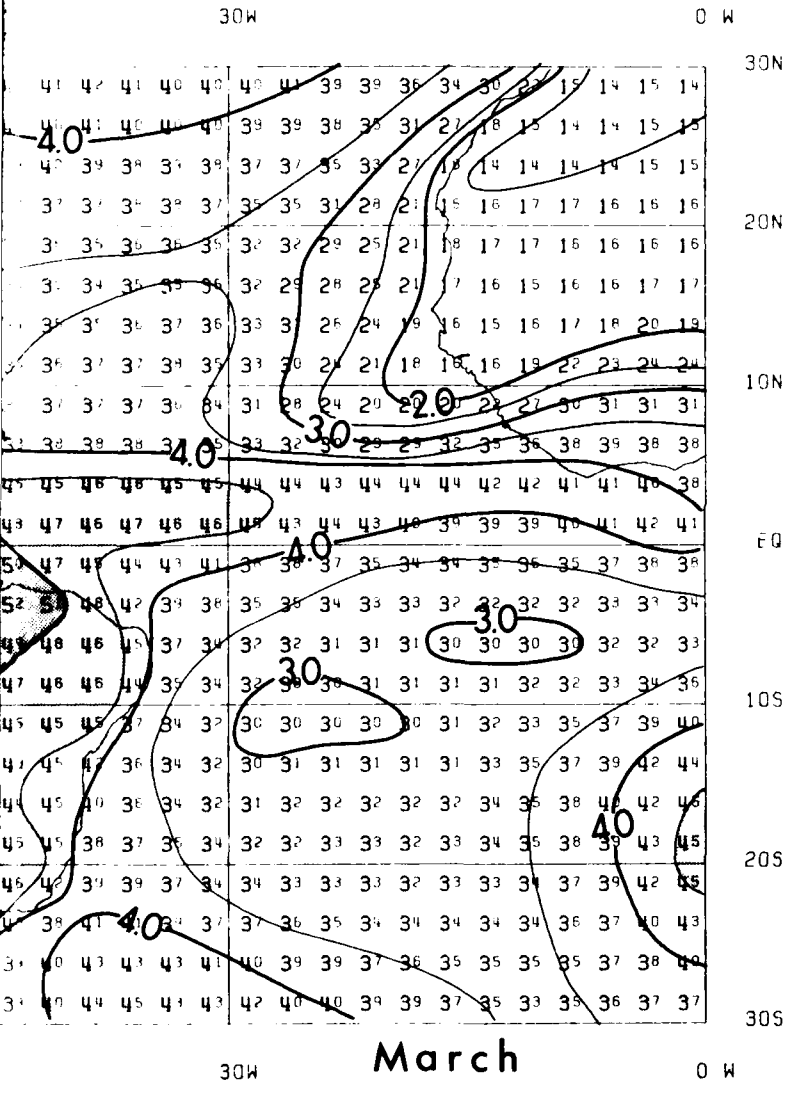
30W
0 W
30N
20N
10N
EQ
10S
20S
30S
4.0
3.0
2.0
3.0
4.0
4.0
4.0
March
30W
0 W

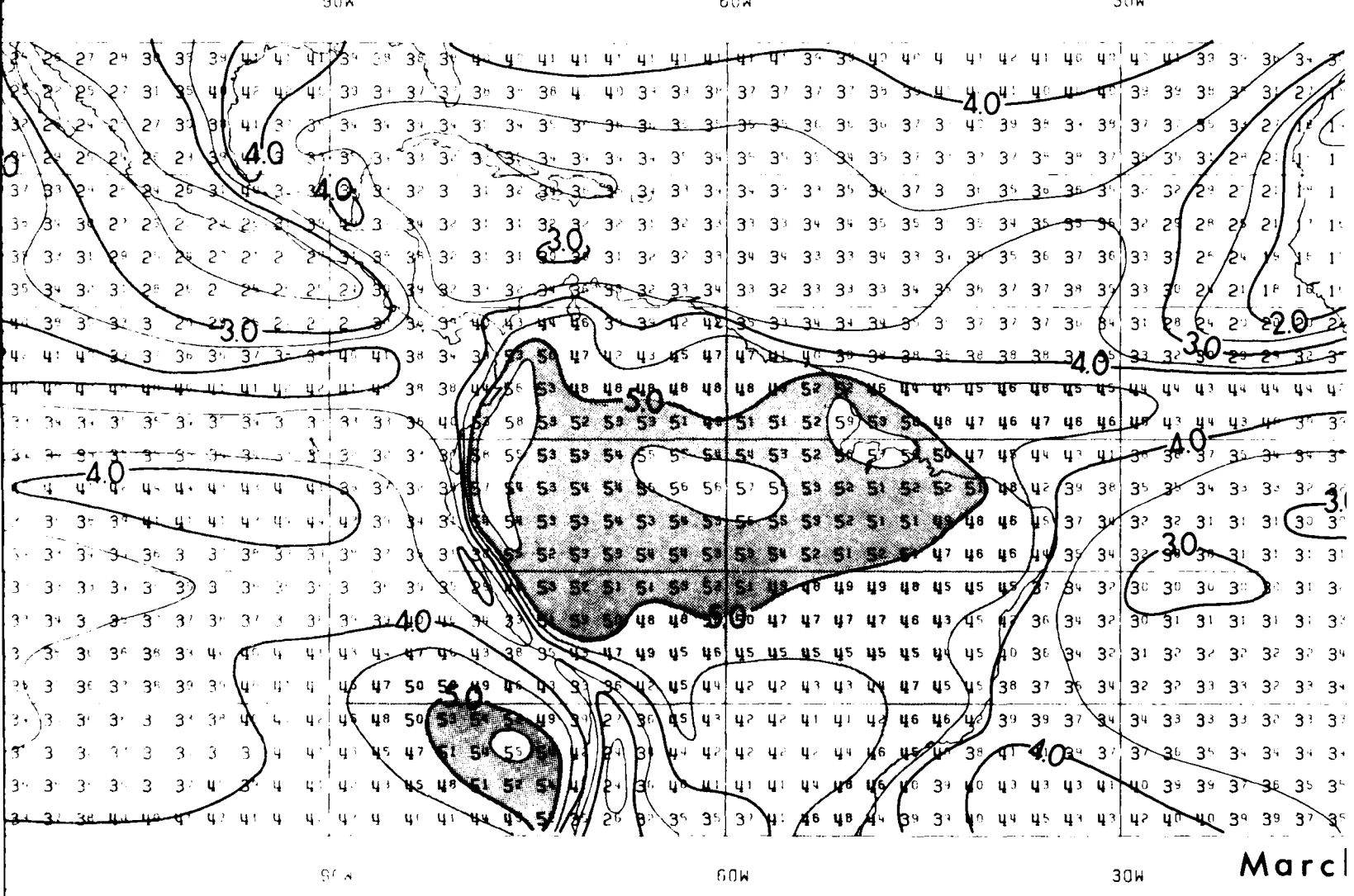
90W
60W
30W
4.0
3.0
5.0
2.0
March

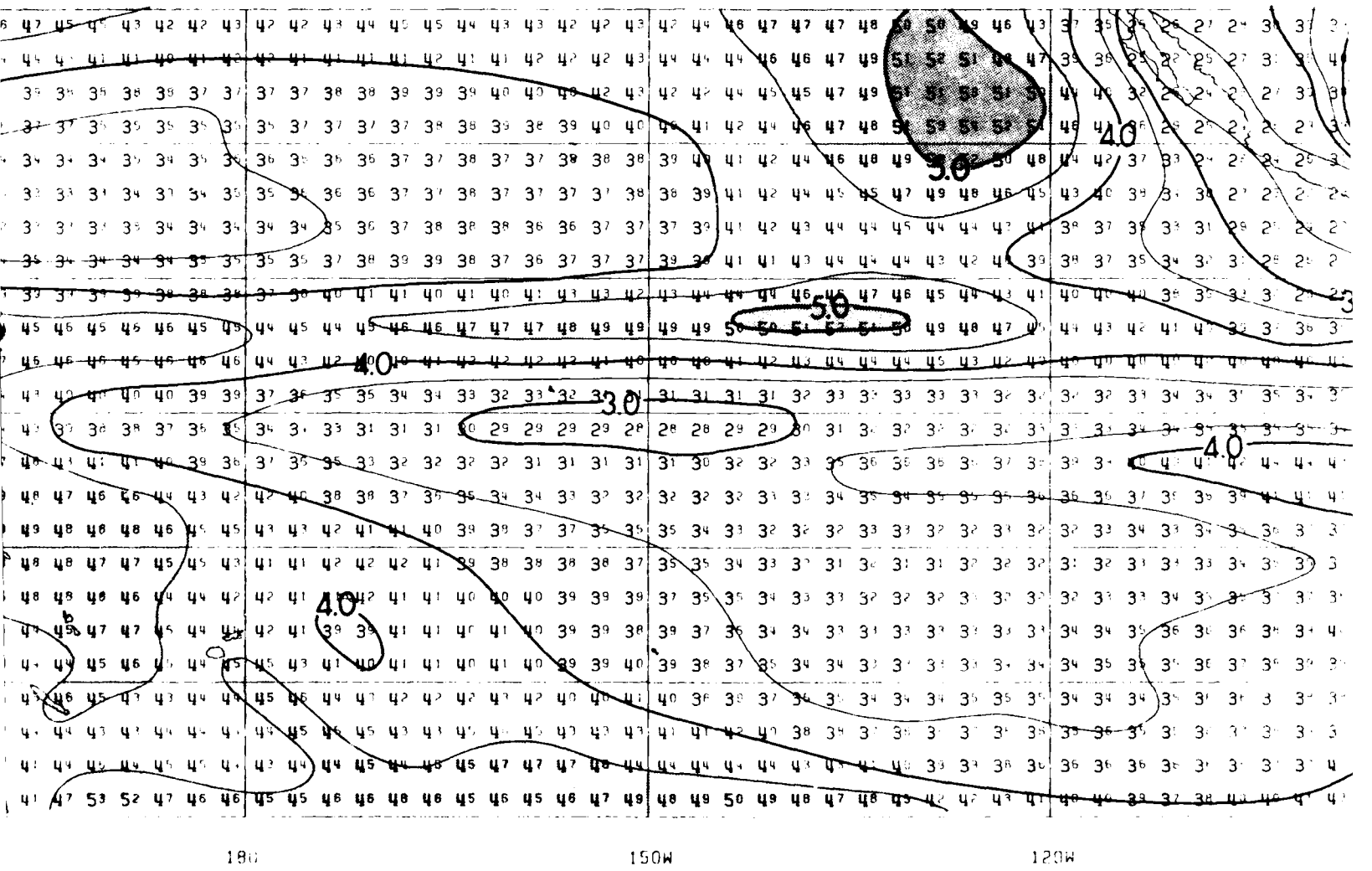
180
150W
120W
5.0
4.0
5.0
3.0
4.0
4.0
180
150W
120W

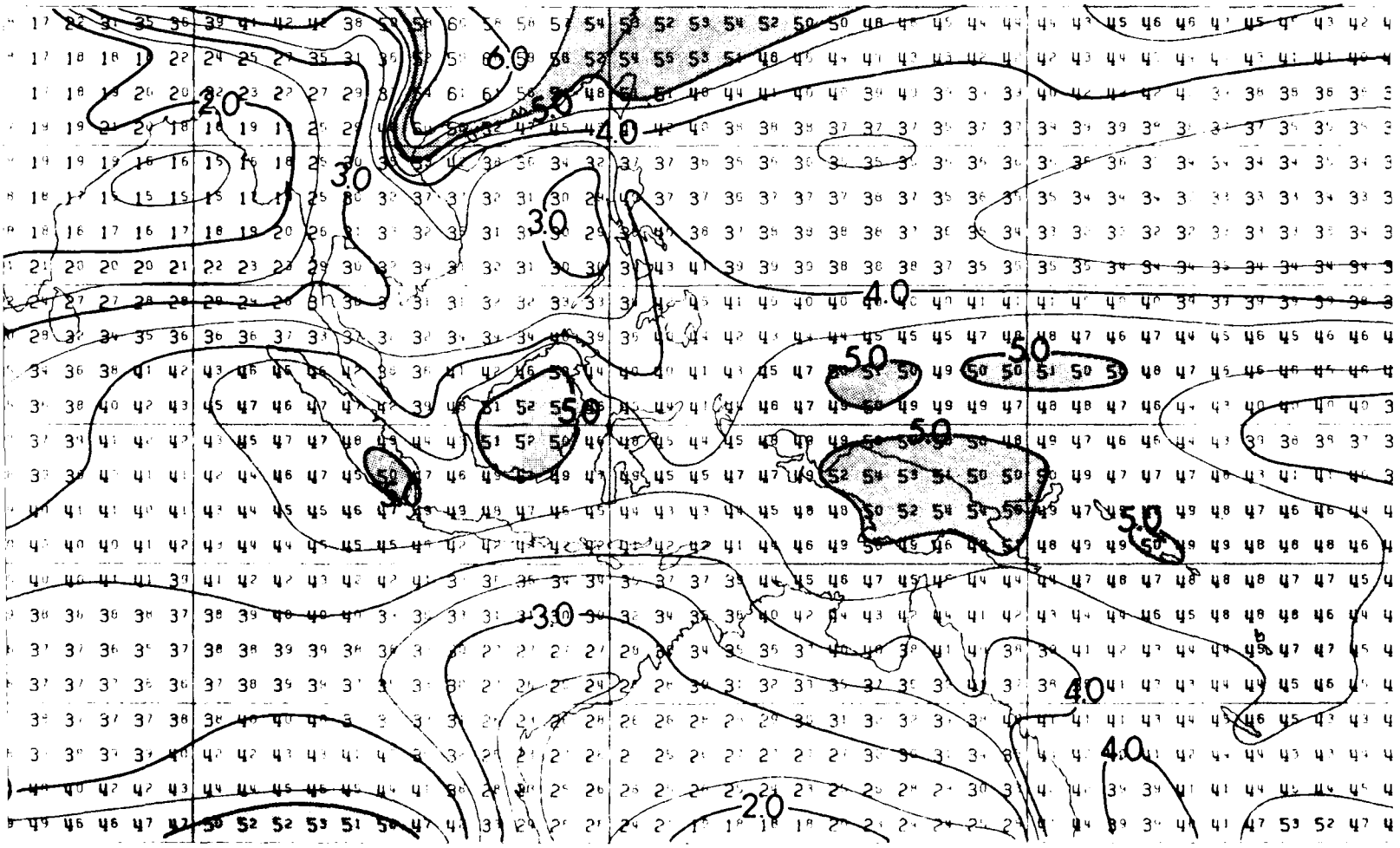
90E
120E
150E
6.0
5.0
4.0
3.0
2.0
5.0
5.0
5.0
5.0
4.0
4.0
3.0
2.0
90E
120E
150E

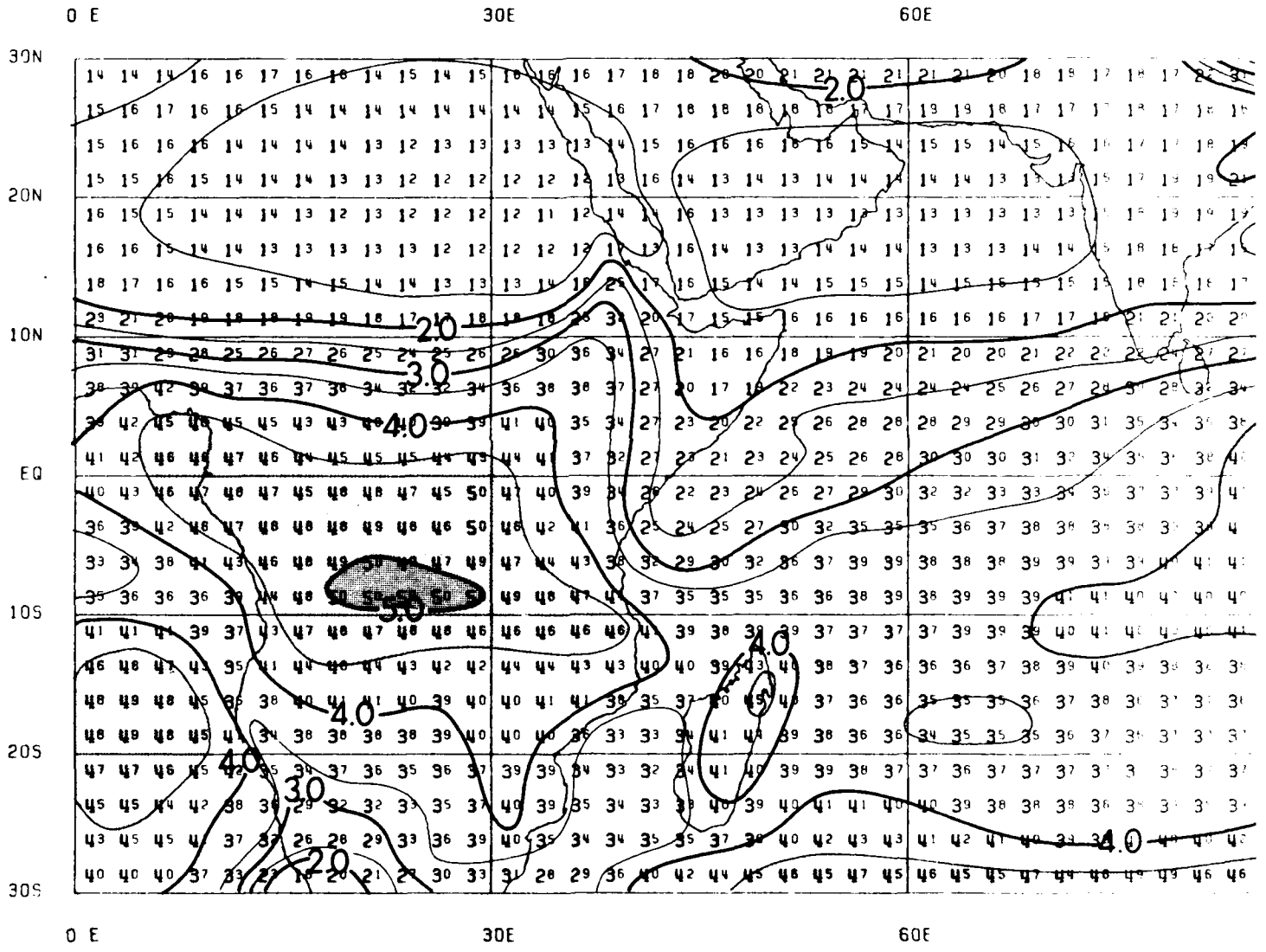

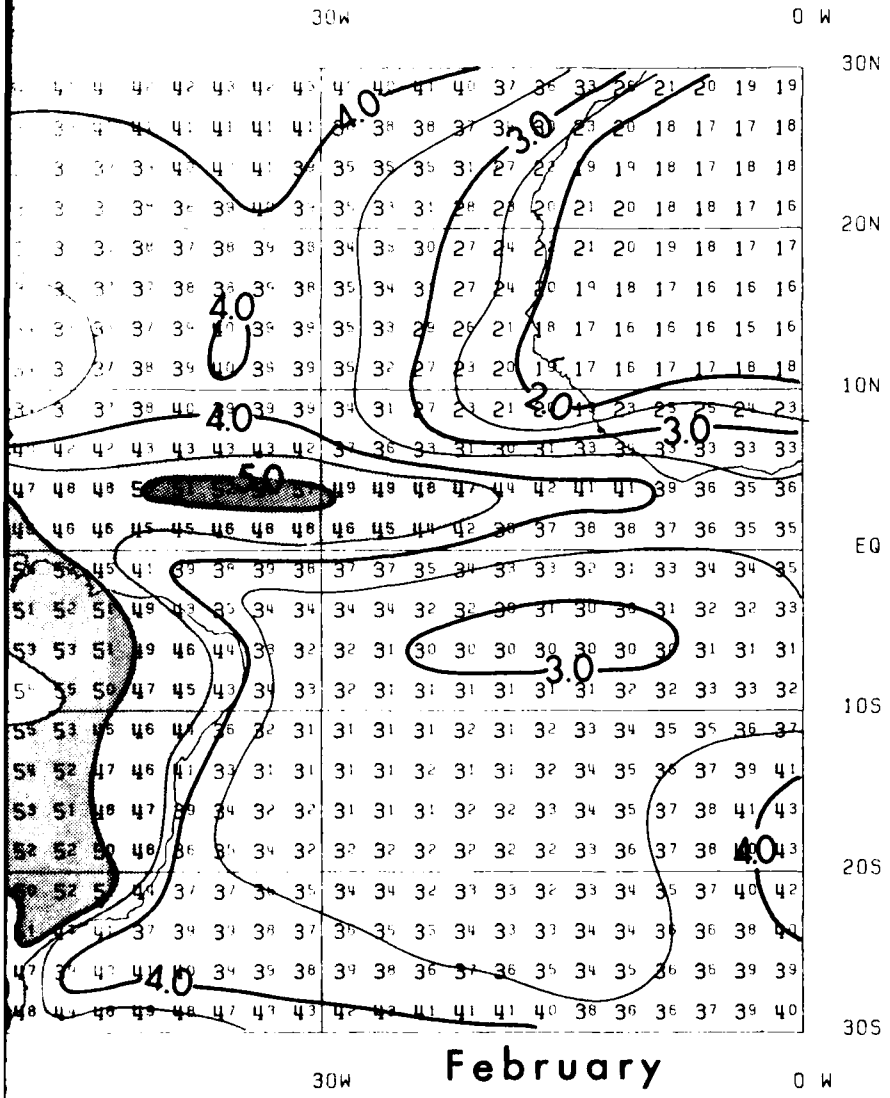
30W
0 W
30N
20N
10N
EQ
10S
20S
30S
4.0
3.0
5.0
February

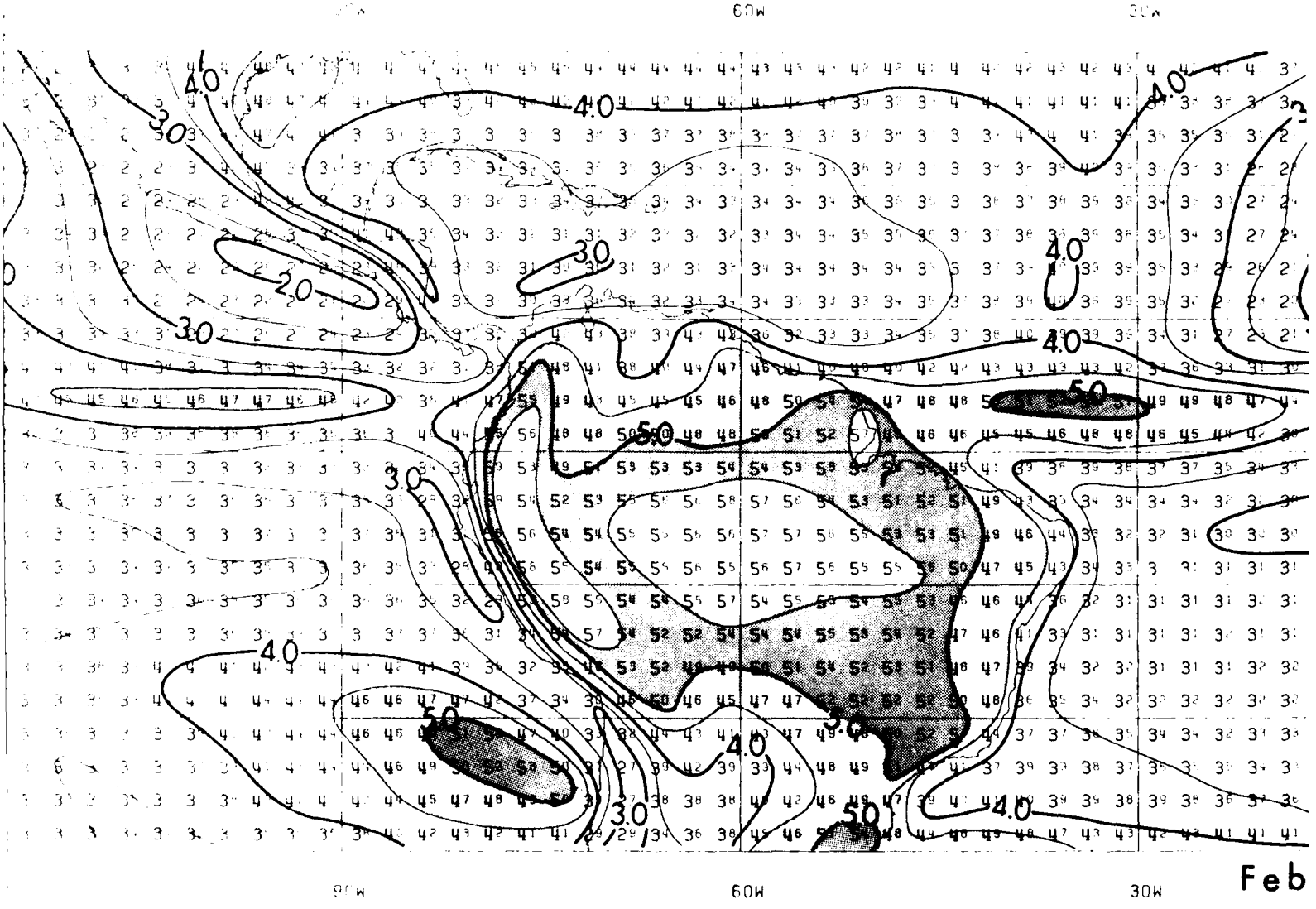
90W
60W
30W
Feb

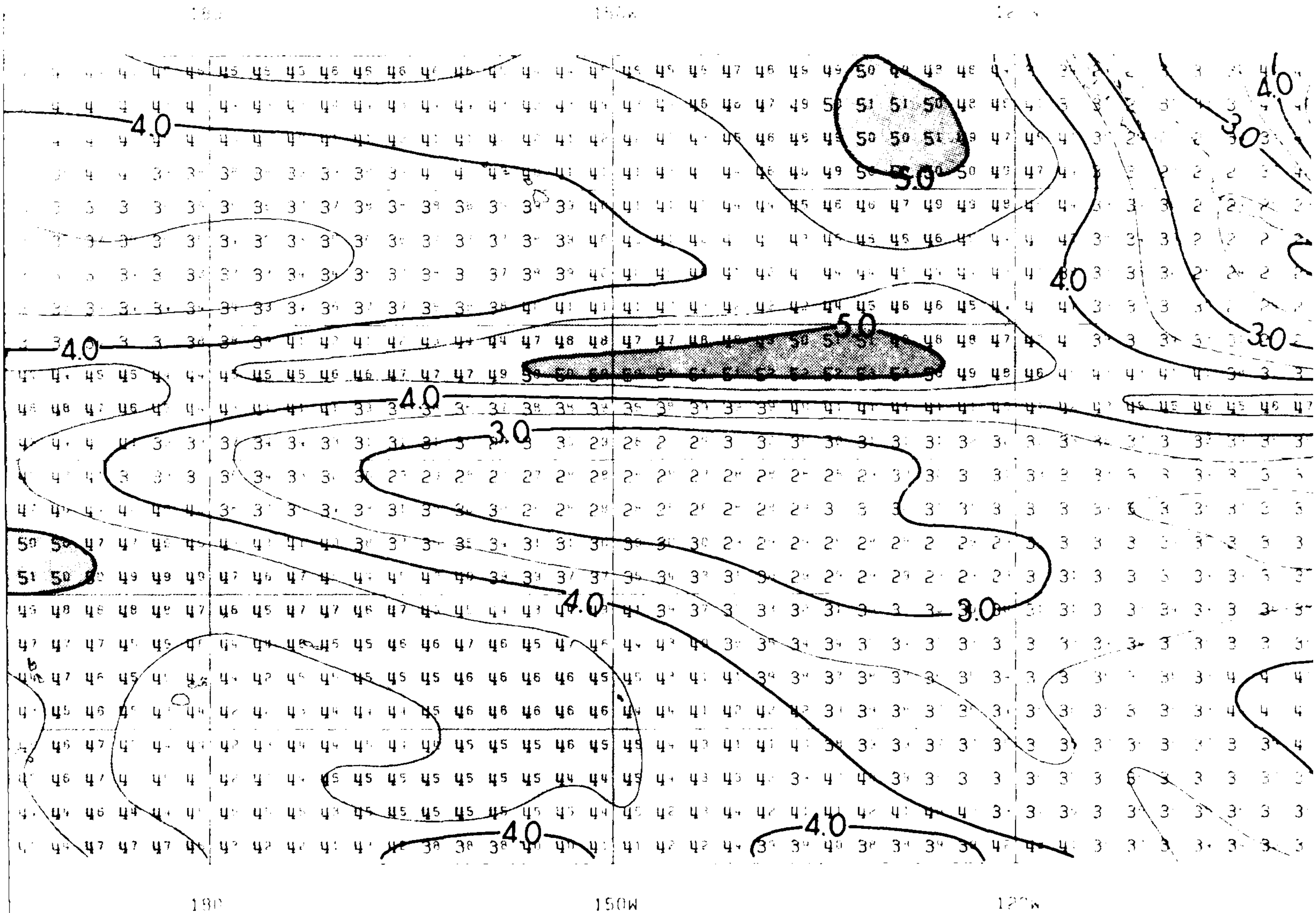
180
150W
4.0
5.0
3.0
4.0
3.0
4.0
3.0
180
150W

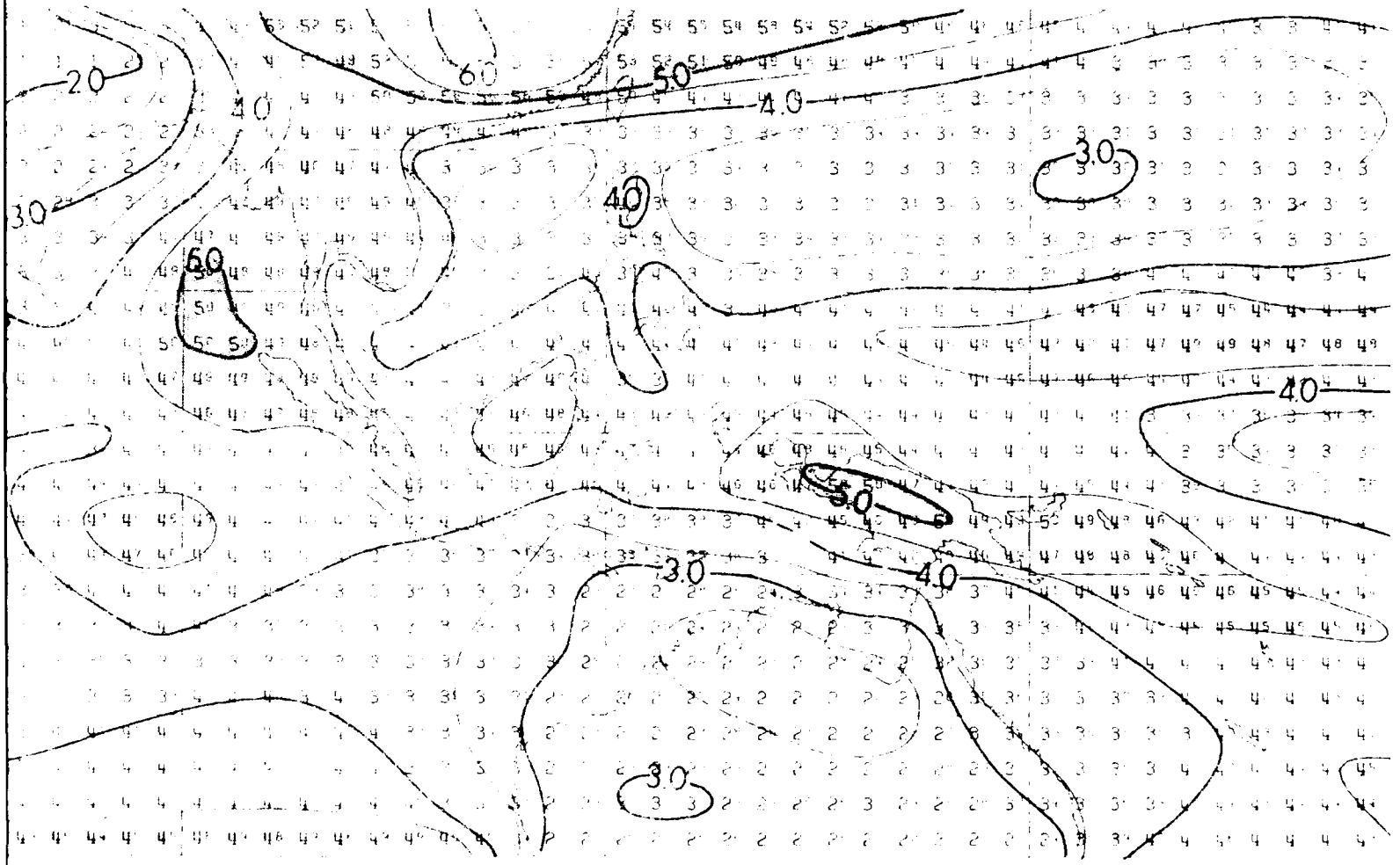
2.0
4.0
6.0
5.0
4.0
3.0
4.0
3.0
6.0
4.0
5.0
3.0
4.0
3.0

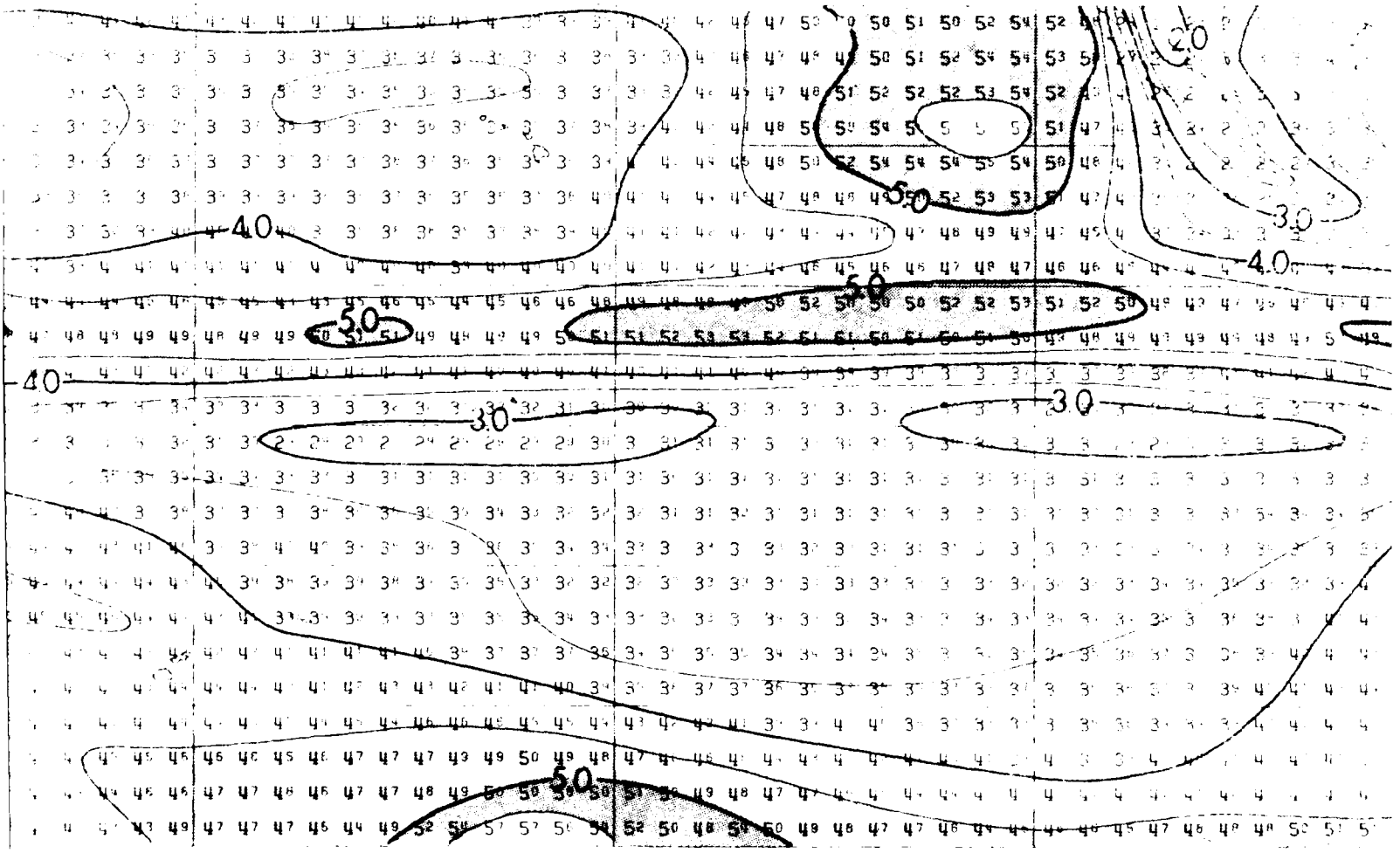
40
50
30
40
50
30
50
40
30

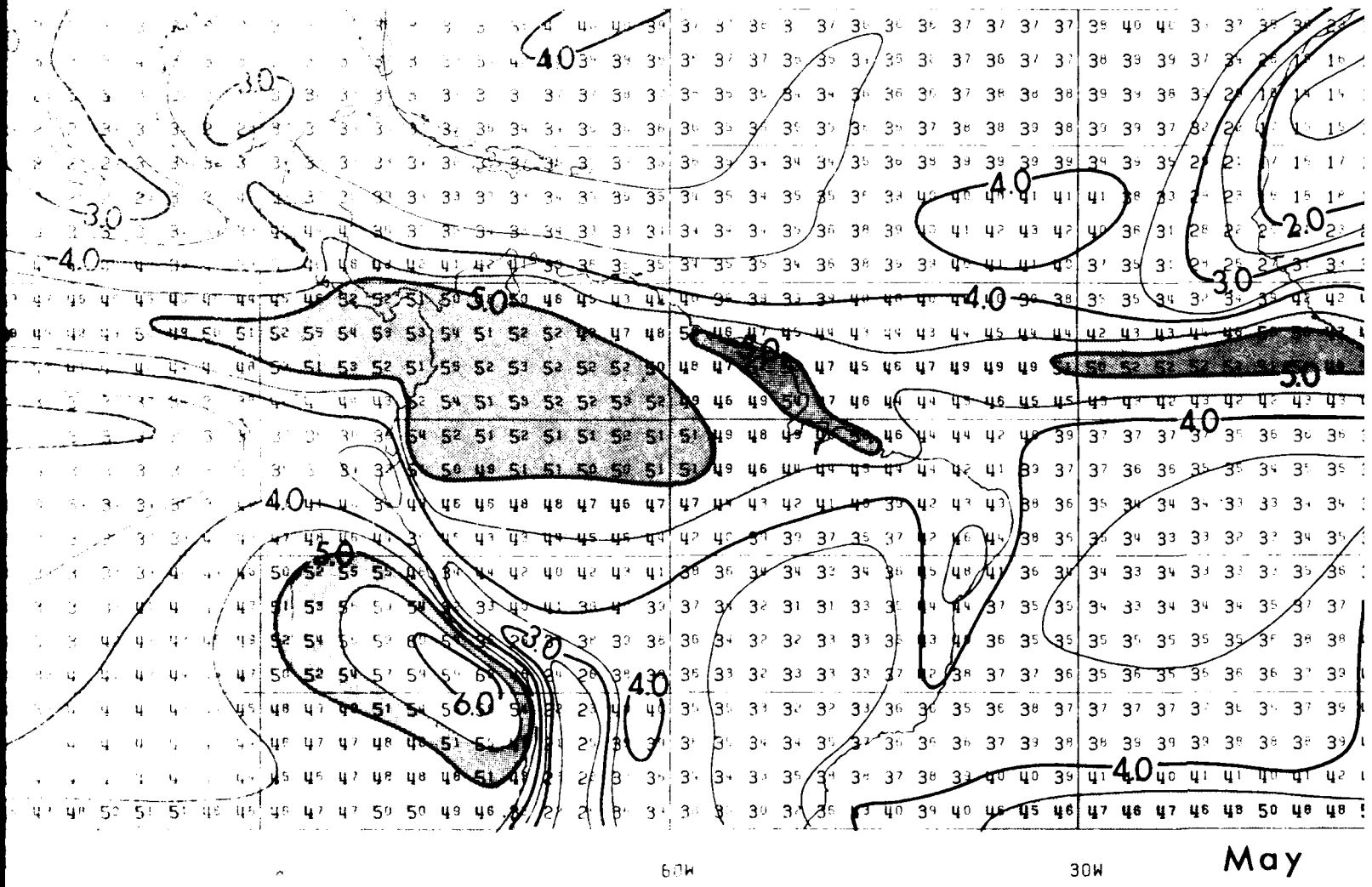

May

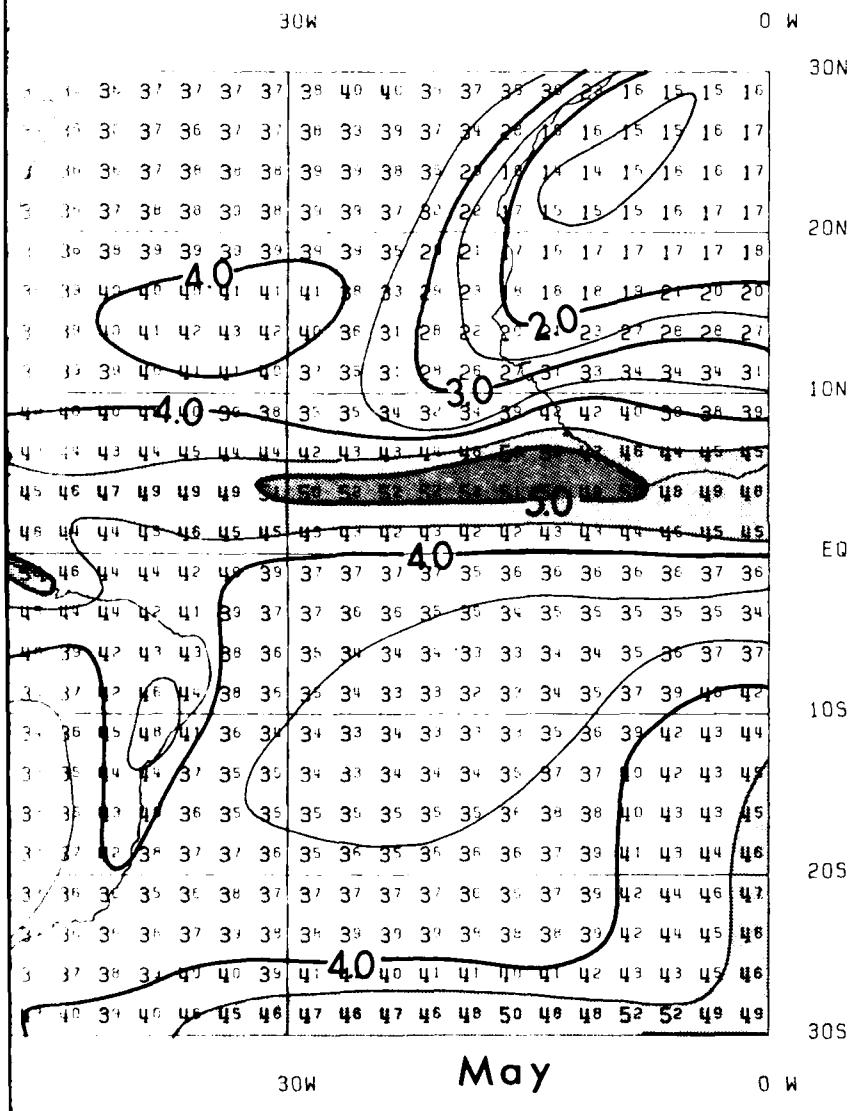
30W
0 W
30N
20N
10N
EQ
10S
20S
30S
4.0
2.0
3.0
4.0
5.0
4.0
4.0
30W
May
0 W

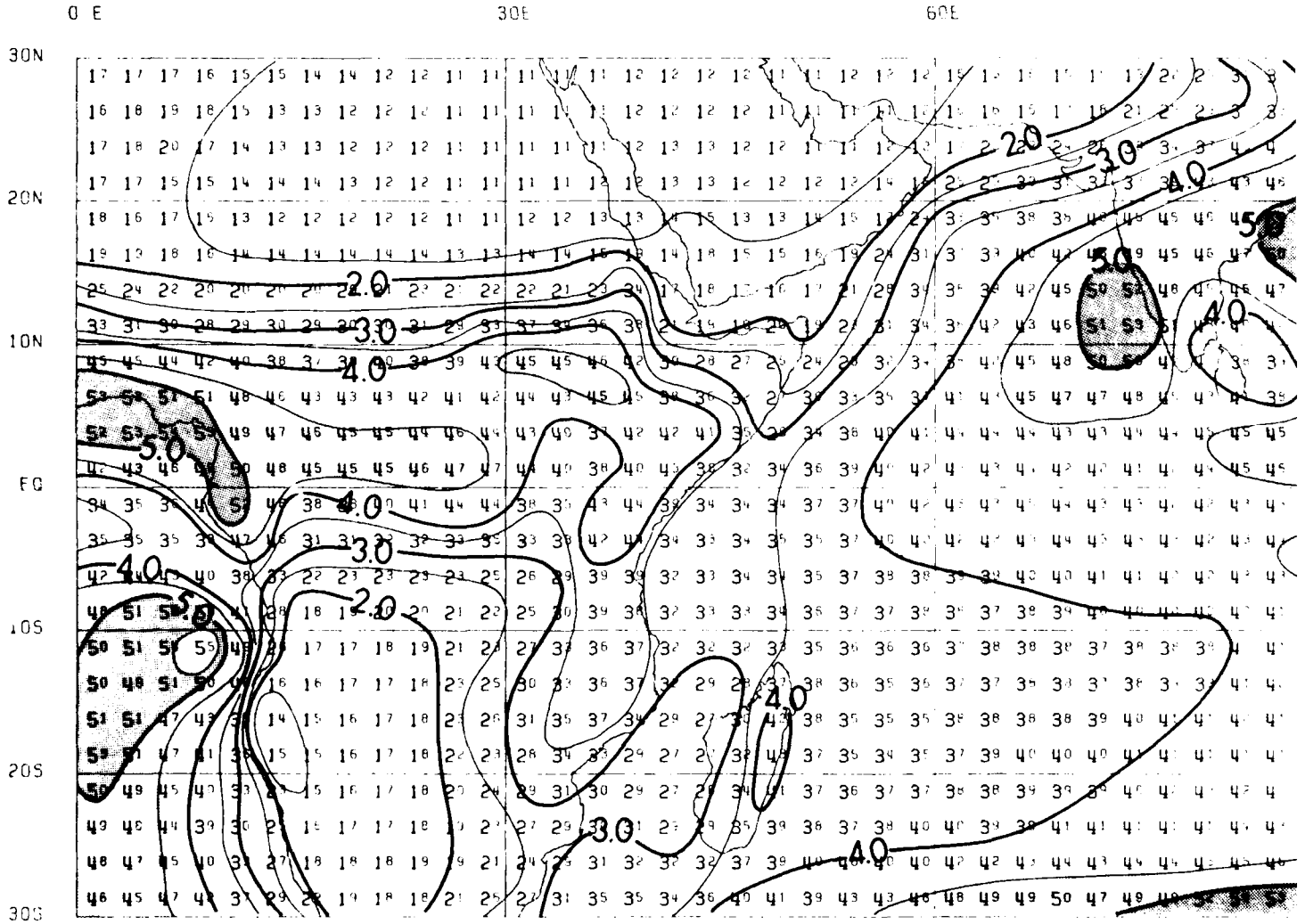

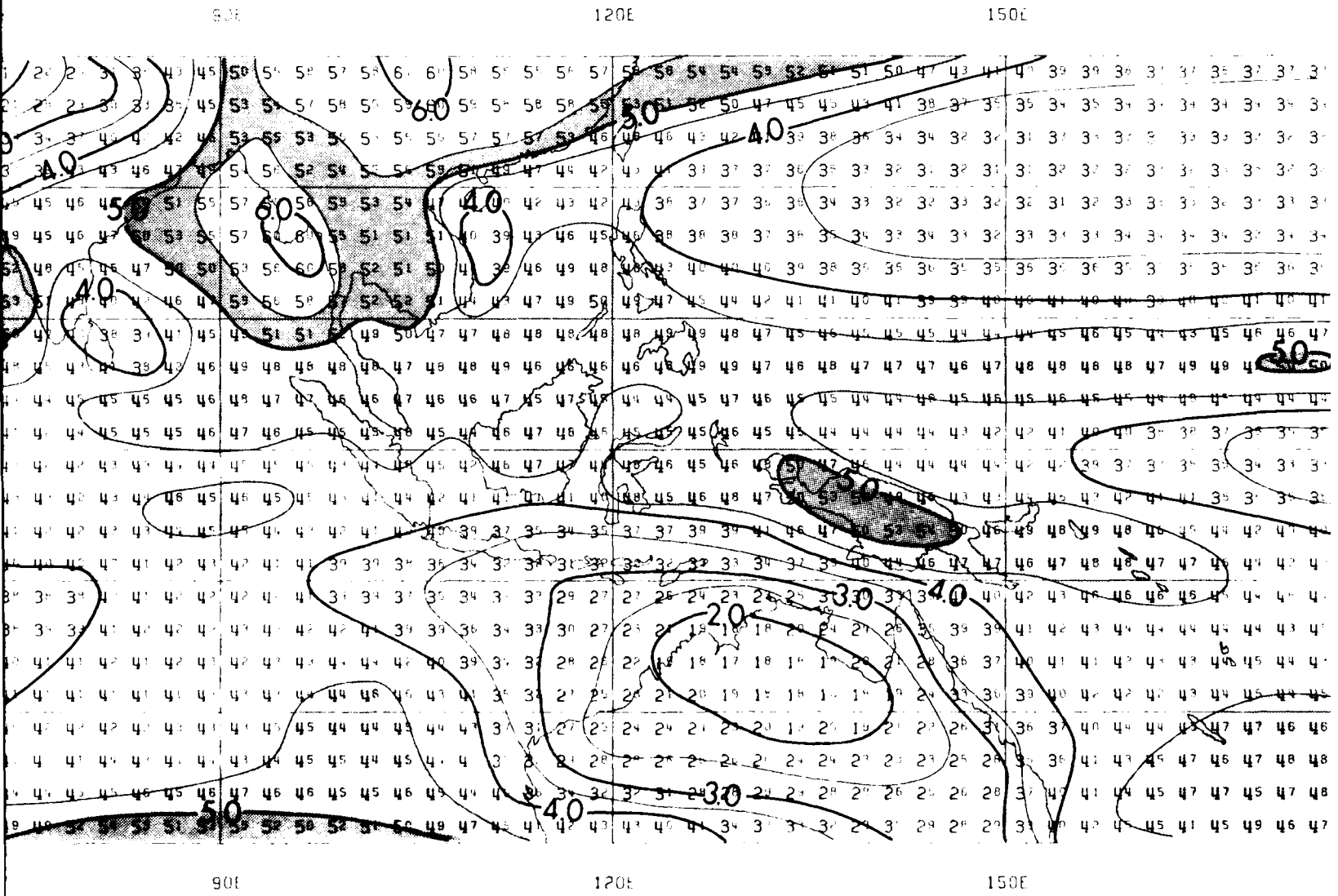
90E
120E
150E
6.0
5.0
4.0
3.0
2.0
5.0
4.0
3.0
2.0
90E
120E
150E

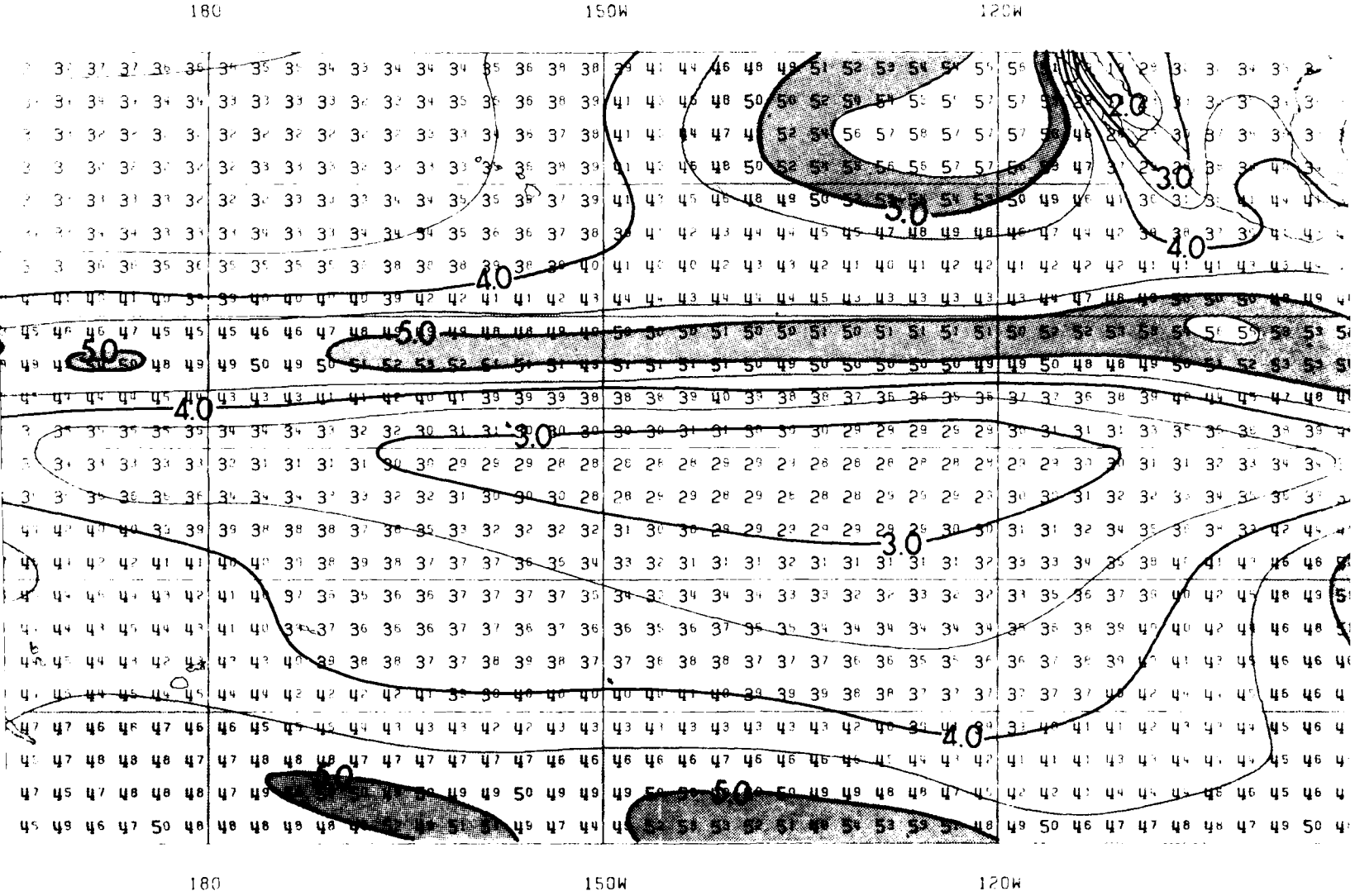
180
150W
120W
2.0
3.0
4.0
5.0
180
150W
120W

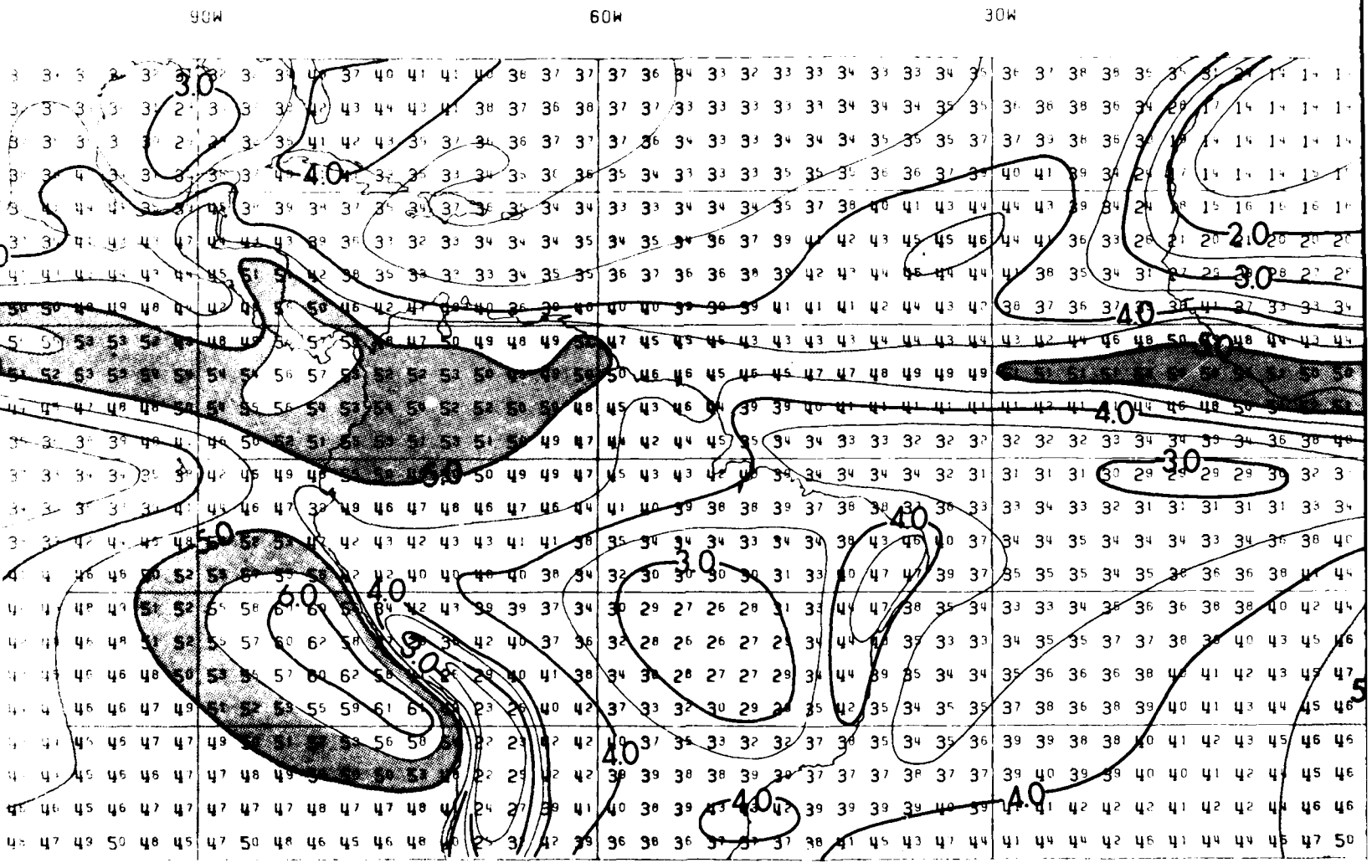

June

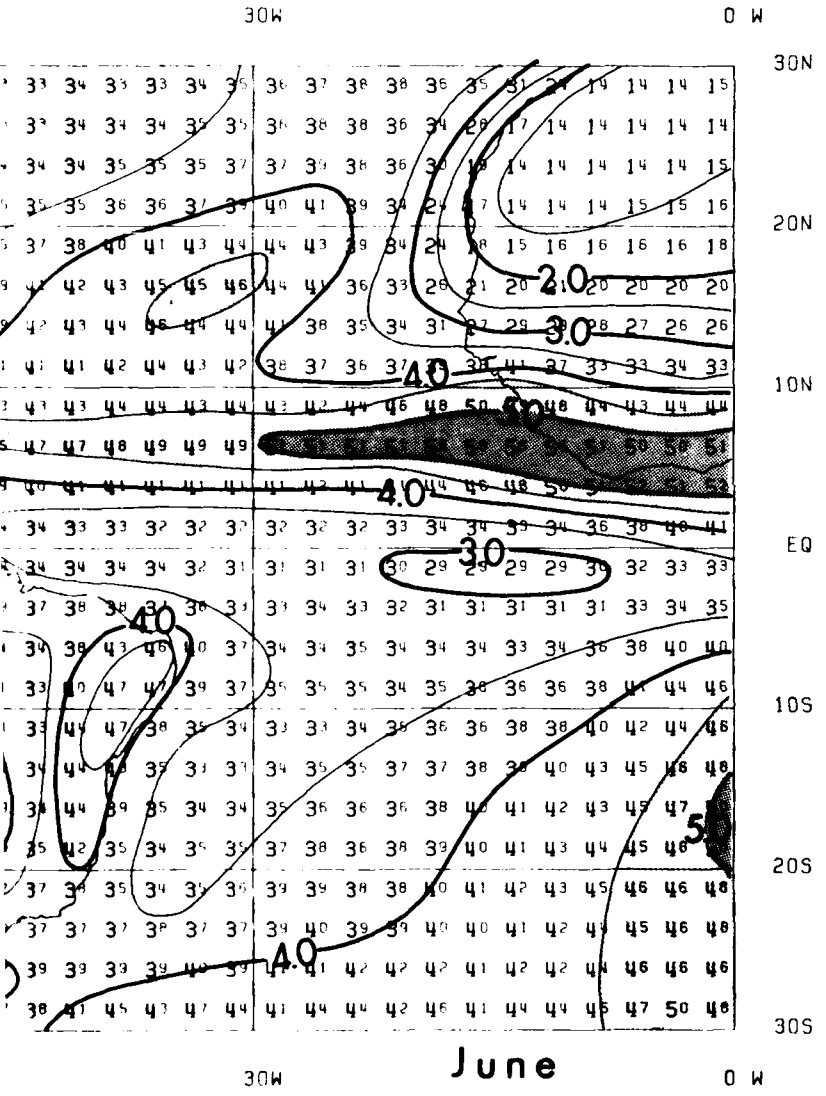
30W
0 W
30N
20N
10N
EQ
10S
20S
30S
2.0
3.0
4.0
5.0
June

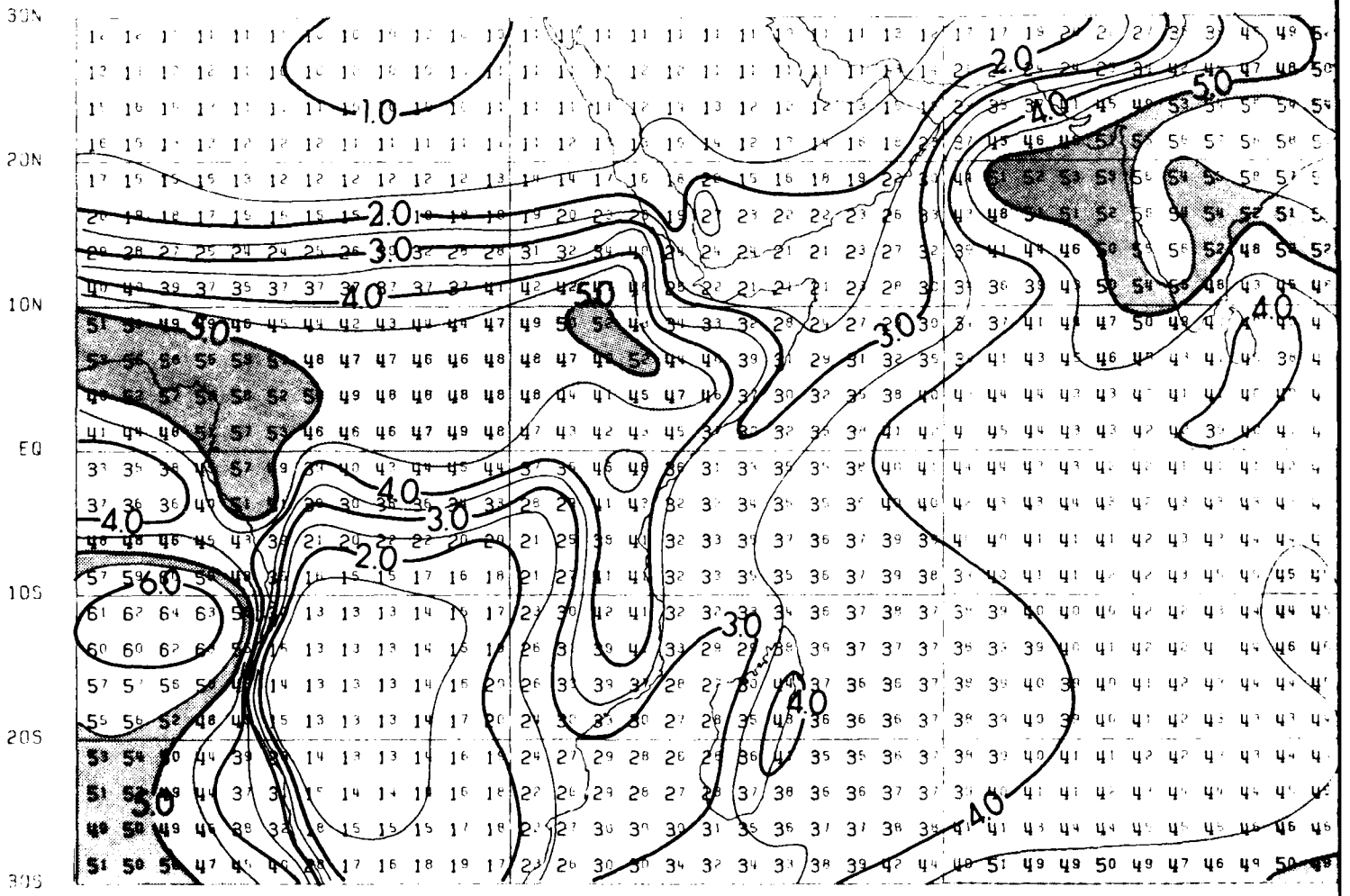

PRECEDING PAGE BLANK-NOT FILMED

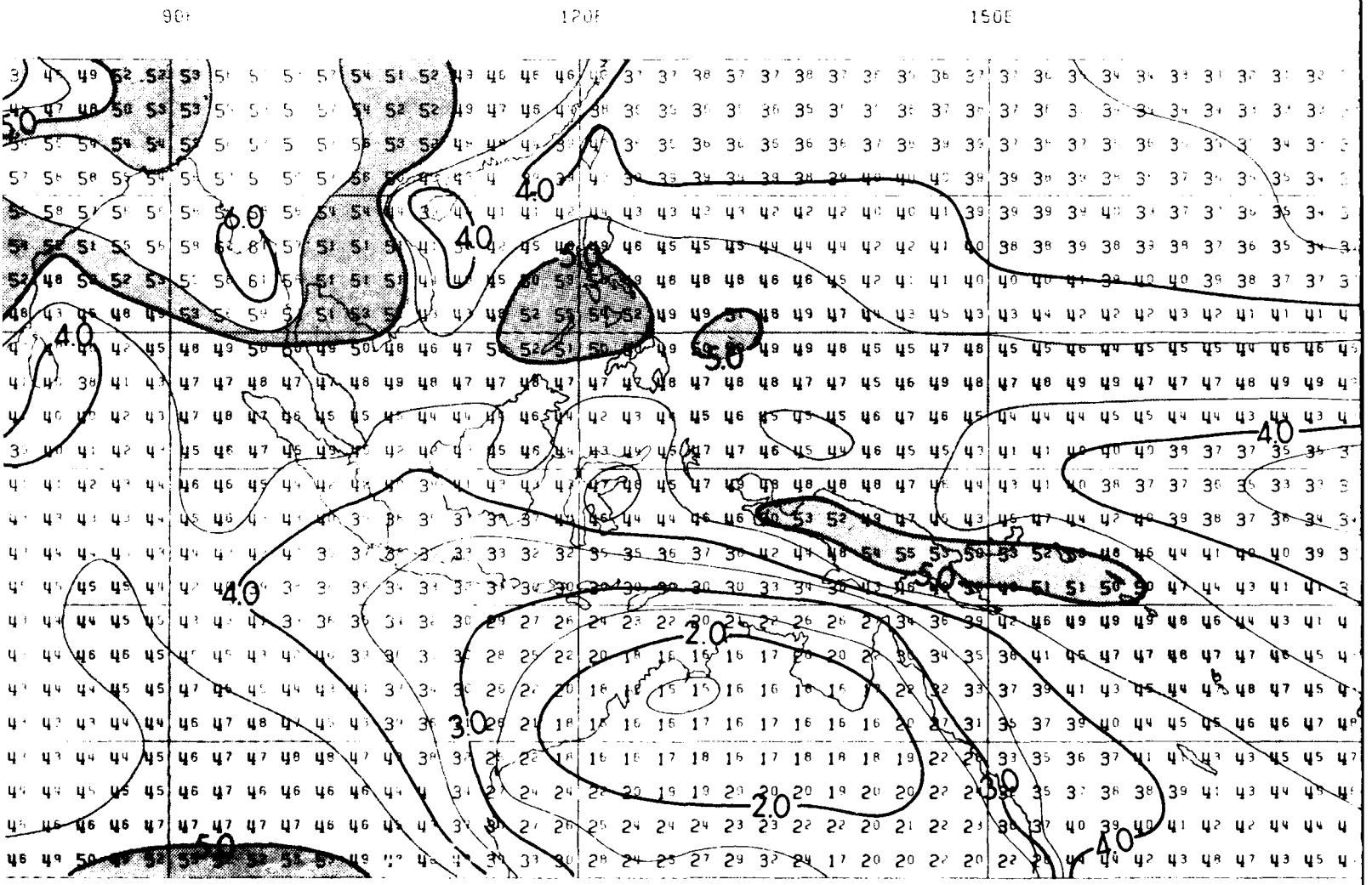
90E
120E
150E
5.0
4.0
3.0
2.0
90E
120E
150E

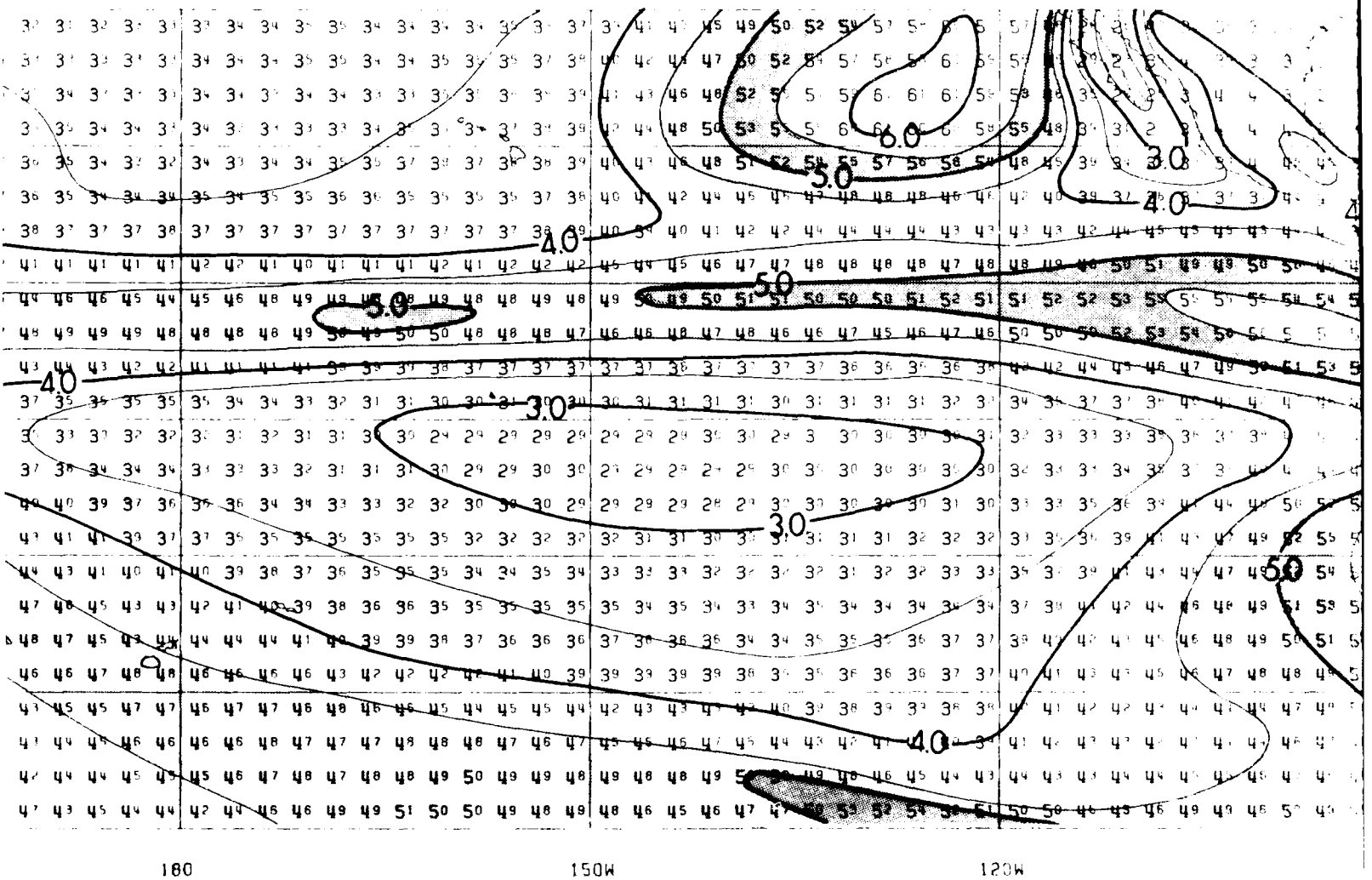
180
150W
120W
6.0
5.0
4.0
3.0
5.0
4.0
3.0
4.0
5.0
180
150W
120W

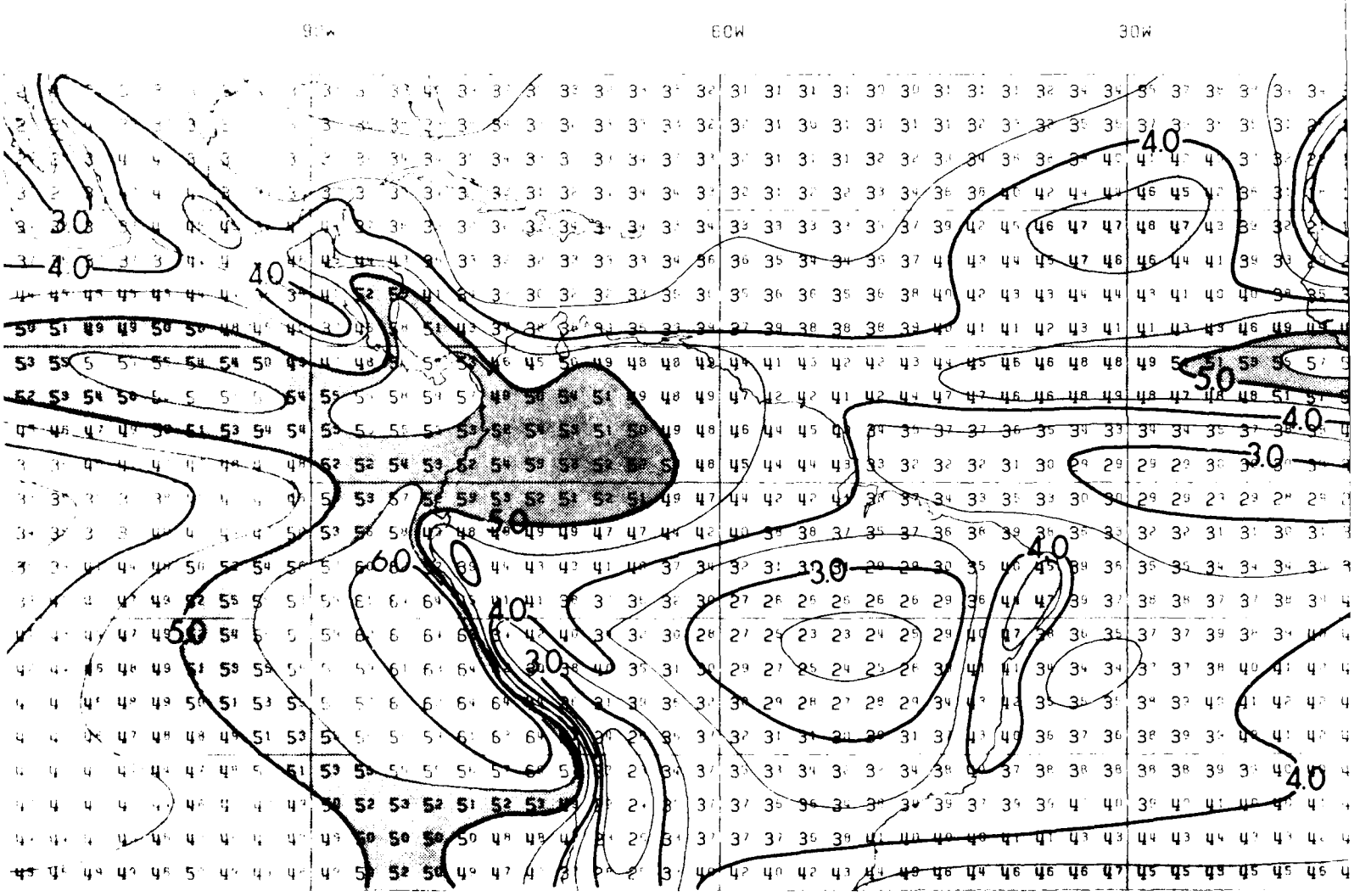
90W
60W
30W
3.0
4.0
5.0
6.0
Jul

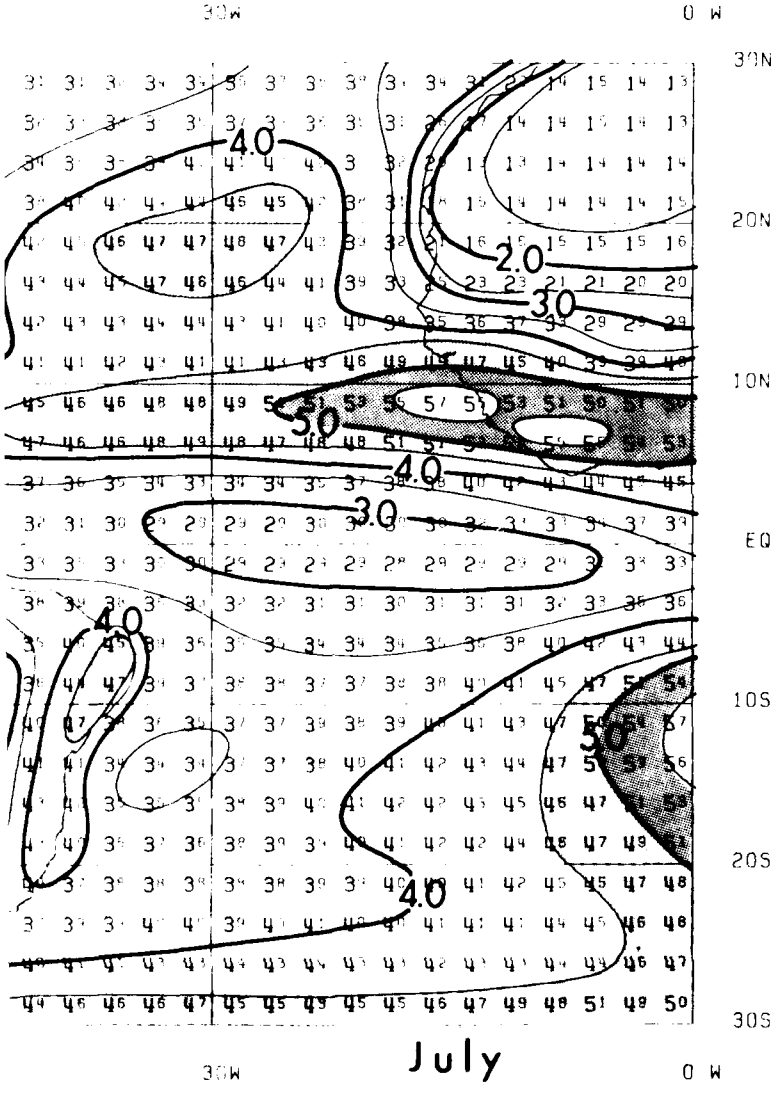
30W
0 W
30N
20N
10N
EQ
10S
20S
30S
2.0
3.0
4.0
5.0
July

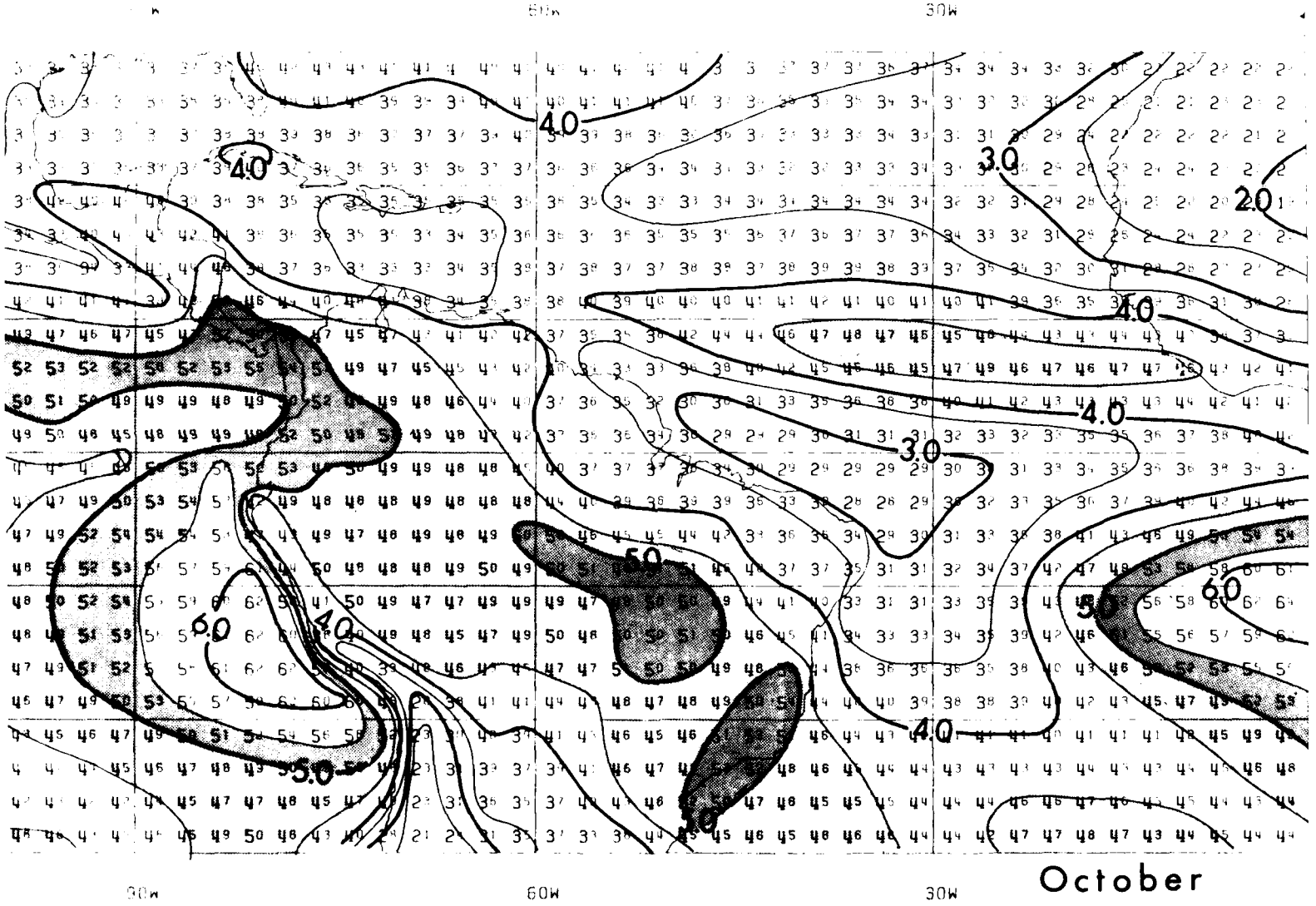

October

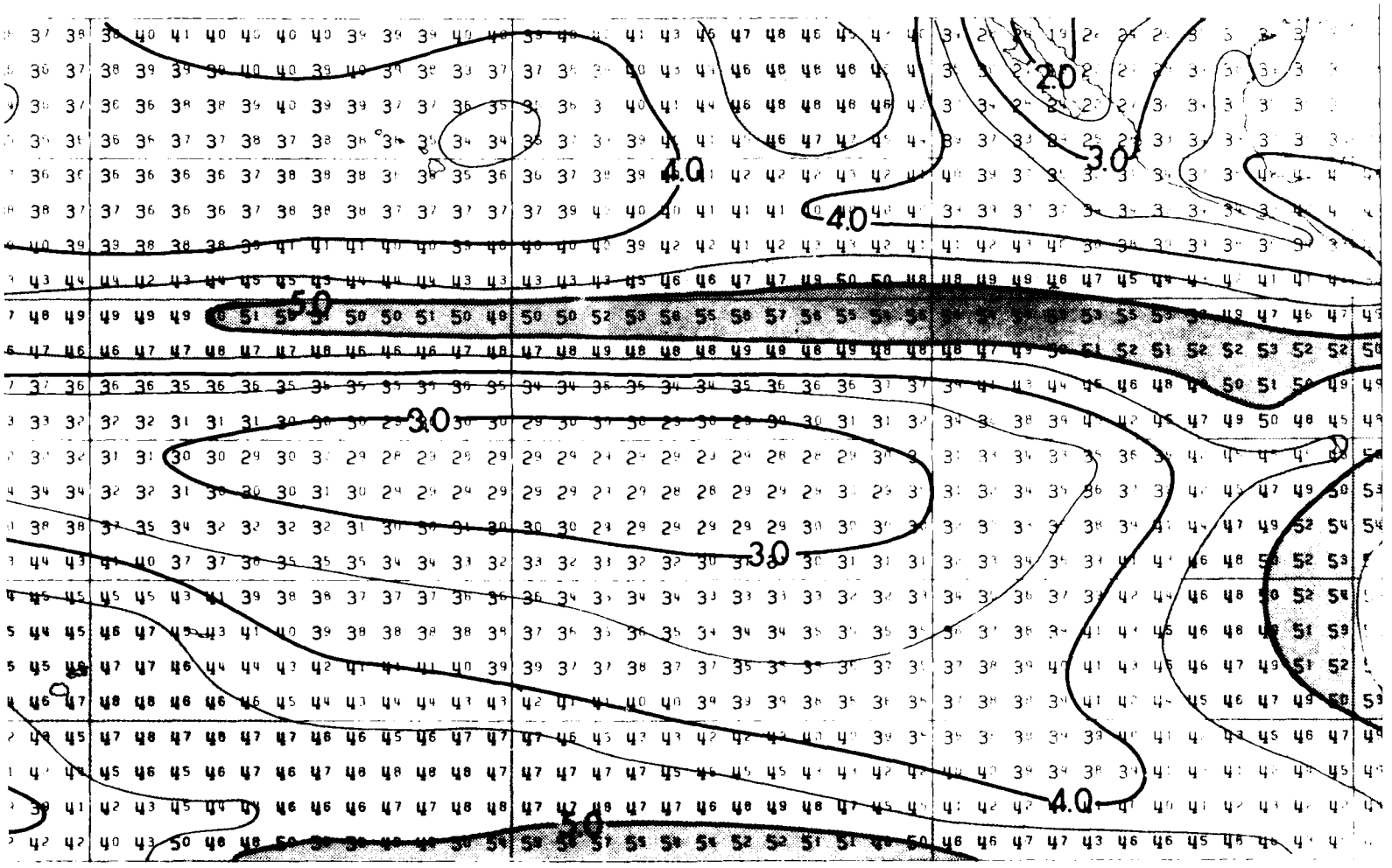
180
150W
120W
2.0
3.0
4.0
5.0
3.0
3.0
4.0
3.0
180
150W
120W

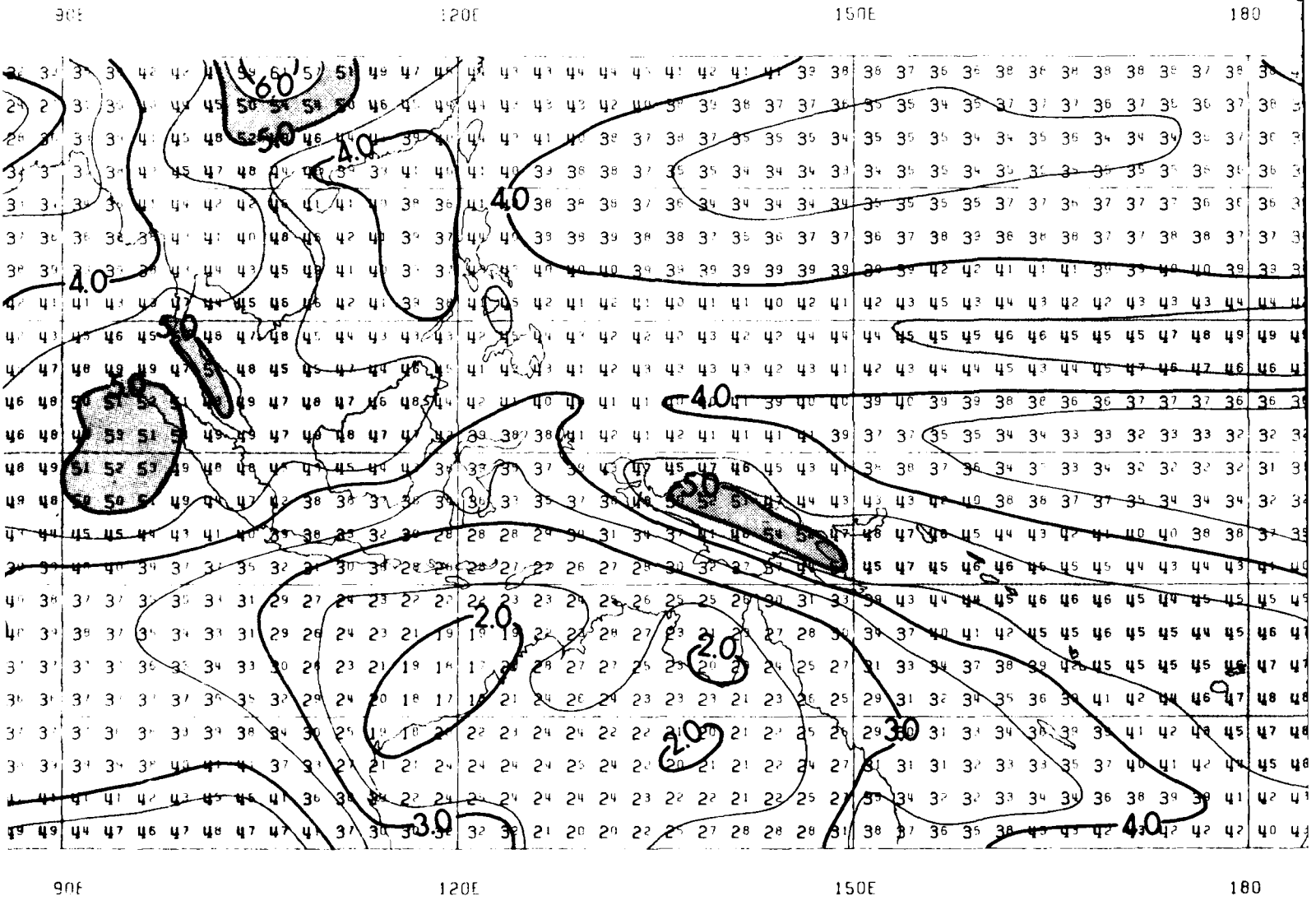
90E
120E
150E
180
6.0
5.0
4.0
4.0
4.0
5.0
4.0
5.0
2.0
2.0
3.0
3.0
4.0
90E
120E
150E
180

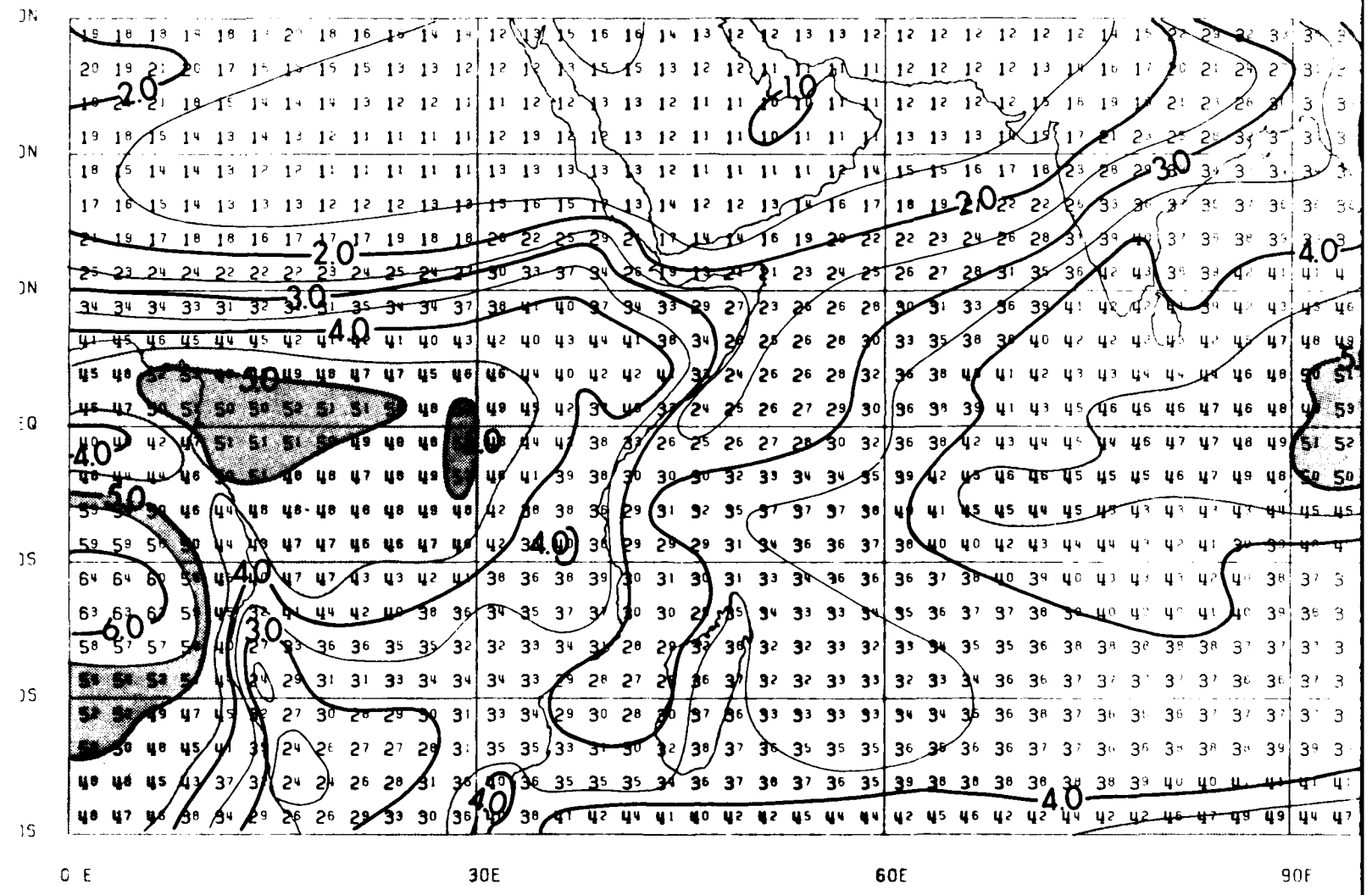

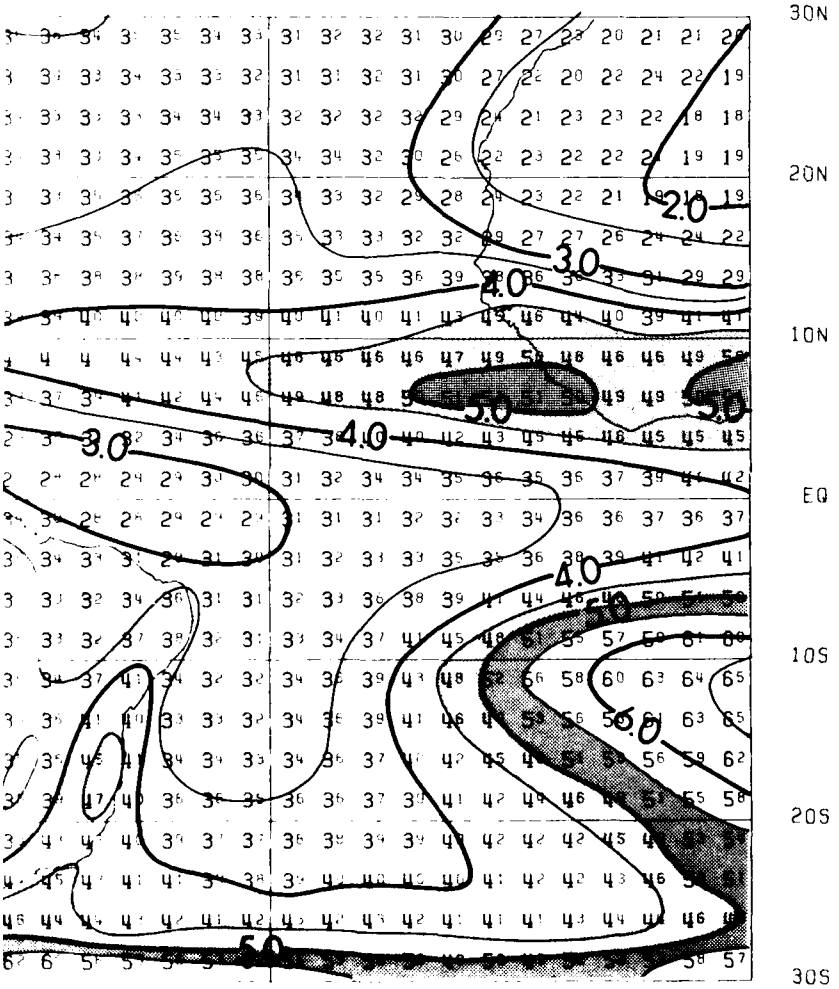

September

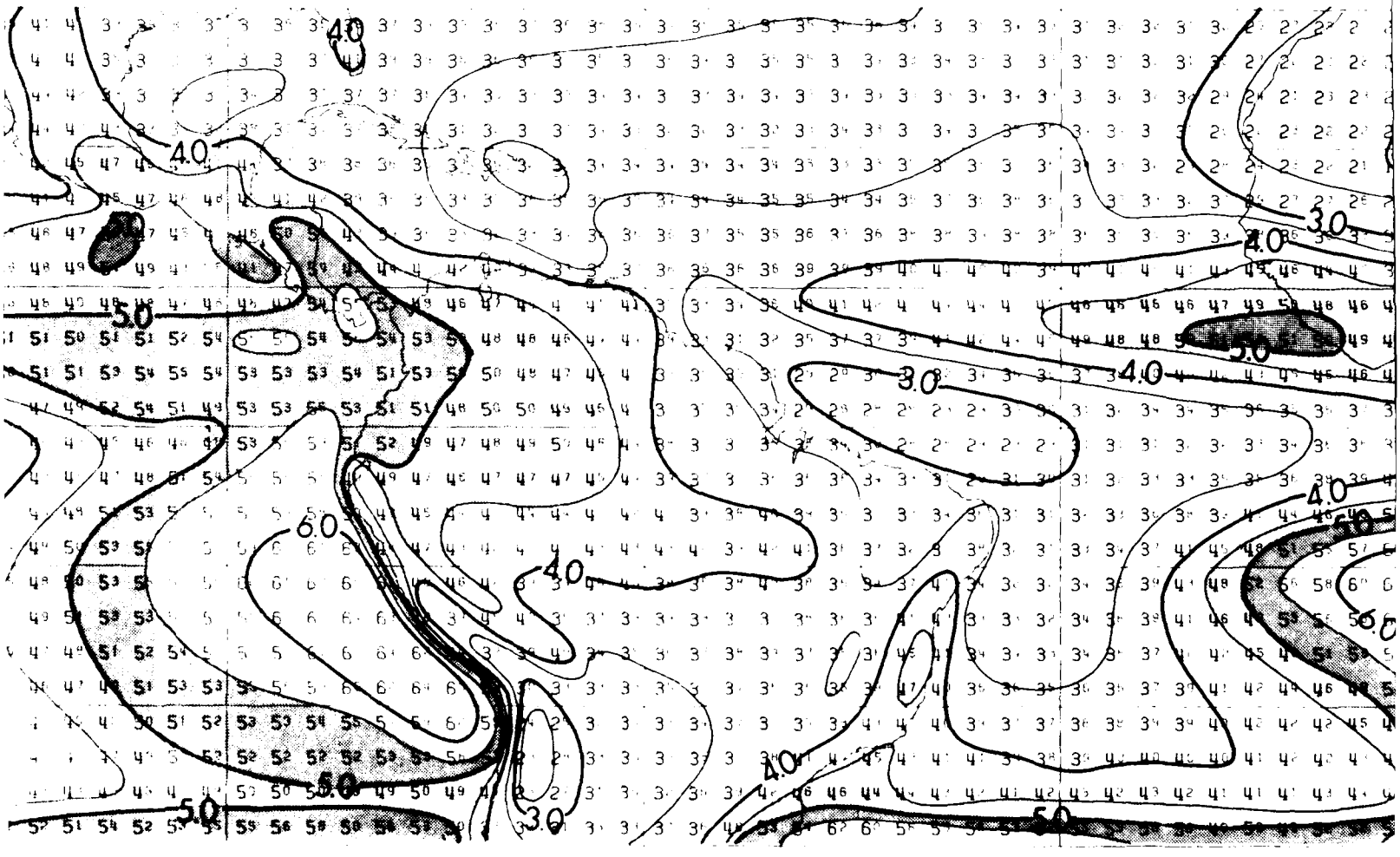

September

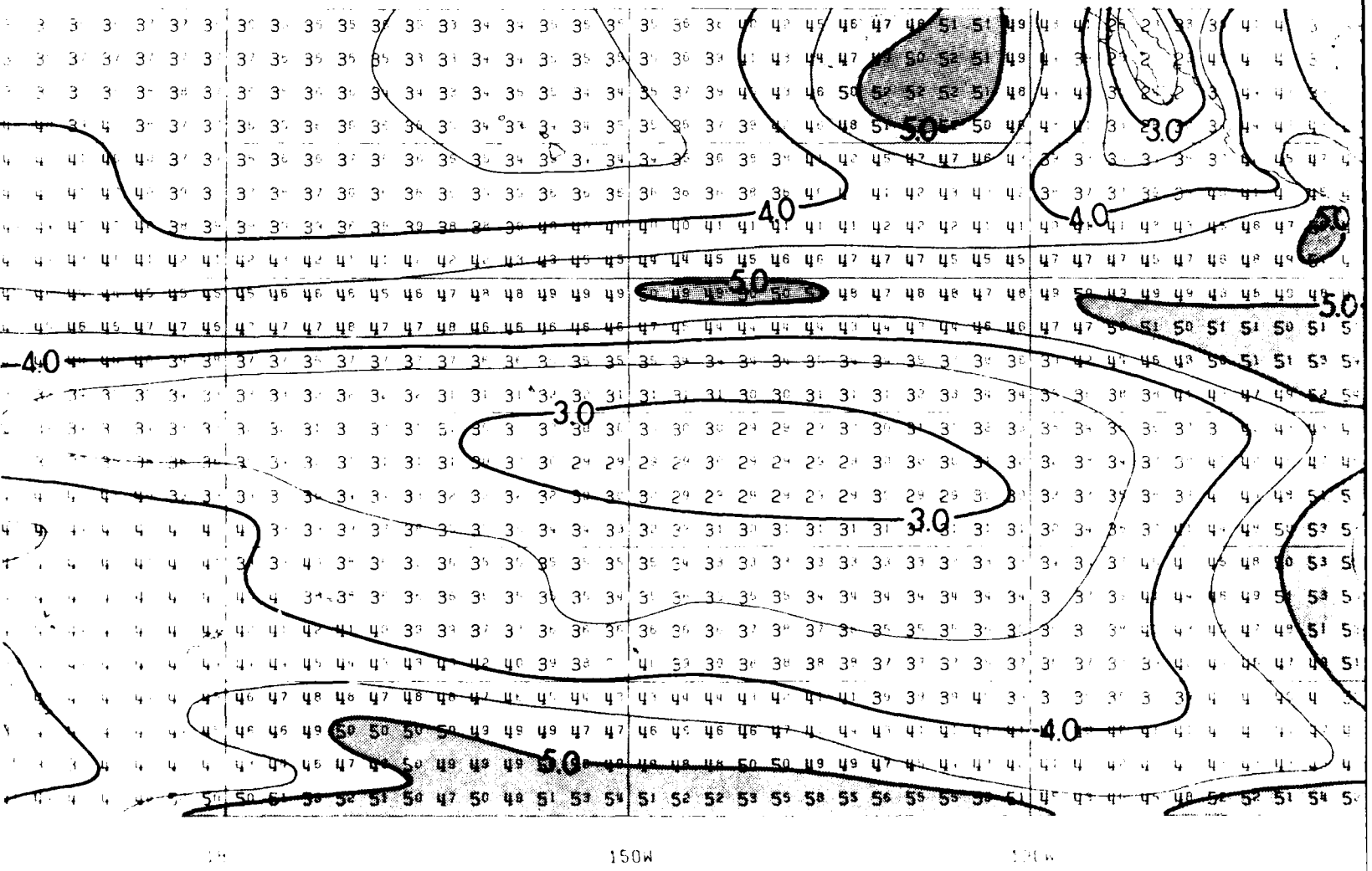
180
150W
120W
3.0
4.0
5.0
3.0
4.0
5.0
3.0
4.0
5.0
150W

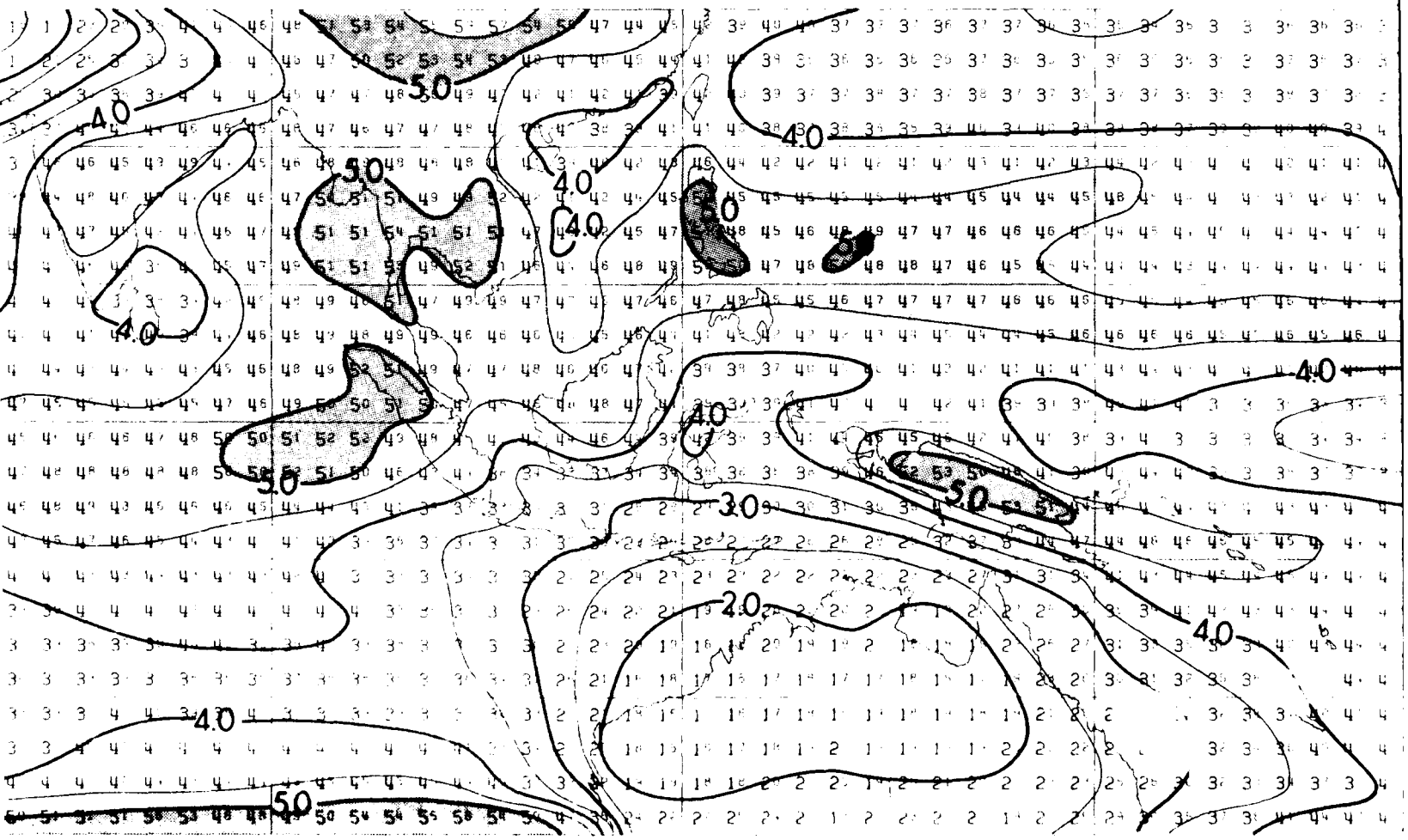
120E
150E
5.0
4.0
3.0
2.0

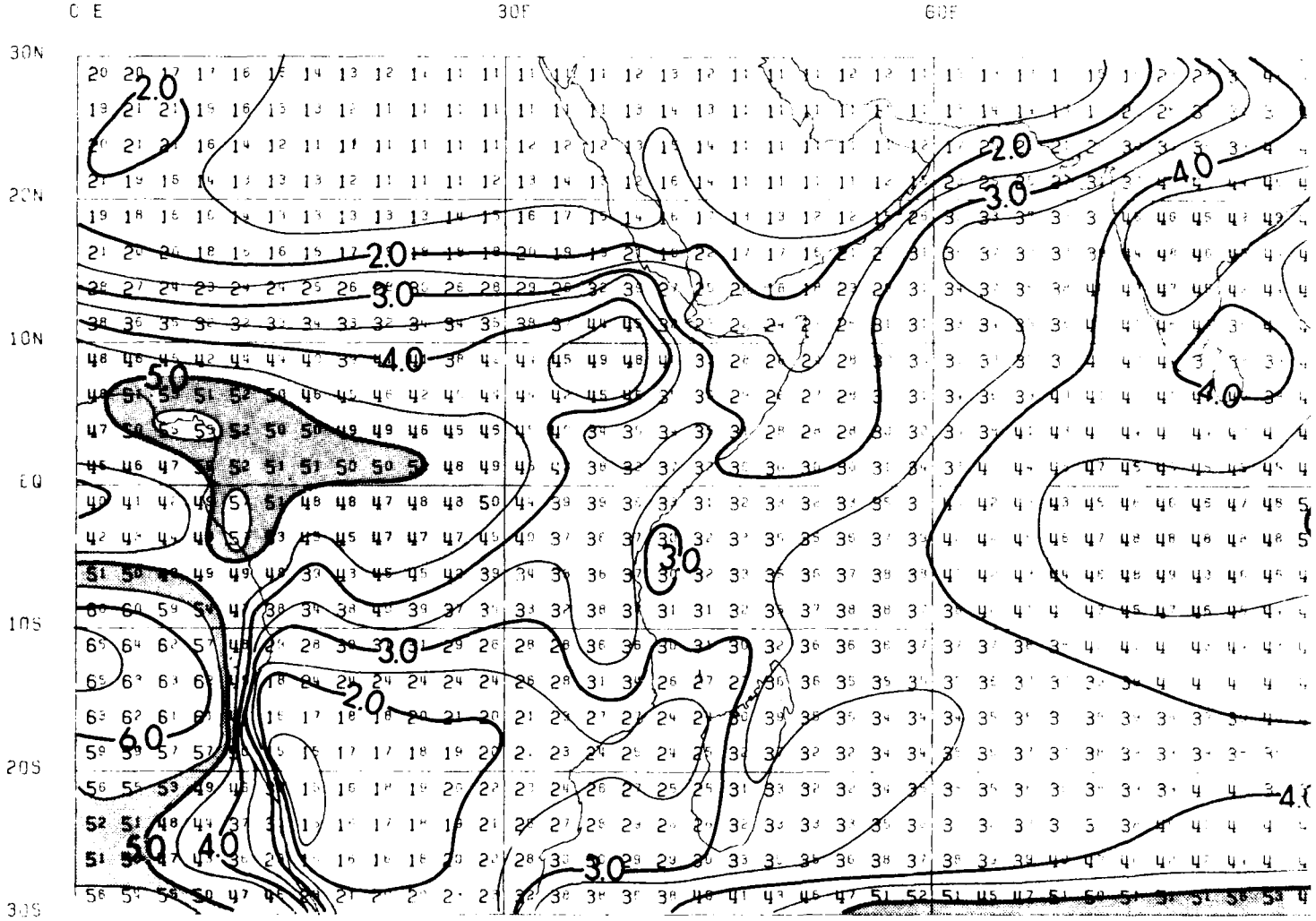

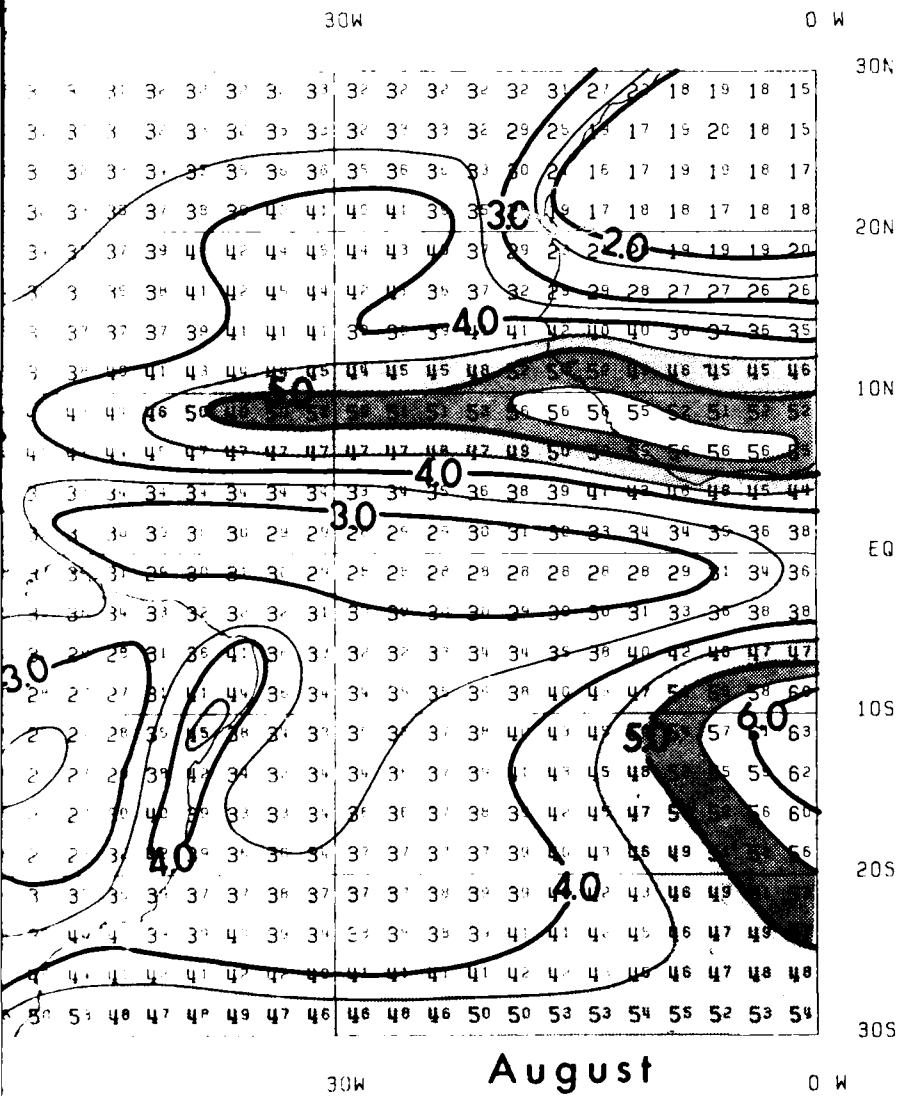
30W
0 W
30N
20N
10N
EQ
10S
20S
30S
2.0
3.0
4.0
5.0
6.0
August

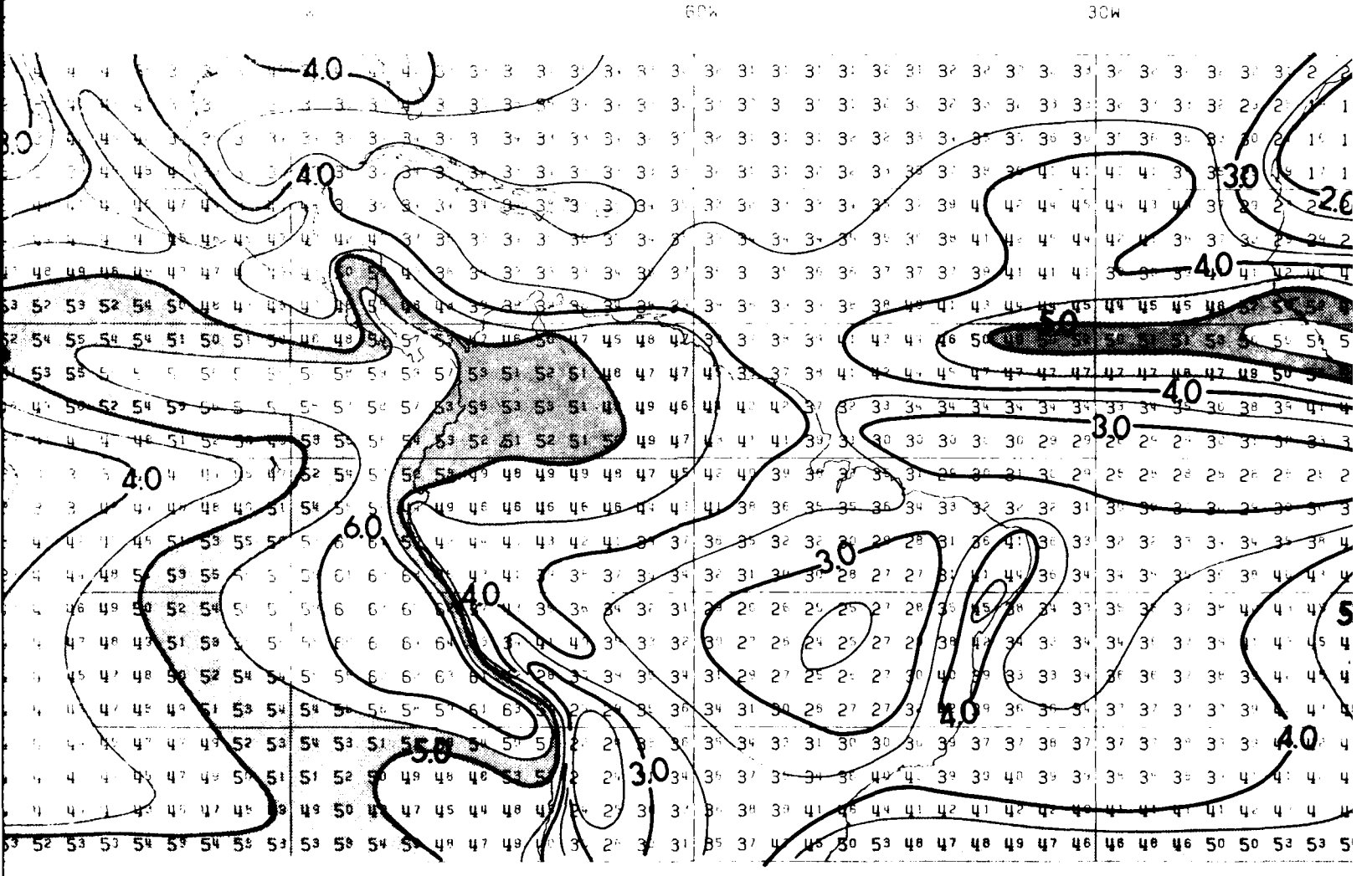

August

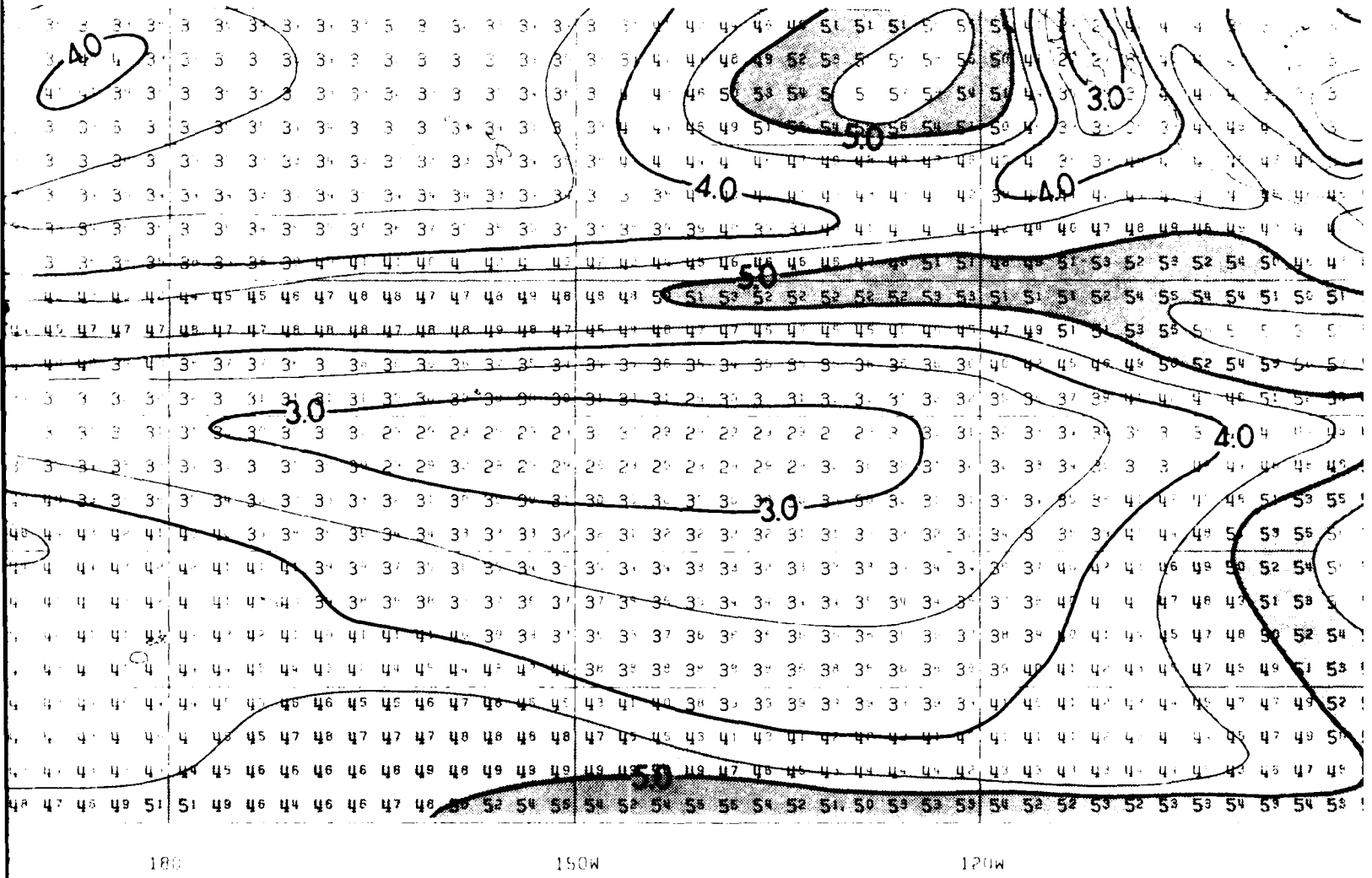

180 150W 120W

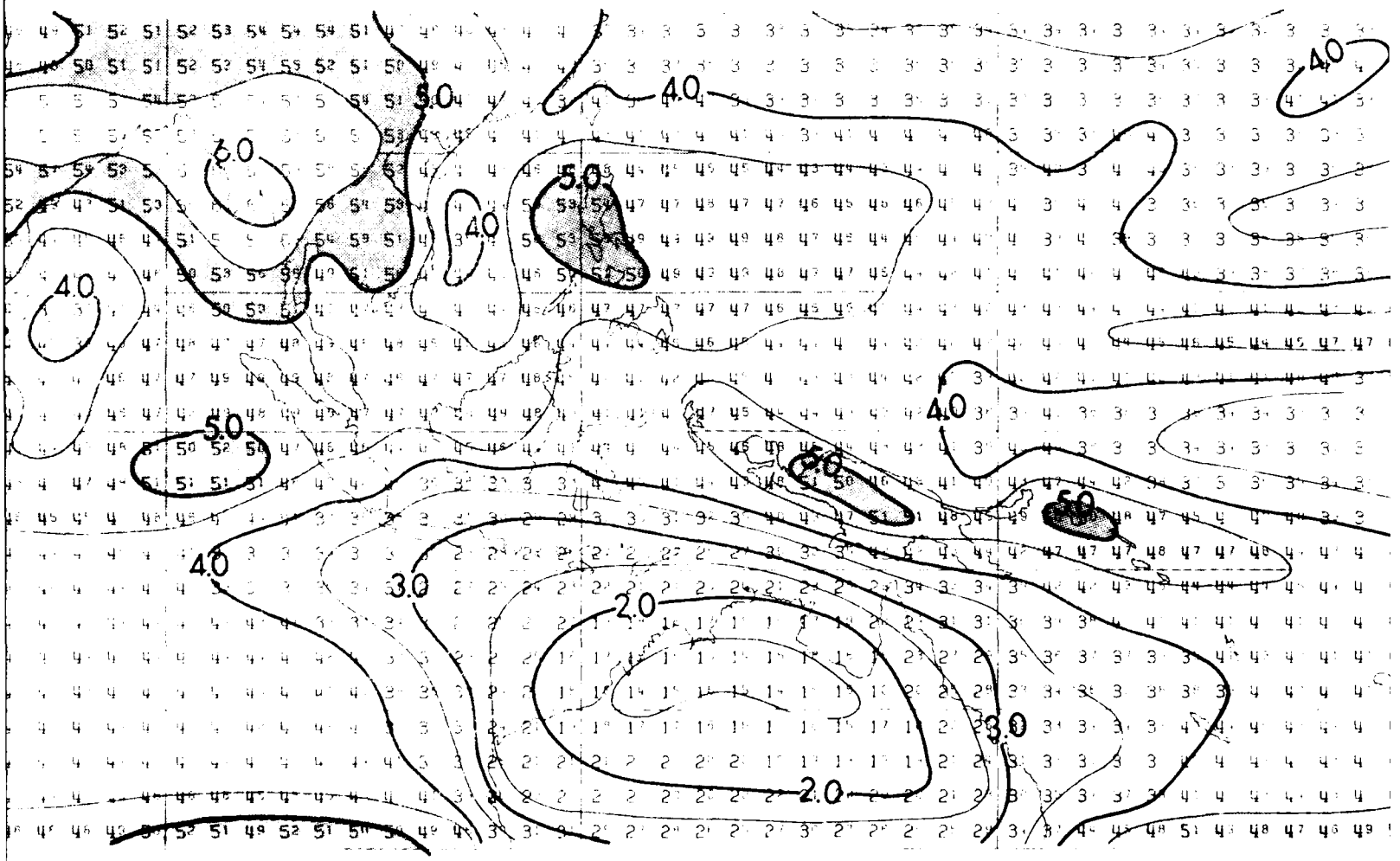
5.0
4.0
5.0
4.0
4.0
5.0
4.0
5.0
4.0
3.0
2.0
3.0
2.0

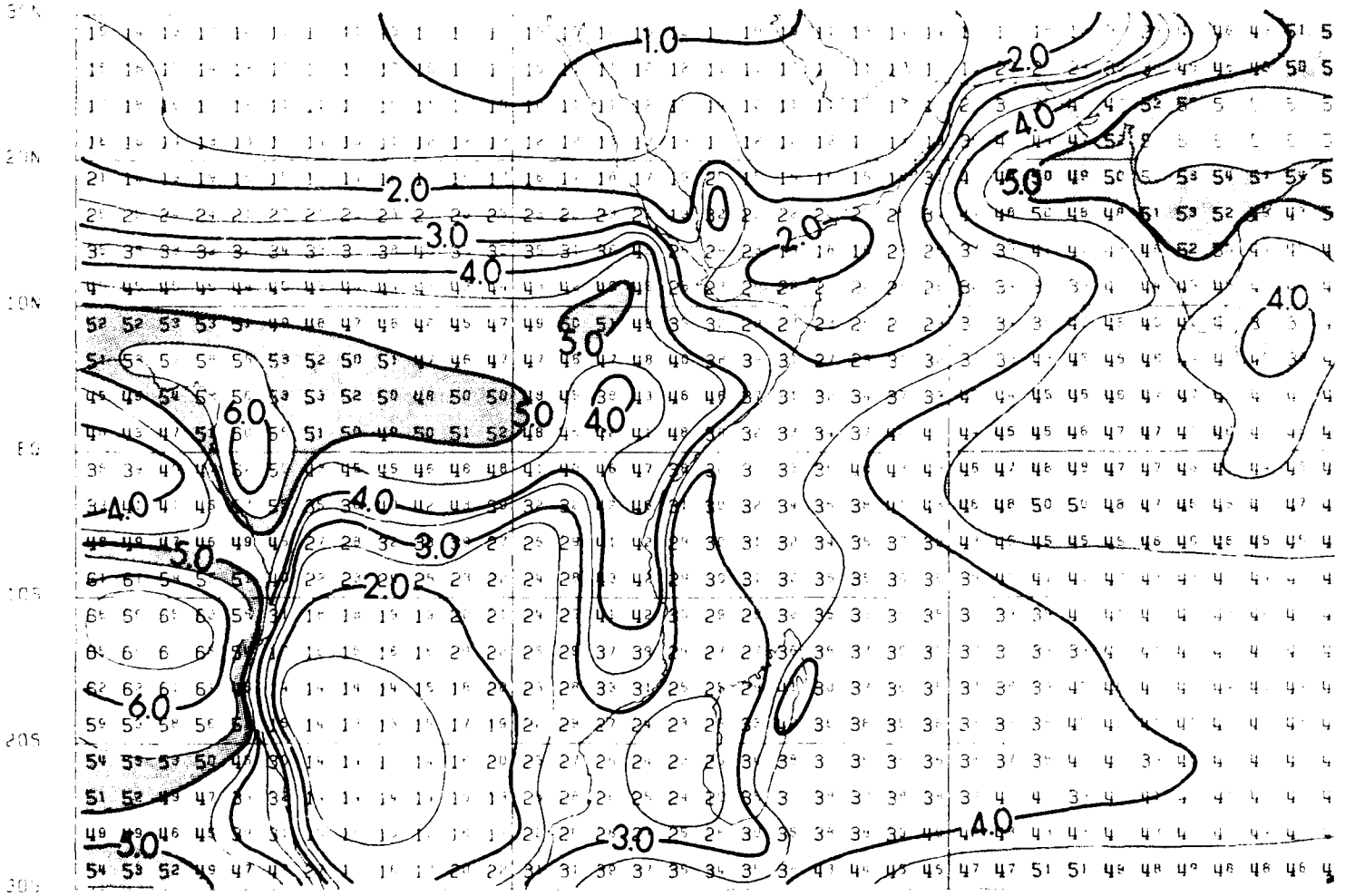

PRECEDING PAGE BLANK-NOT FILMED

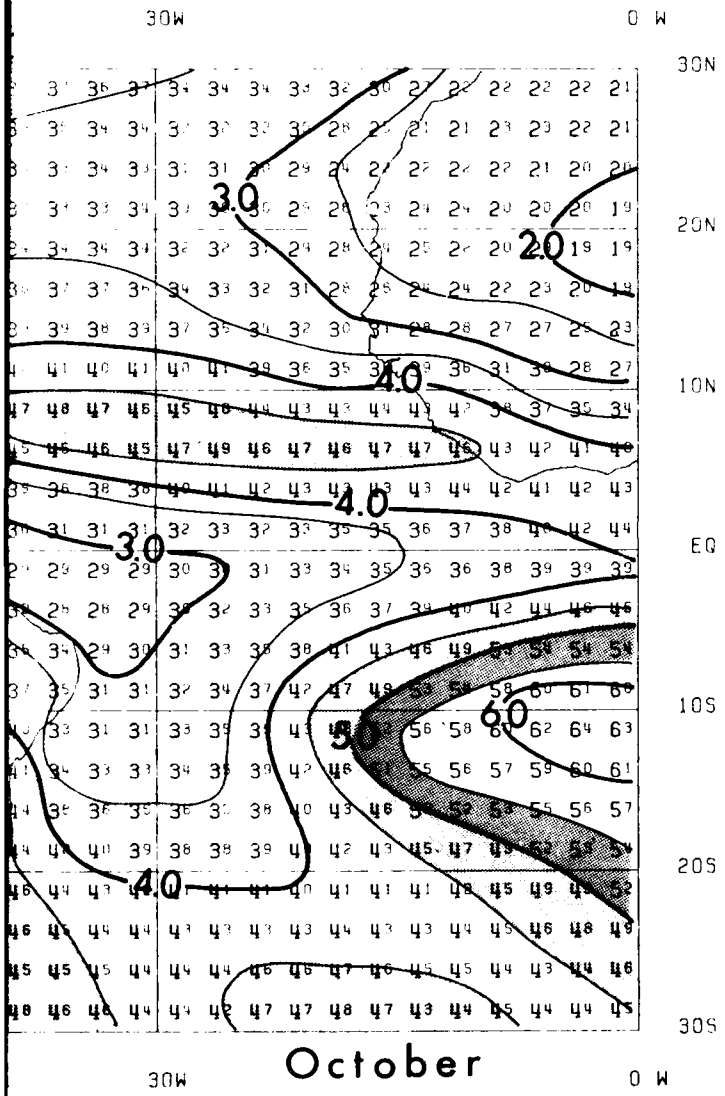
30W
0 W
30N
20N
10N
EQ
10S
20S
30S
3.0
4.0
2.0
5.0
6.0
October

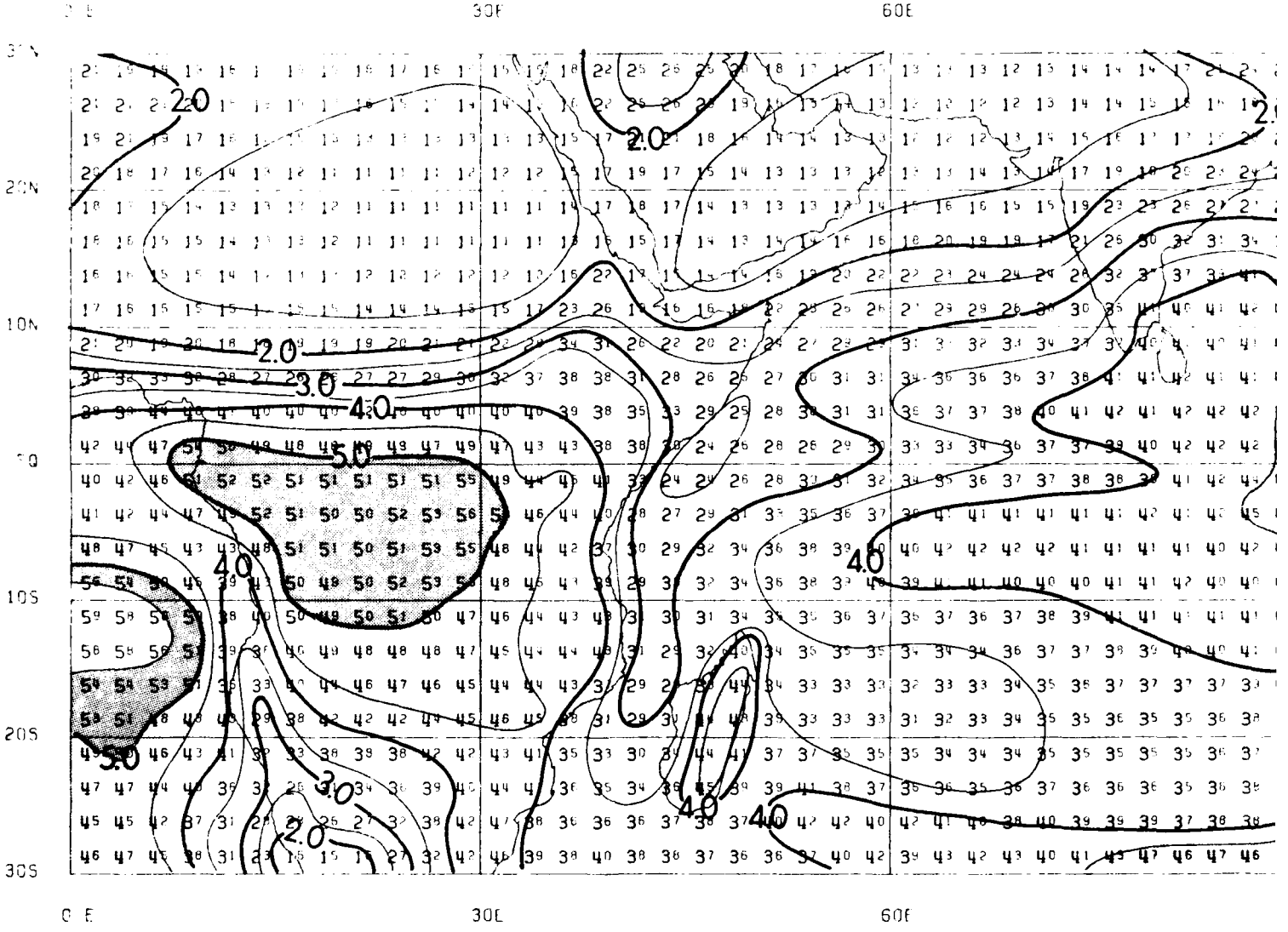

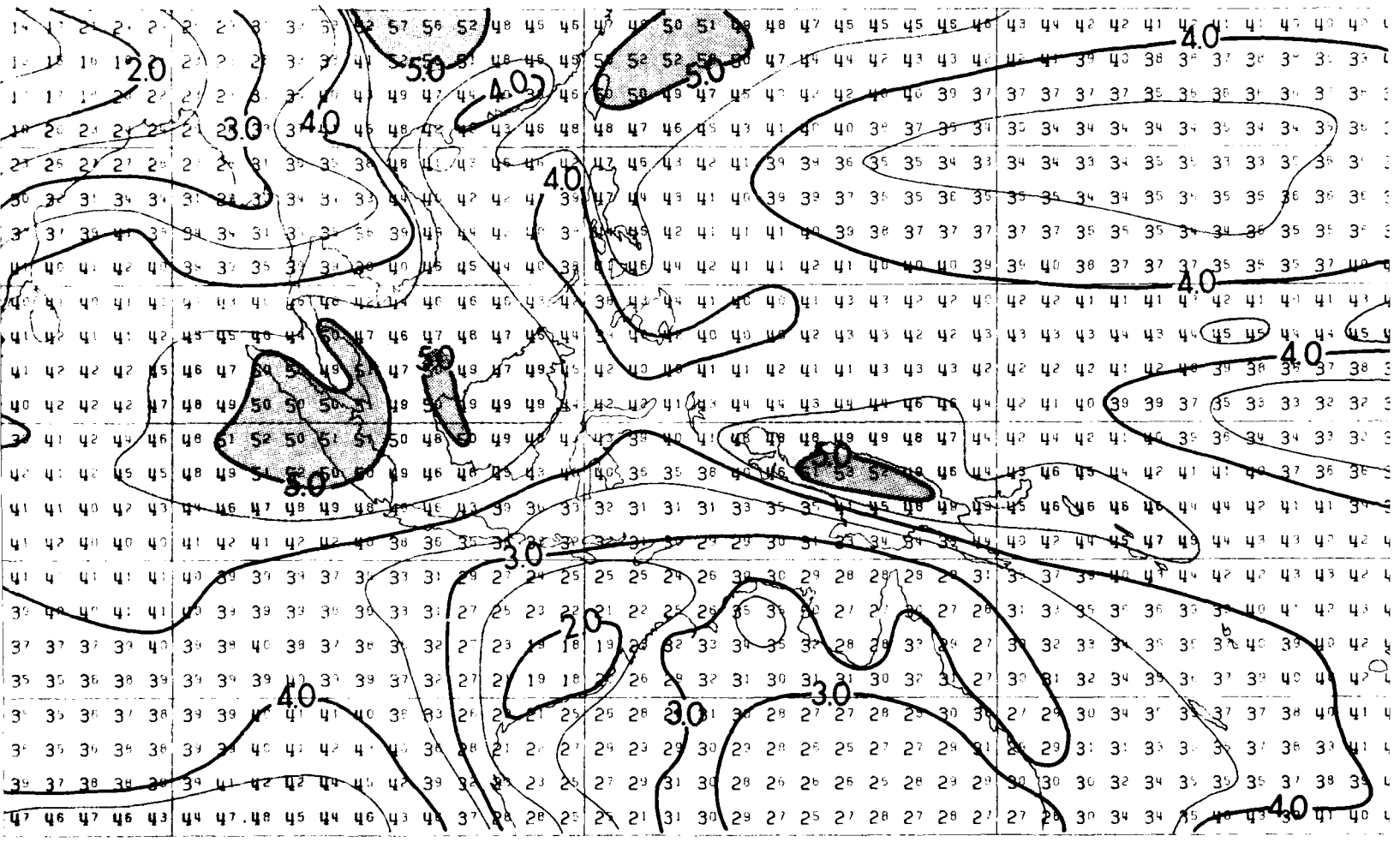
90E
120E
150E
2.0
3.0
4.0
5.0

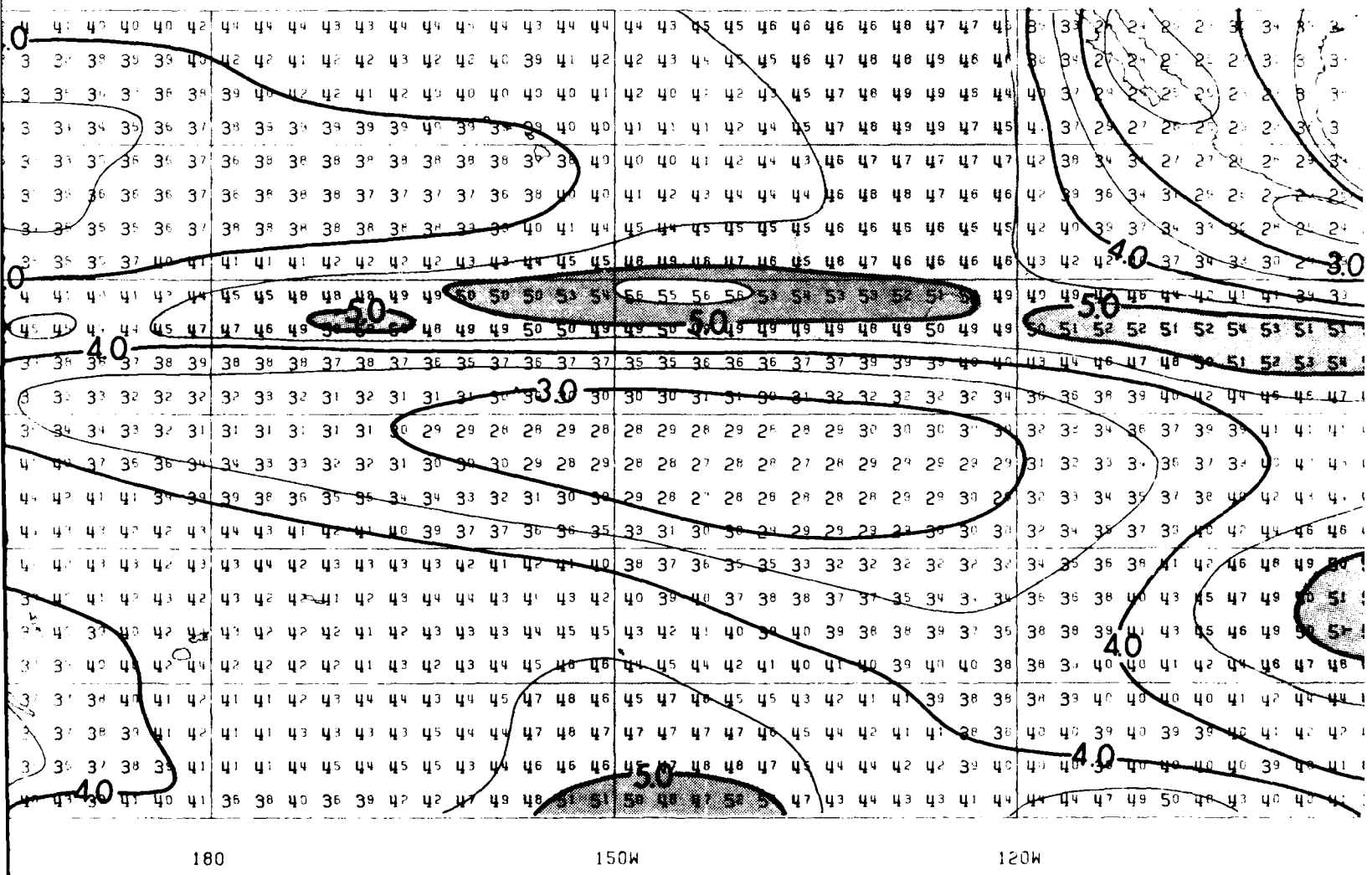
180
150W
120W
5.0
4.0
3.0
180
150W
120W

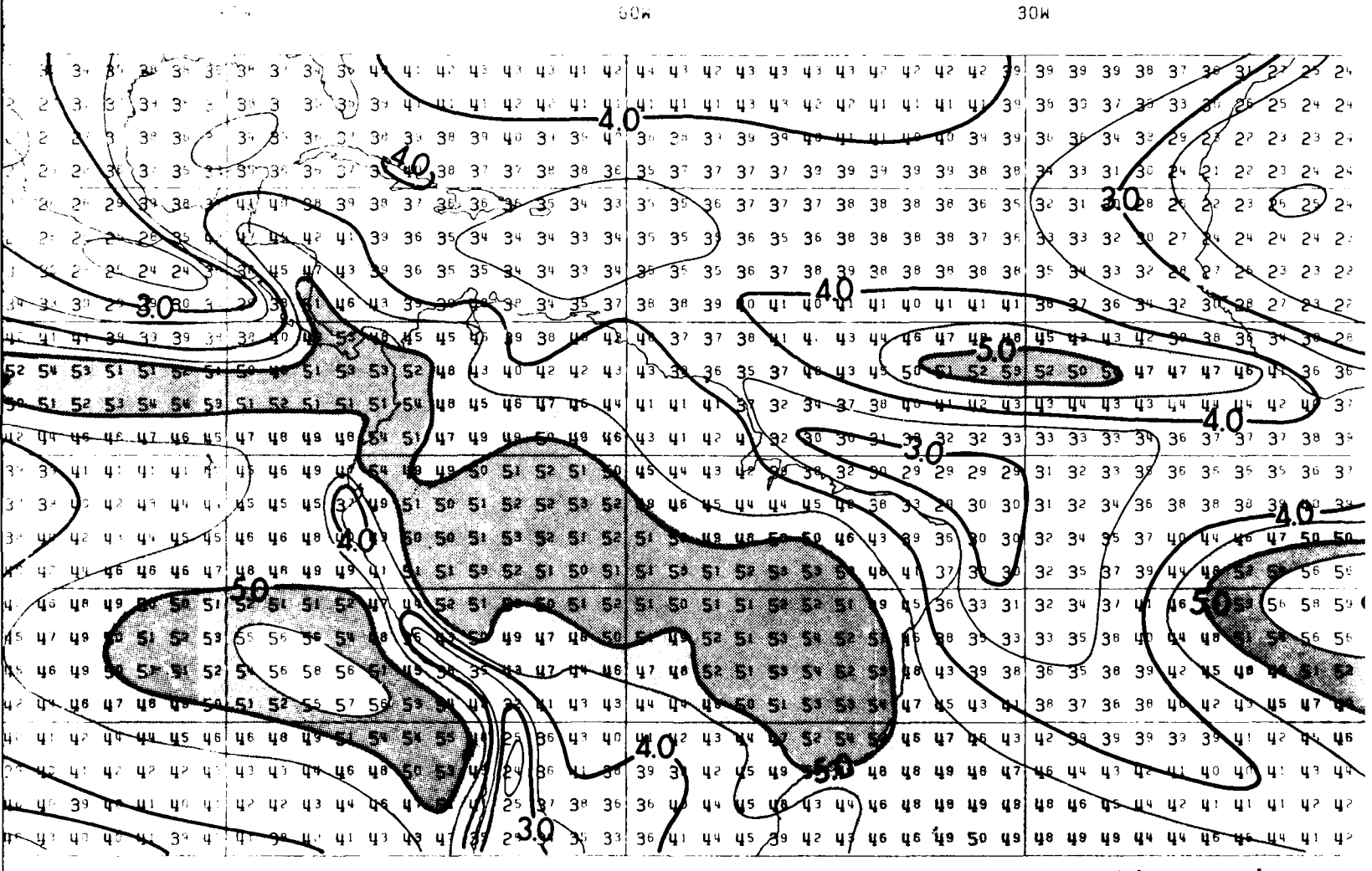

November

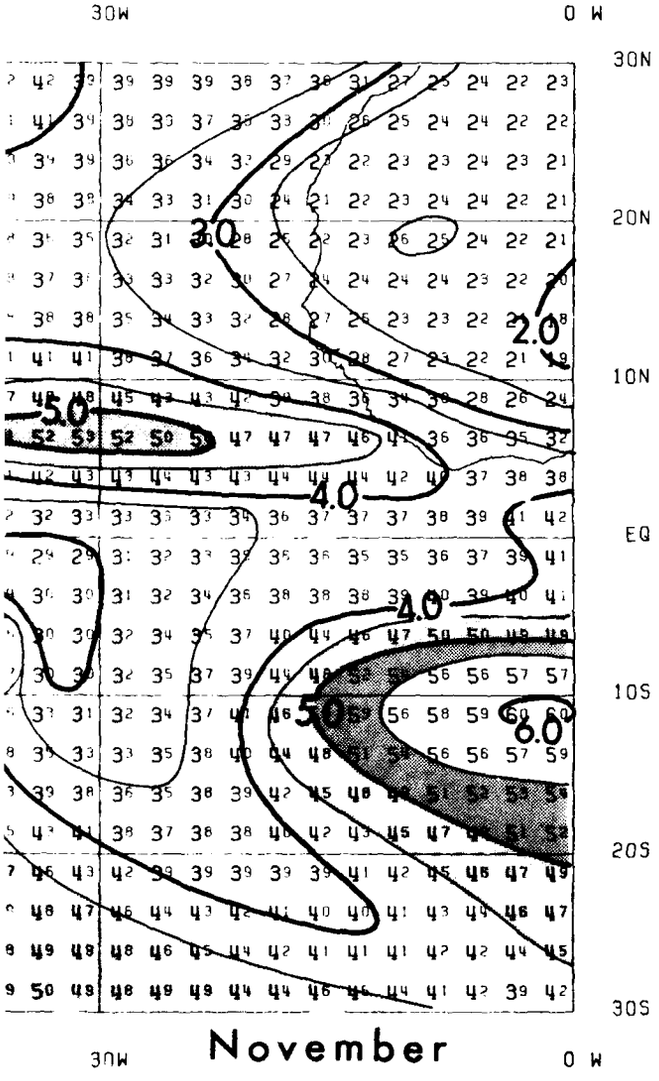

November

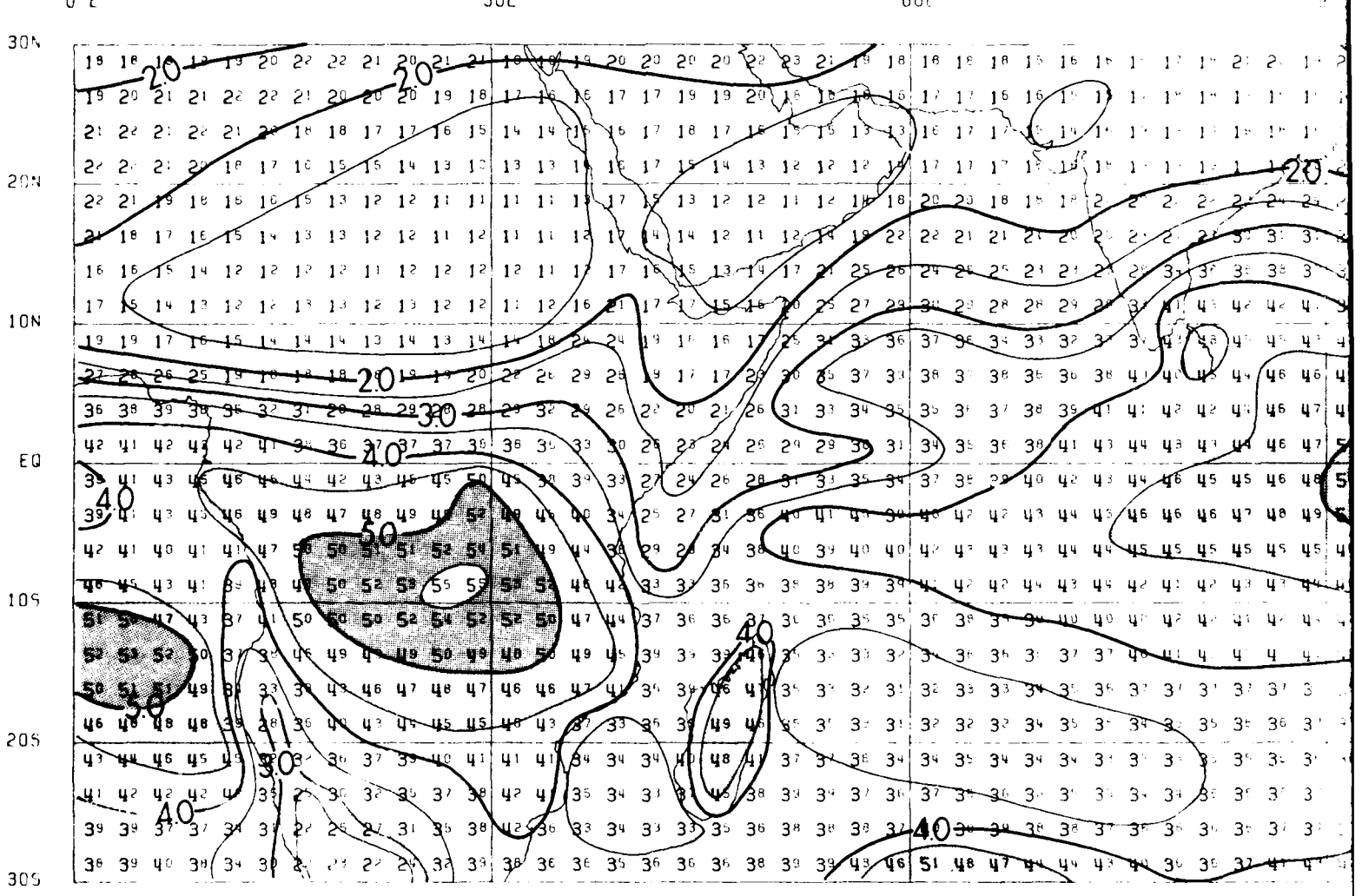

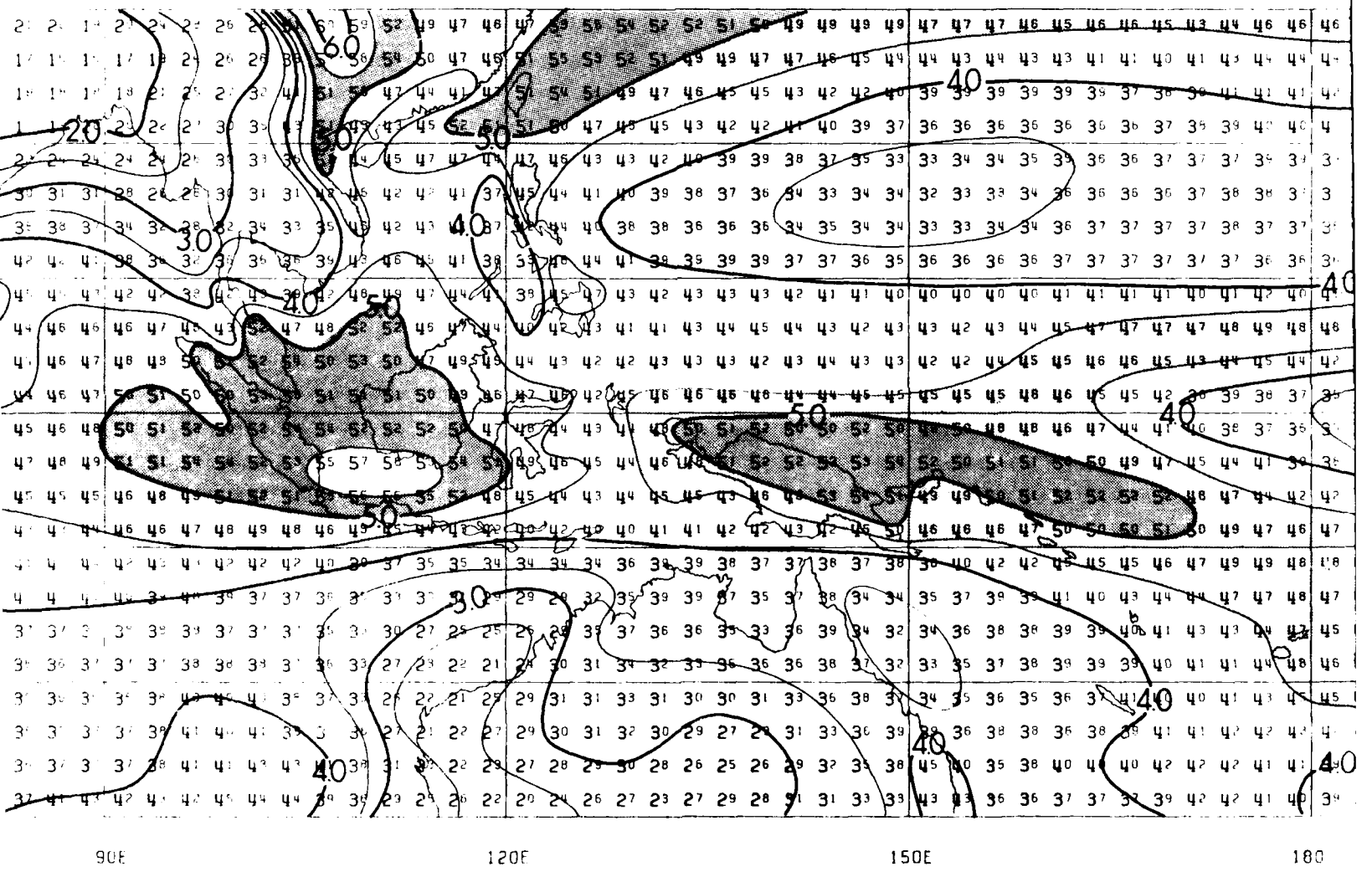
90E
120E
150E
180
90E
120E
150E
180

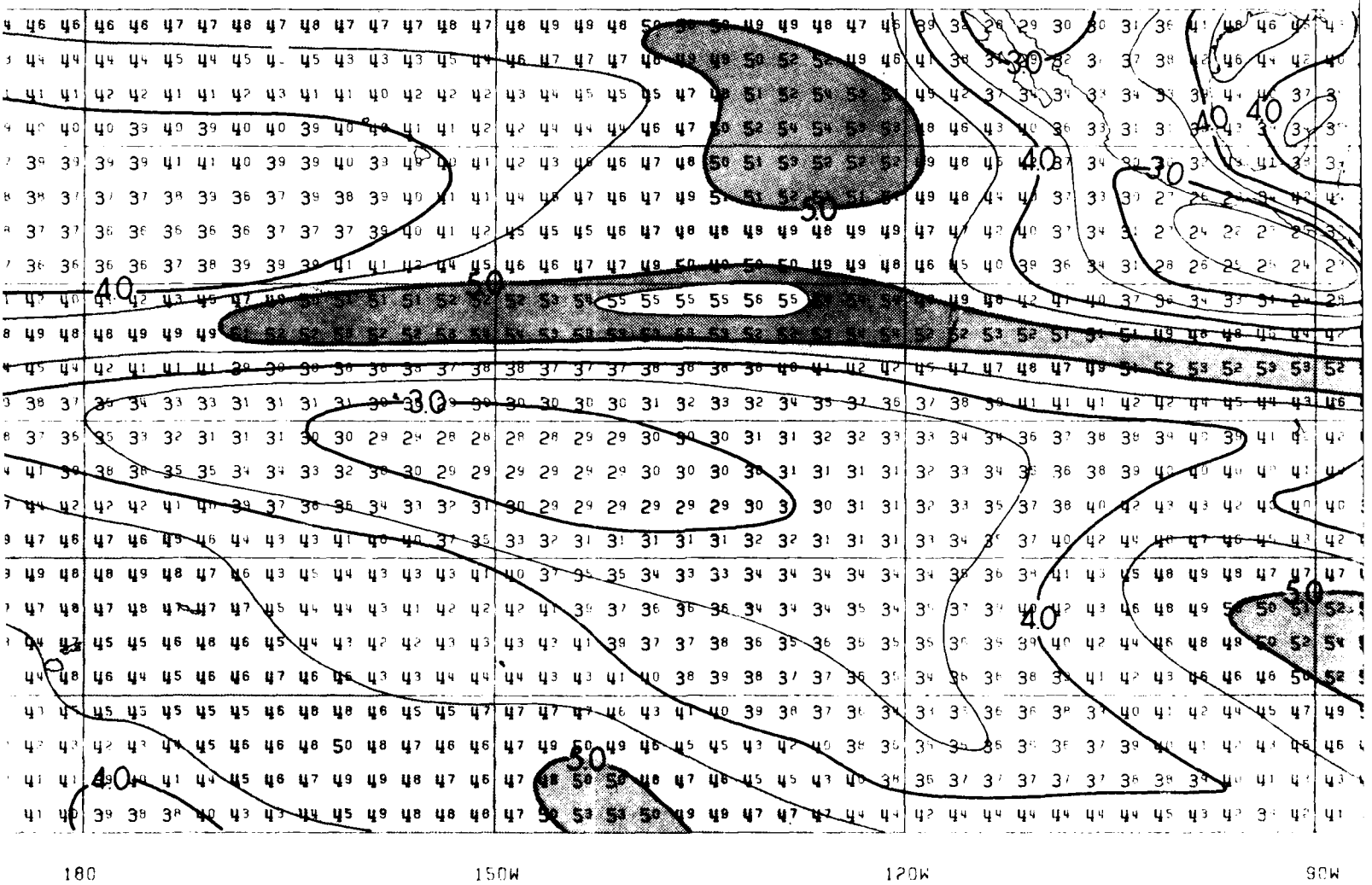
180
150W
120W
90W
40
50
30
40
50
30
40
50
180
150W
120W
90W

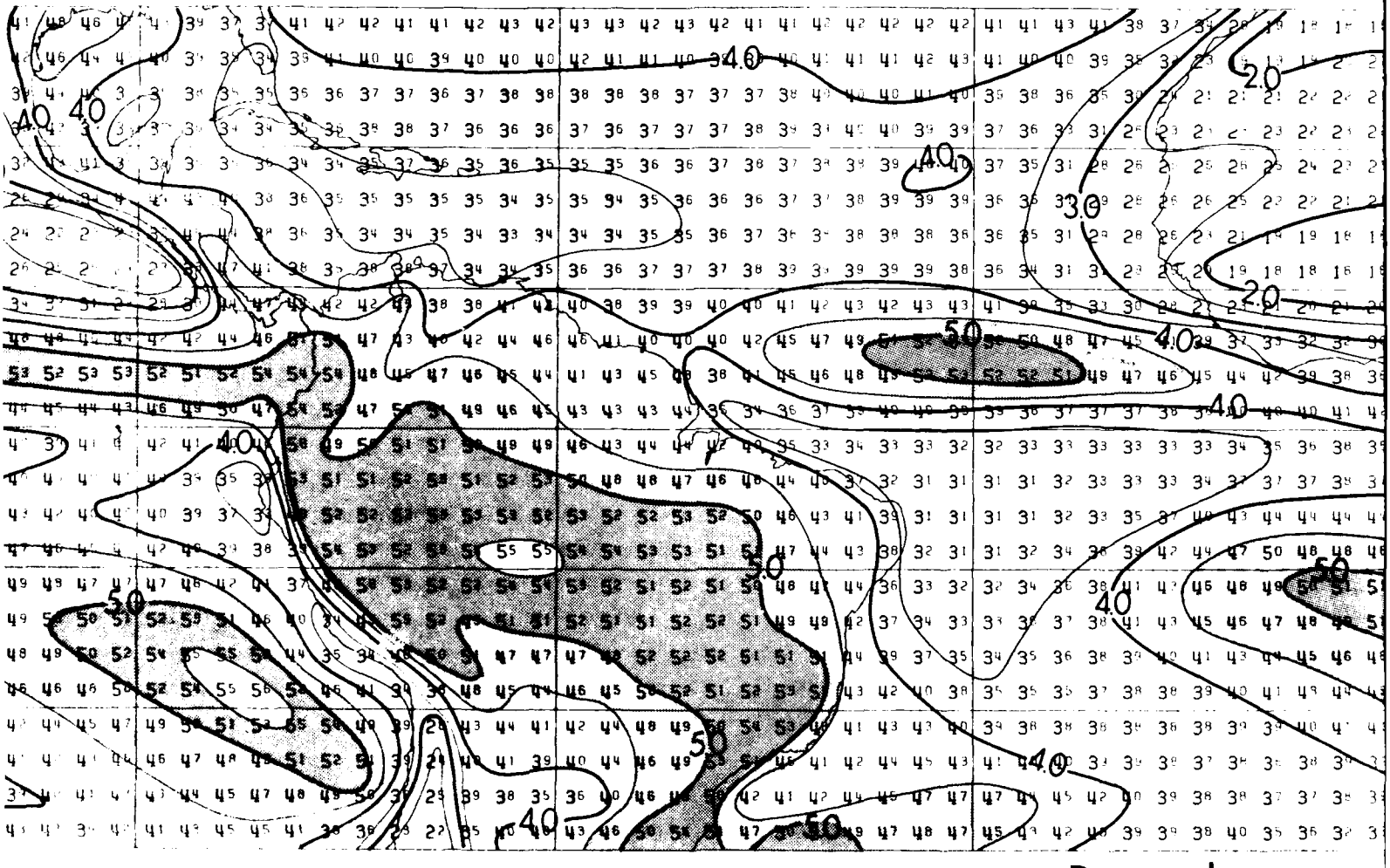

December

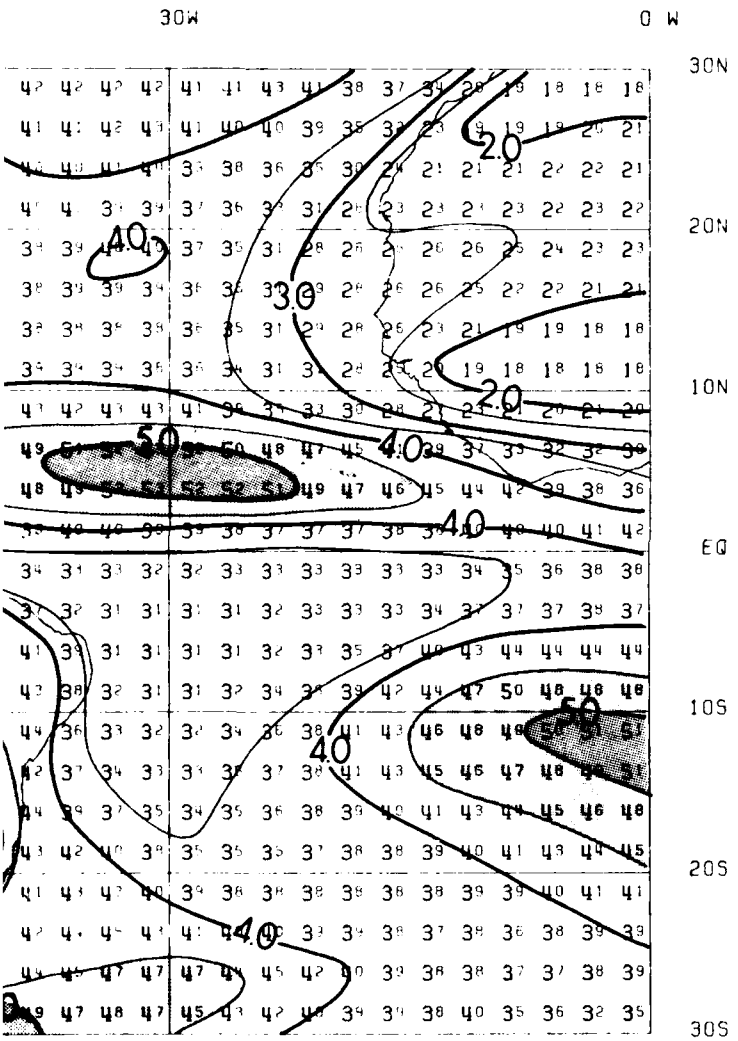
30W
0 W
30N
20N
10N
EQ
10S
20S
30S
2.0
3.0
4.0
5.0
December

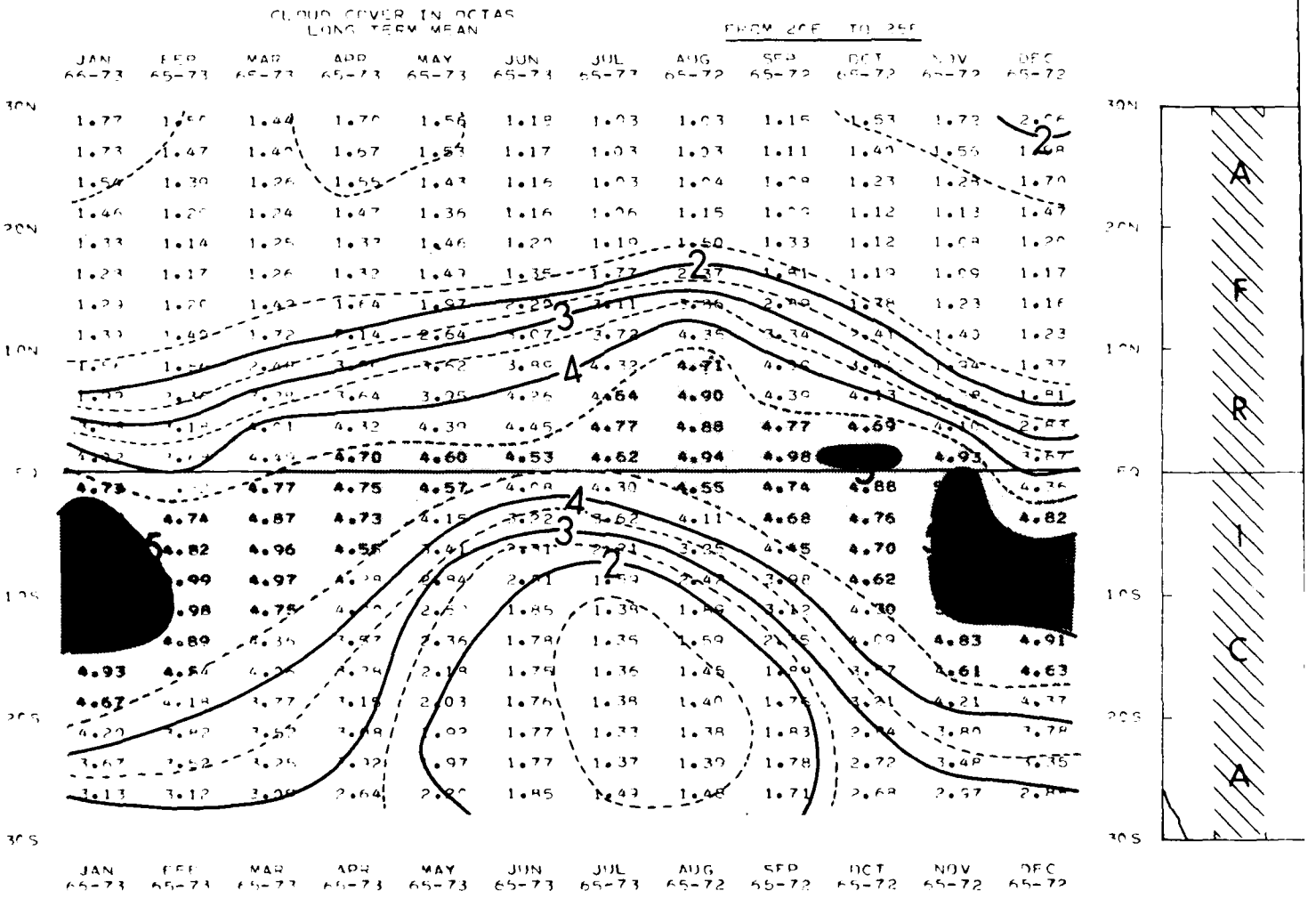

PRECEDING PAGE BLANK-NOT FILMED

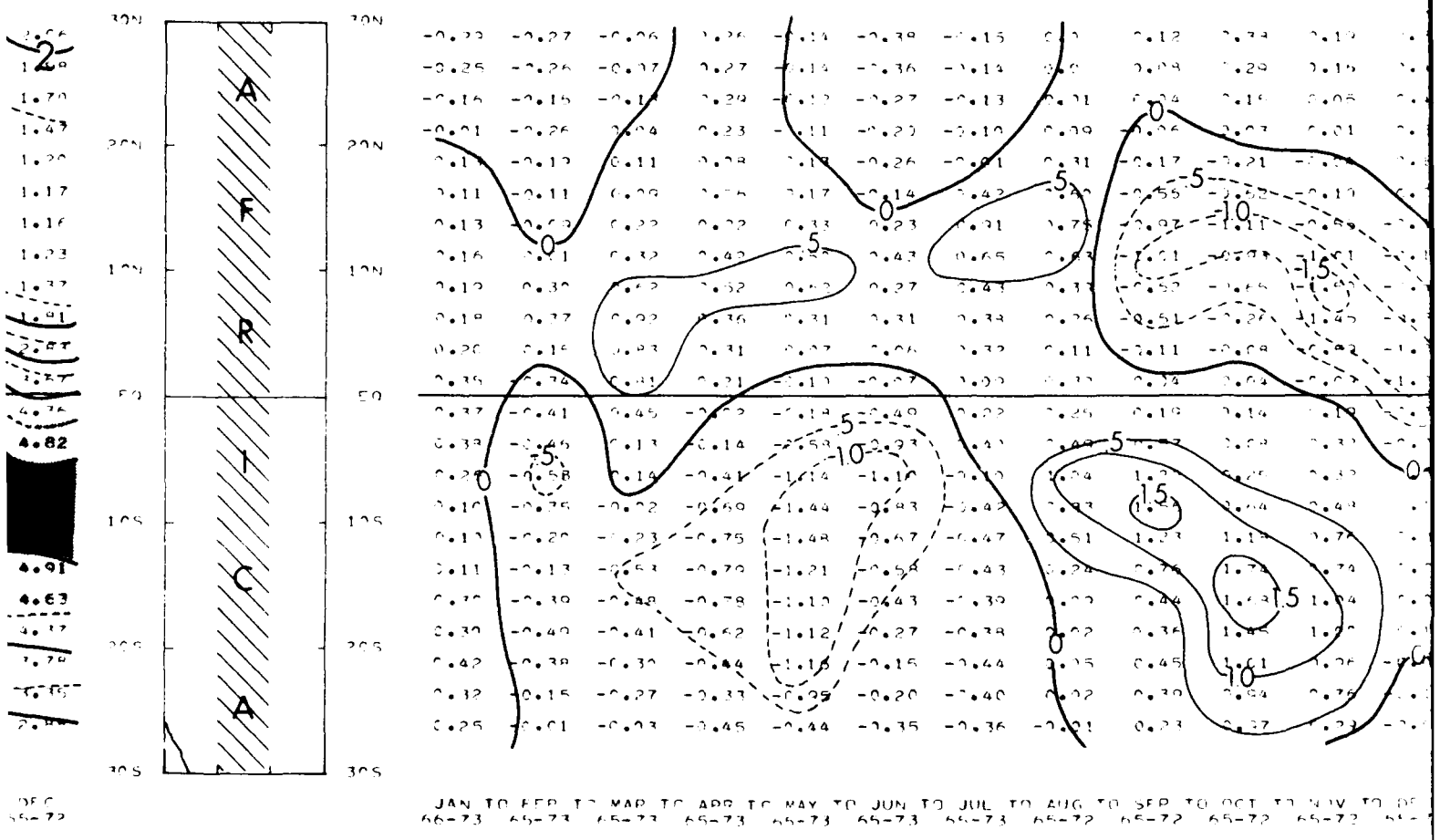
CLOUD COVER IN OCTAS
MONTH TO MONTH CHANGE IN LONG TERM MEAN FROM 30S TO 30N
JAN TO FEB 66-73
FEB TO MAR 65-73
MAR TO APR 65-73
APR TO MAY 65-73
MAY TO JUN 65-73
JUN TO JUL 65-73
JUL TO AUG 65-72
AUG TO SEP 65-72
SEP TO OCT 65-72
OCT TO NOV 65-72
30N
20N
10N
EQ
10S
20S
30S
AFRICA
-0.33 -0.27 -0.06 0.26 -0.14 -0.38 -0.15 0.12 0.34 0.12
-0.25 -0.26 -0.17 0.27 -0.14 -0.36 -0.14 0.09 0.29 0.15
-0.16 -0.15 -0.14 0.29 -0.12 -0.27 -0.13 0.01 0.24 0.16 0.05
-0.01 -0.26 0.04 0.23 -0.11 -0.20 -0.10 0.09 0.26 0.07 0.01
0.14 -0.13 0.11 0.38 0.10 -0.26 -0.01 0.31 -0.17 -0.21
0.11 -0.11 0.09 0.25 0.17 -0.14 0.43 0.20 -0.55 -0.52 -0.10
0.13 -0.03 0.22 0.32 0.33 0.23 0.31 0.75 -0.02 -1.11 -0.69
0.16 0.01 0.32 0.43 0.38 0.43 0.65 0.83 -1.01 -0.94 -1.01
0.19 0.30 0.42 0.52 0.50 0.27 0.43 0.33 -0.52 -1.65 -1.49
0.18 0.27 0.33 0.36 0.31 0.31 0.38 0.26 -0.51 -0.27 -1.45
0.20 0.15 0.23 0.31 0.27 0.06 0.32 0.11 -0.11 -0.08 -0.03
0.36 -0.24 0.31 0.21 -0.10 -0.07 0.03 0.33 0.24 0.04 -0.07
0.37 -0.41 0.45 -0.03 -0.18 -0.49 0.22 0.25 0.19 0.14 0.19
0.33 -0.46 0.13 0.14 -0.58 -0.93 0.41 0.48 0.57 0.09 0.33
0.20 -0.58 0.19 -0.41 -1.14 -1.10 0.10 1.04 1.27 0.25 0.32
0.10 -0.25 -0.02 -0.69 -1.44 -0.83 -0.43 0.83 1.25 1.04 0.48
0.13 -0.20 -0.23 -0.75 -1.48 -0.67 -0.47 0.51 1.23 1.19 0.74
0.11 -0.13 -0.53 -0.70 -1.21 -0.58 -0.43 0.28 0.76 1.28 0.74
0.28 -0.39 -0.48 -0.78 -1.10 -0.43 -0.39 0.22 0.44 1.43 1.04
0.39 -0.40 -0.41 -0.62 -1.12 -0.27 -0.38 0.22 0.36 1.45 1.22
0.42 -0.38 -0.39 -0.44 -1.15 -0.15 -0.44 0.25 0.45 1.61 1.26
0.32 -0.15 -0.27 -0.33 -0.95 -0.20 -0.40 0.02 0.30 0.94 0.76
0.25 -0.01 -0.03 -0.45 -0.44 -0.35 -0.36 -0.01 0.23 0.37 0.23
0 5 10 15

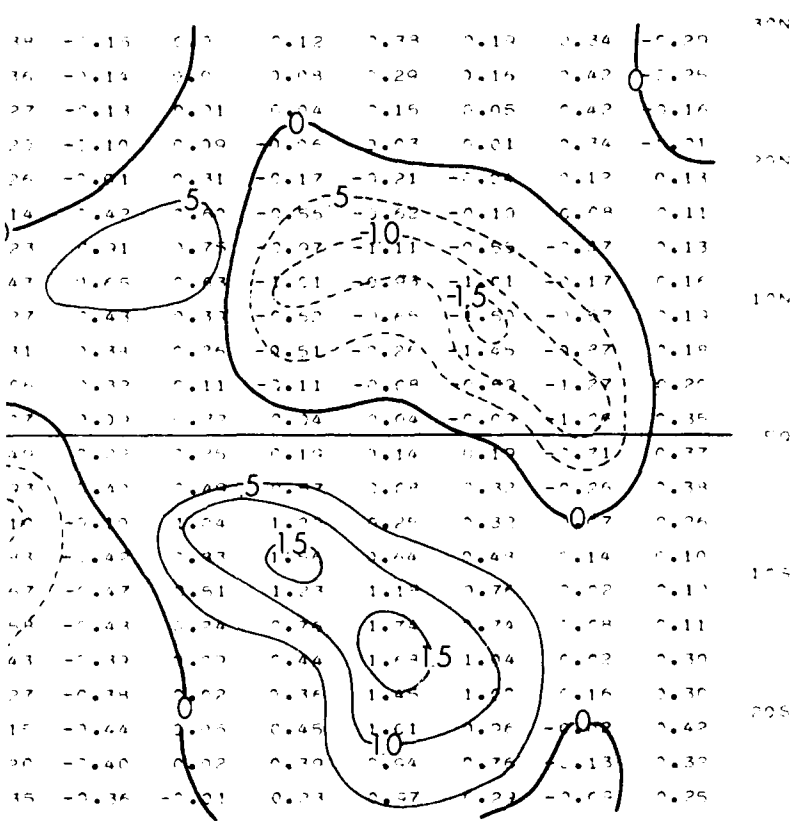
0
-5
-10
-15
5
-5
1.5
0
1.5
1.0
0

AD-A156 188 MEAN CLOUDINESS OVER THE GLOBAL TROPICS FROM SATELLITE OBSERVATIONS(U) HAWAII UNIV HONOLULU DEPT OF METEOROLOGY J C SADLER ET AL. DEC 84 UHMET-84-1 2/2

UNCLASSIFIED NEPRF-CR-84-09 N00014-83-K-0498 F/G 4/2 NL

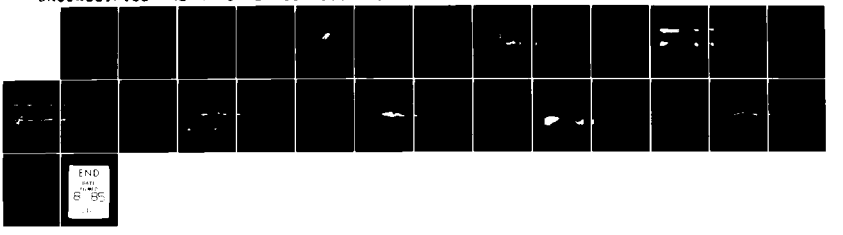

END
DATE FILMED
8 85

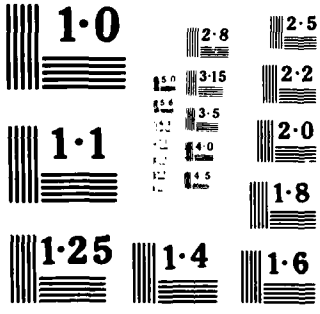
1·0
1·1
1·25
2·8
3·15
3·5
4·0
4·5
1·4
2·5
2·2
2·0
1·8
1·6

CLOUD COVER IN OCTAS
LONG TERM MEAN

FROM 60E TO 55E

	JAN 66-72	FEB 65-73	MAR 65-73	APR 65-73	MAY 65-73	JUN 65-73	JUL 65-73	AUG 65-72	SEP 65-72	OCT 65-72	NOV 65-72	DEC 65-72
30N	2.37	2.68	2.09	2.68	1.67	1.14	1.13	1.20	1.14	1.25	1.75	2.17
	2.15	1.83	1.79	2.42	1.49	1.07	1.12	1.09	1.07	1.11	1.33	1.73
	1.77	1.62	1.56	2.05	1.39	1.12	1.27	1.13	1.05	1.04	1.19	1.47
20N	1.60	1.72	1.33	1.76	1.28	1.21	1.43	1.22	1.11	1.04	1.32	1.20
	1.44	1.43	1.25	1.53	1.25	1.44	1.87	1.53	1.24	1.10	1.39	1.14
	1.67	1.64	1.39	1.45	1.32	1.73	2.25	2.08	1.82	1.34	1.38	1.32
10N	2.37	1.92	1.45	1.60	1.62	1.37	2.17	1.89	2.02	1.74	1.72	1.88
	2.54	2.15	1.67	1.79	2.15	2.10	2.21	2.06	2.41	2.15	2.37	2.26
	2.80	2.37	1.84	2.12	2.26	2.53	2.53	2.43	2.60	2.45	2.56	2.78
EQ	3.19	2.79	2.22	2.41	2.85	3.10	3.01	2.93	2.76	2.56	2.82	3.25
	3.26	3.00	2.54	2.69	3.33	3.58	3.35	3.20	2.92	2.69	2.90	3.18
	3.39	3.04	2.41	3.03	3.33	3.74	3.62	3.56	3.09	2.80	2.98	3.30
10S	3.52	3.07	2.64	2.73	3.36	3.73	3.67	3.77	3.26	2.75	2.91	3.22
	3.95	3.32	3.14	3.14	3.41	3.58	3.57	3.66	3.43	3.32	3.35	3.66
	4.13	4.06	3.50	3.37	3.42	3.56	3.69	3.44	3.64	3.58	3.66	3.86
20S	4.35	4.11	3.65	3.44	3.39	3.62	3.62	3.48	3.75	3.64	3.70	3.88
	4.37	4.26	3.91	3.46	3.35	3.56	3.69	3.60	3.61	3.35	3.43	3.67
	4.33	4.01	3.88	3.58	3.43	3.65	3.80	3.77	3.57	3.39	3.42	3.49
30S	4.07	3.69	3.91	3.77	3.46	3.68	3.67	3.76	3.48	3.22	3.35	3.40
	3.73	3.58	3.94	3.77	3.53	3.63	3.61	3.56	3.22	3.19	3.40	3.46
	3.66	3.50	3.90	3.90	3.56	3.65	3.49	3.58	3.19	3.32	3.55	3.74
	3.71	3.62	4.02	3.94	3.65	3.74	3.57	3.74	3.33	3.65	3.97	3.86
	3.90	3.91	4.09	4.09	3.88	3.98	3.71	3.80	3.53	3.73	4.13	3.69
40S	4.26	4.25	4.55	4.59	4.68	4.03	3.82	4.31	4.63	4.34	3.64	3.90

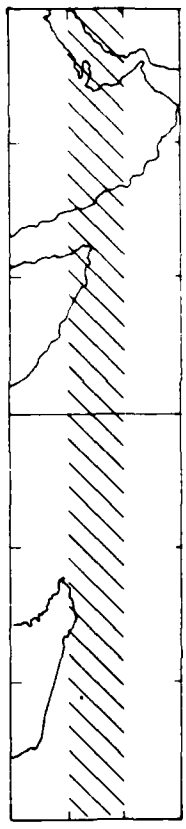

CLOUD COVER IN OCTAS
MONTH TO MONTH CHANGE IN LONG TERM MEAN FROM 60E TO 60E

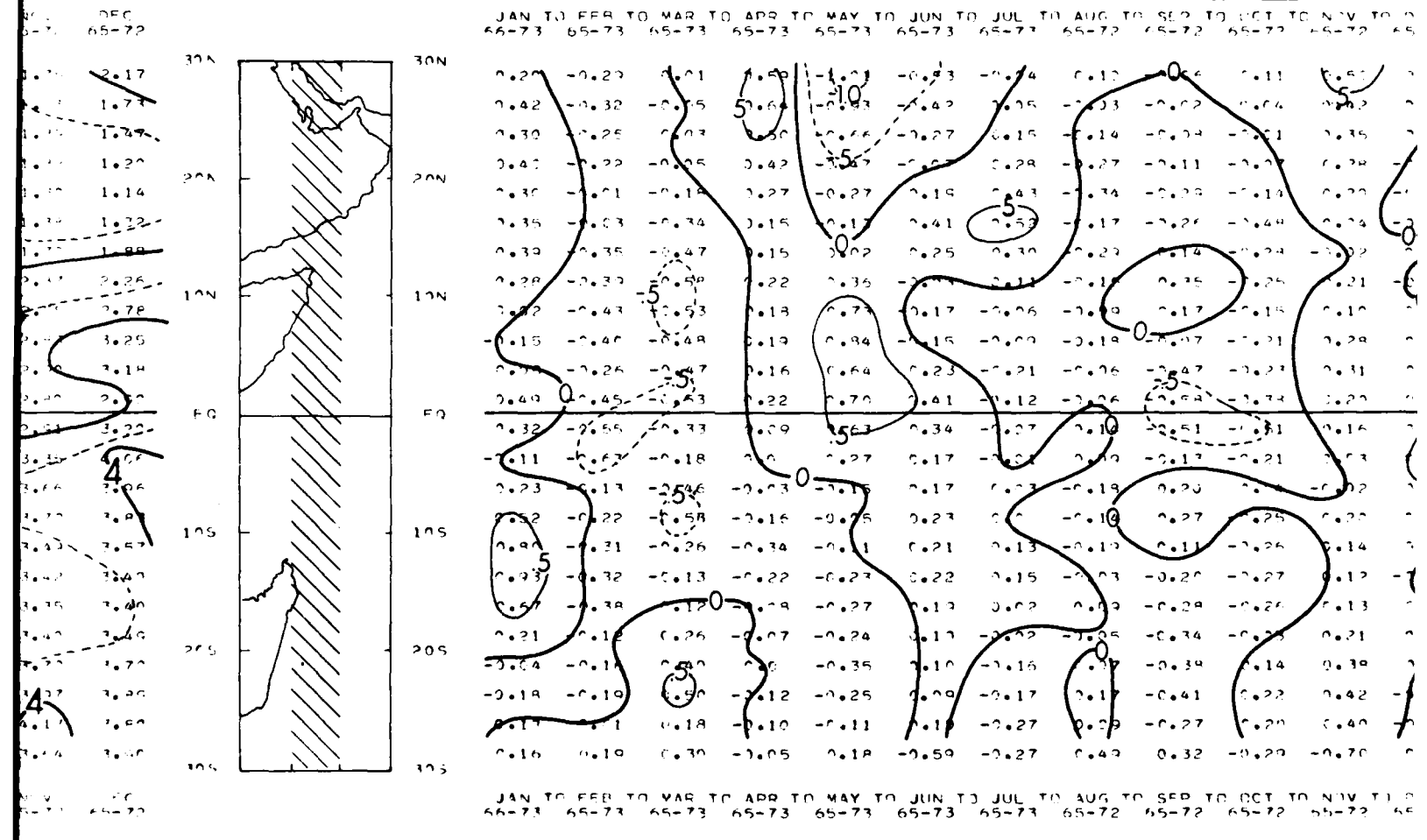

TERM MEAN FROM 50E TO 55E

JUL TO AUG 65-72	AUG TO SEP 65-72	SEP TO OCT 65-72	OCT TO NOV 65-72	NOV TO DEC 65-72	DEC TO JAN 66-73	
.14	0.13	-0.06	0.11	0.53	0.43	0.27
.26	-0.03	-0.02	0.04	0.02	0.23	0.42
.15	-0.14	-0.08	-0.01	0.35	0.08	0.30
.28	-0.27	-0.11	-0.07	0.28	-0.12	0.40
.43	-0.34	-0.09	-0.14	0.20	-0.16	0.30
.37	-0.17	-0.26	-0.48	0.24	-0.05	0.36
.30	0.23	0.14	-0.08	-0.02	0.16	0.39
.11	-0.15	0.35	-0.25	0.21	-0.11	0.28
.26	-0.03	0.17	-0.15	0.10	-0.23	0.02
.21	-0.19	-0.07	-0.21	0.28	0.42	0.15
.21	-0.06	-0.47	-0.23	0.31	0.28	0.08
.13	-0.06	-0.58	-0.38	0.20	0.16	0.49
.27	0.10	-0.61	-0.31	0.16	0.20	0.32
.23	0.02	-0.17	-0.21	0.03	0.35	-0.11
.23	-0.18	0.20	-0.08	-0.02	0.30	0.23
.2	-0.10	0.27	-0.25	0.20	0.13	0.02
.13	-0.13	0.11	-0.26	0.14	0.28	0.08
.15	-0.03	-0.20	-0.27	0.13	-0.02	0.03
.03	0.03	-0.28	-0.26	0.13	0.05	0.07
.22	-0.25	-0.34	-0.20	0.21	0.03	0.21
.16	-0.07	-0.38	0.14	0.38	0.00	0.04
.17	-0.17	-0.41	-0.22	0.42	-0.04	-0.18
.27	-0.29	-0.27	-0.20	0.40	-0.33	-0.14
.27	0.43	0.32	-0.22	-0.70	0.26	0.16

JUL TO AUG 65-72	AUG TO SEP 65-72	SEP TO OCT 65-72	OCT TO NOV 65-72	NOV TO DEC 65-72	DEC TO JAN 66-73

30N
20N
10N
EQ
10S
20S
30S

CLOUD COVER IN OCTAS
LONG TERM MEAN

FROM 70E TO 75E

	JAN 66-73	FEB 65-73	MAR 65-73	APR 65-73	MAY 65-73	JUN 65-73	JUL 65-73	AUG 65-72	SEP 65-72	OCT 65-72	NOV 65-72	DEC 65-72
30N	1.76	1.65	1.76	1.91	1.38	1.69	2.46	2.57	1.66	1.20	1.34	1.63
	1.51	1.58	1.71	1.82	1.33	1.80	3.14	3.41	1.86	1.33	1.33	1.51
	1.48	1.41	1.56	1.72	1.33	2.70	3.73	4.24	2.79	1.54	1.41	1.53
20N	1.51	1.36	1.41	1.66	1.41	3.55	4.30	4.44	3.37	1.62	1.55	1.70
	1.61	1.36	1.41	1.75	1.70	4.20	4.55	4.16	3.02	1.72	1.72	1.80
	1.74	1.42	1.46	1.83	2.18	4.71	4.83	4.96	4.18	2.41	1.89	1.98
	1.86	1.47	1.56	2.01	2.66	4.88	4.83	4.44	4.15	2.97	2.47	2.39
10N	2.29	1.75	1.75	2.32	3.44	4.83	4.83	4.34	4.05	3.54	2.86	2.88
	2.84	2.33	2.23	2.96	3.89	4.83	4.83	4.53	4.08	4.01	3.35	3.23
	3.21	2.77	2.76	3.38	4.32	4.75	4.53	4.55	4.15	4.06	3.75	3.58
	3.49	3.11	3.04	3.59	4.46	4.32	4.28	4.62	4.45	4.22	4.01	3.89
EQ	3.72	3.25	3.28	3.76	4.41	4.12	4.23	4.68	4.56	4.35	4.23	4.17
	4.10	3.45	3.48	4.60	4.00	4.29	4.20	4.69	4.52	4.42	4.71	4.24
	4.41	3.97	3.83	3.78	3.69	4.29	4.22	4.73	4.72	4.55	4.06	4.37
	4.56	4.56	3.92	3.82	3.60	4.07	4.18	4.52	4.72	4.46	4.13	4.39
	4.60	4.92	4.06	3.62	3.56	3.97	4.18	4.25	4.42	4.26	4.02	4.25
10S	4.20	4.55	4.04	3.68	3.59	3.76	4.11	4.11	4.03	3.96	3.87	3.97
	4.13	4.11	3.95	3.86	3.49	3.74	4.16	4.03	3.87	3.84	3.71	3.70
	3.85	3.86	3.79	3.41	3.60	3.98	4.06	4.03	3.92	3.68	3.57	3.56
	3.67	3.72	3.67	3.40	3.78	4.02	4.06	4.06	3.96	3.61	3.49	3.49
20S	3.29	3.59	3.68	3.51	3.75	3.94	4.13	3.93	3.80	3.71	3.56	3.35
	3.28	3.65	3.75	3.59	4.05	4.12	4.25	4.04	3.81	3.72	3.62	3.47
	3.46	3.80	3.92	3.85	4.26	4.34	4.41	4.24	3.97	3.75	3.91	3.73
30S												

	JAN 66-73	FEB 65-73	MAR 65-73	APR 65-73	MAY 65-73	JUN 65-73	JUL 65-73	AUG 65-72	SEP 65-72	OCT 65-72	NOV 65-72	DEC 65-72

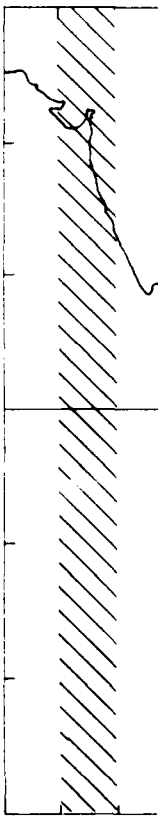

CLOUD COVER IN OCTAS
MONTH TO MONTH CHANGE IN LONG TERM MEAN FROM 75E TO 75E

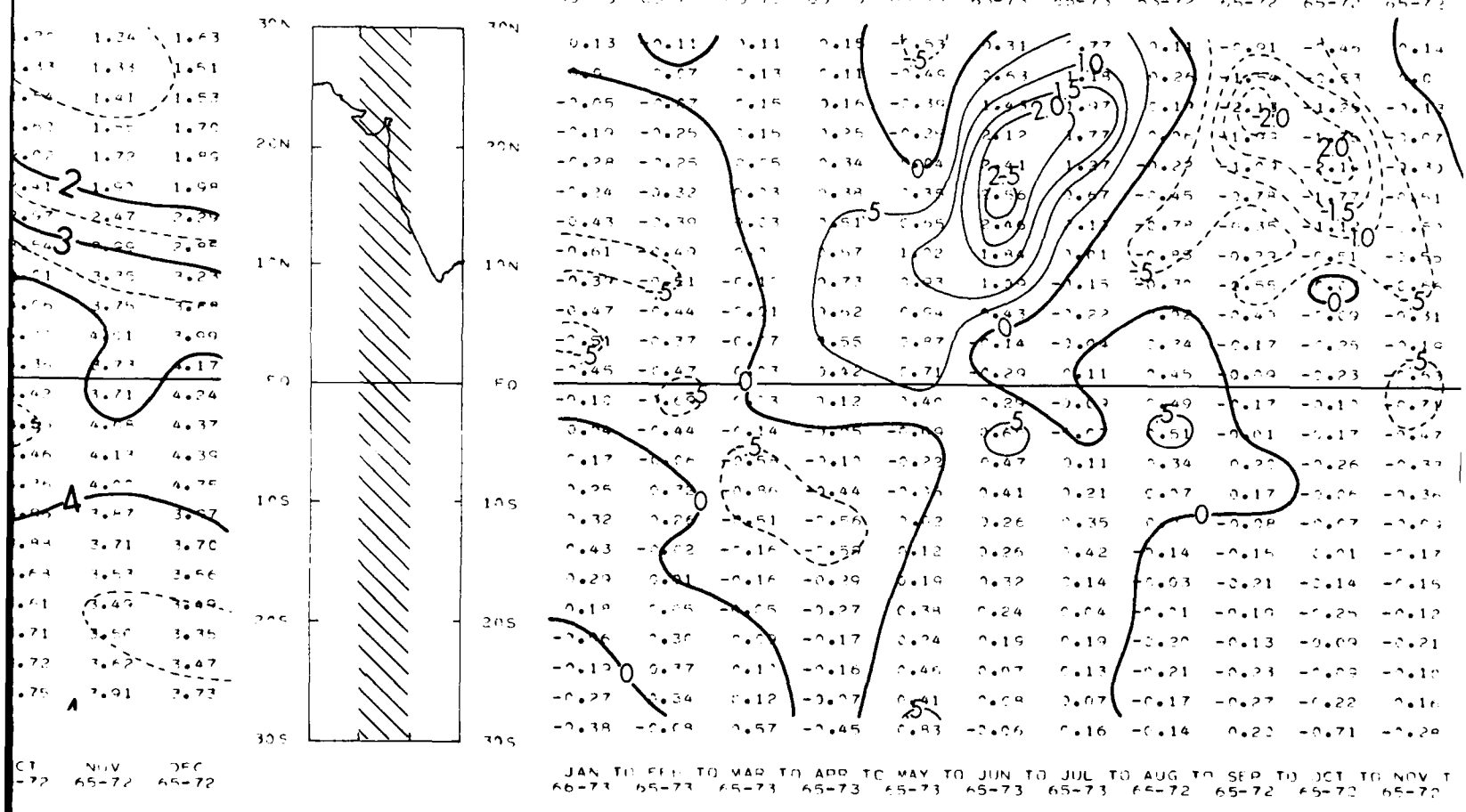

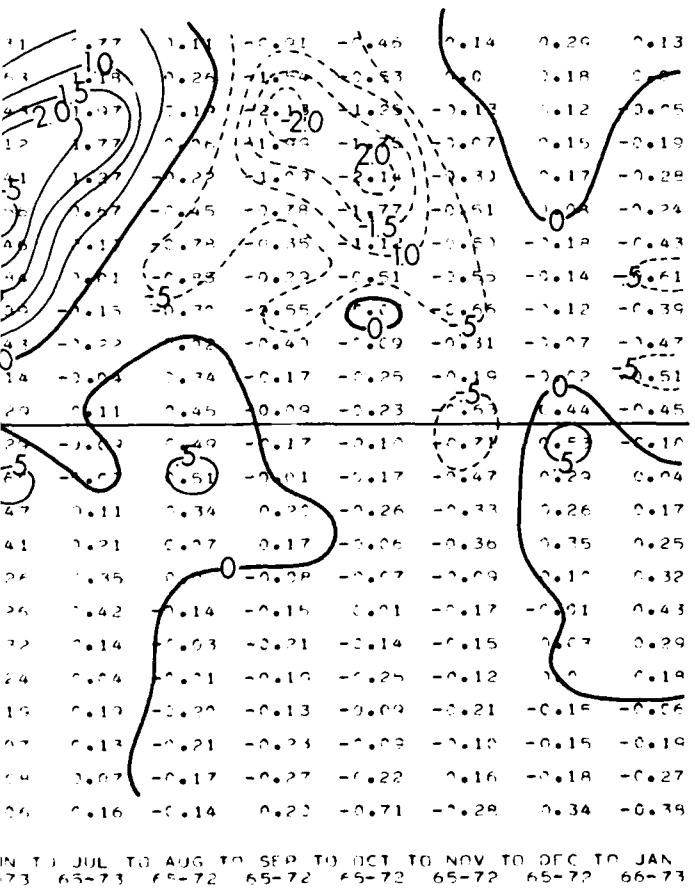
LONG TERM MEAN FROM 75E TO 75E
TO JUL TO AUG TO SEP TO OCT TO NOV TO DEC TO JAN
73 65-73 65-72 65-72 65-72 65-72 65-72 66-73
30N
20N
10N
EQ
10S
20S
30S
-2.0
-1.5
-1.0
-.5
0
.5
1.0
1.5
2.0

CLOUD COVER IN OCTAS
LONG TERM MEAN

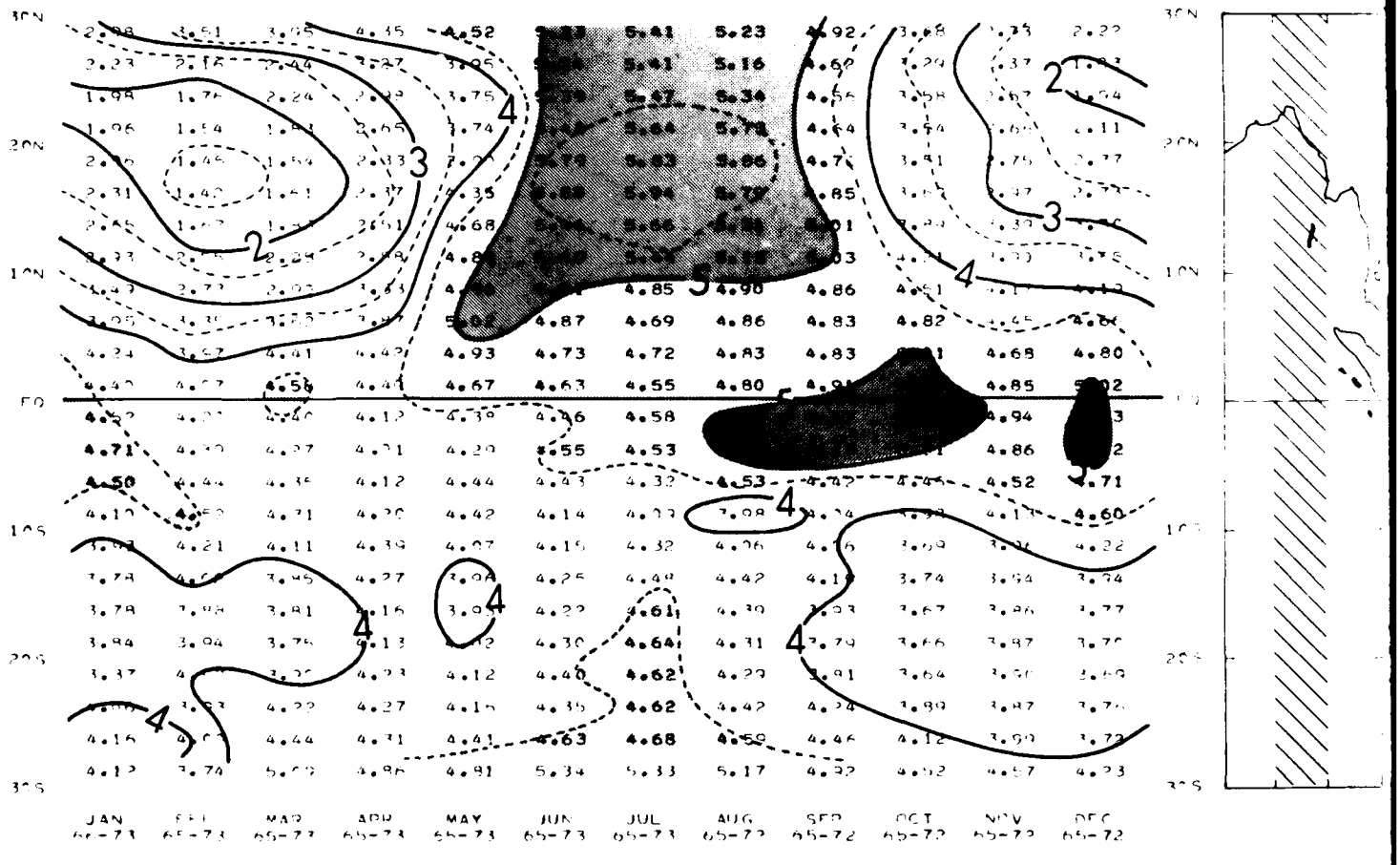

CLOUD COVER IN OCTAS
MONTH TO MONTH CHANGE IN LONG TERM MEAN FROM [illegible] TO [illegible]

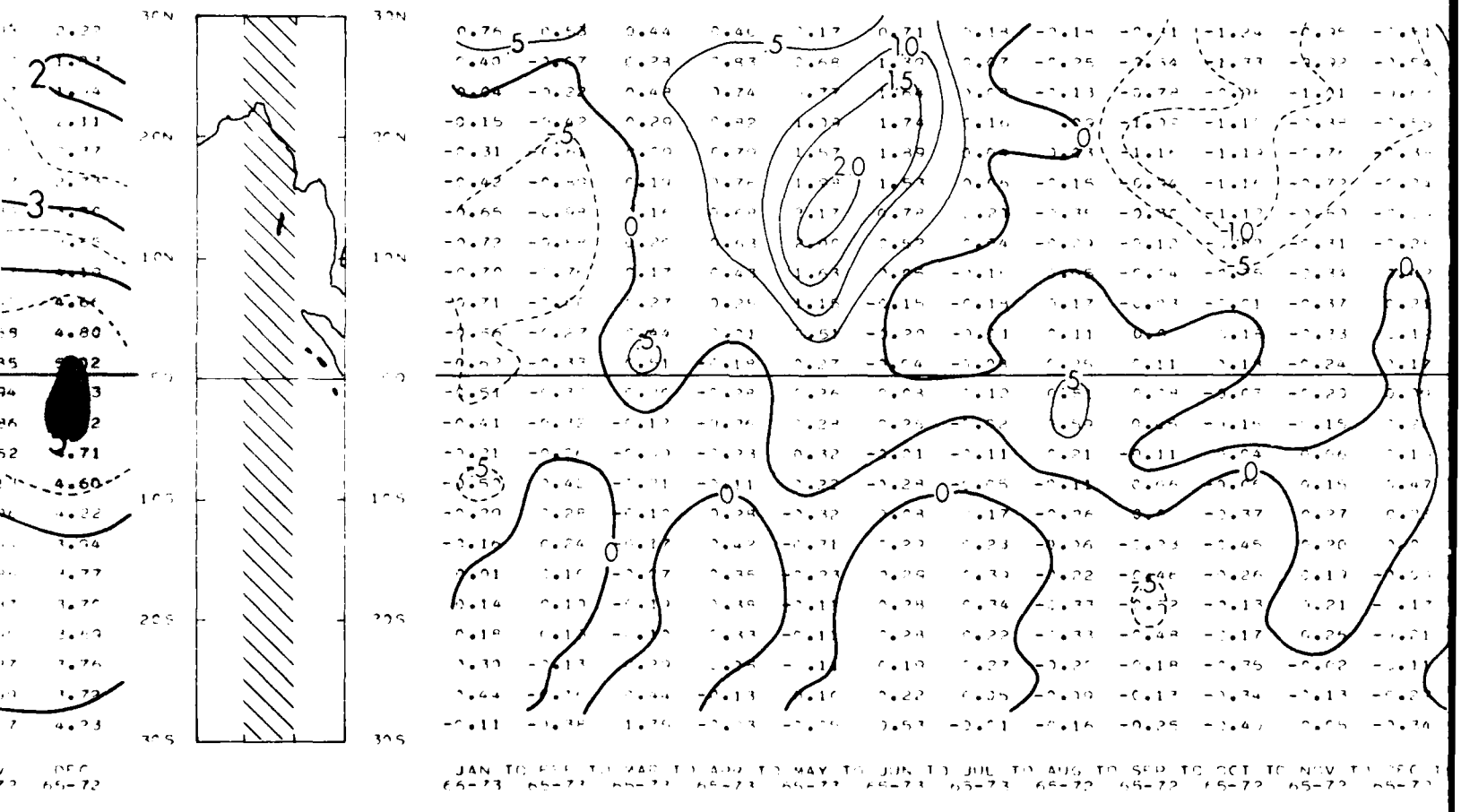

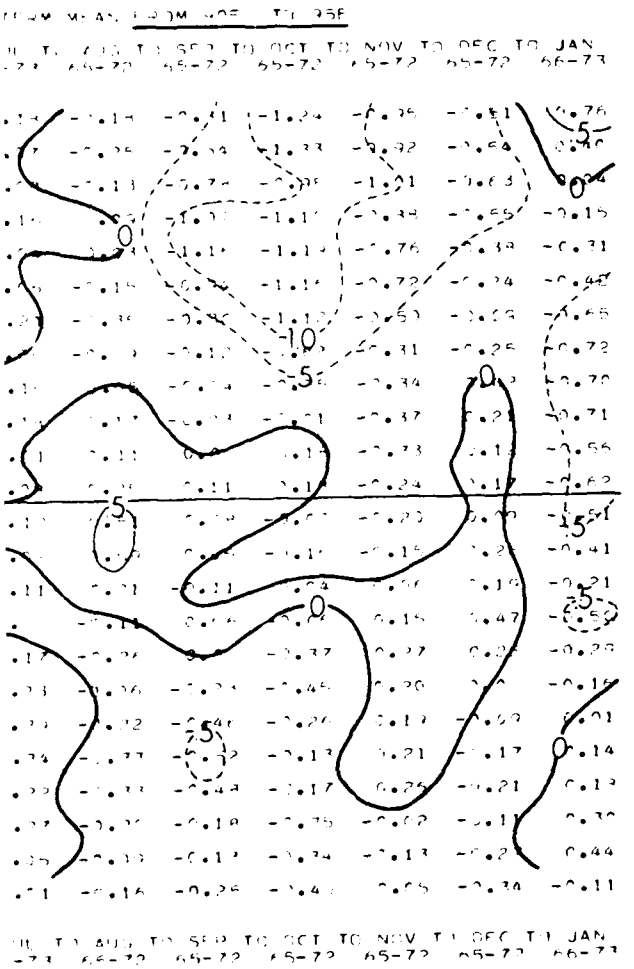
30N
20N
10N
EQ
10S
20S
30S

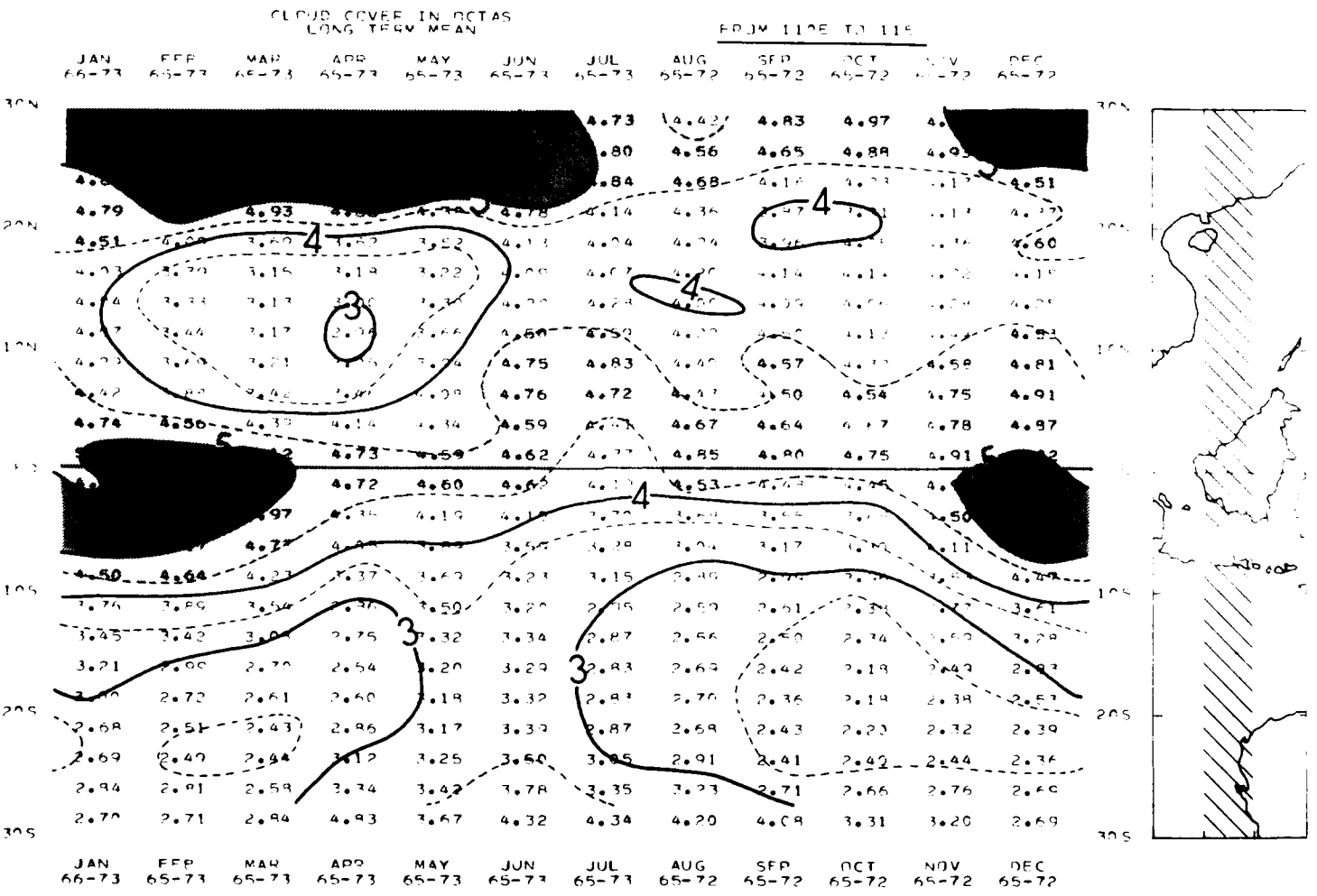

CLOUD COVER IN OCTAS
MONTH TO MONTH CHANGE IN LONG TERM MEAN FROM 1156 TO 1156

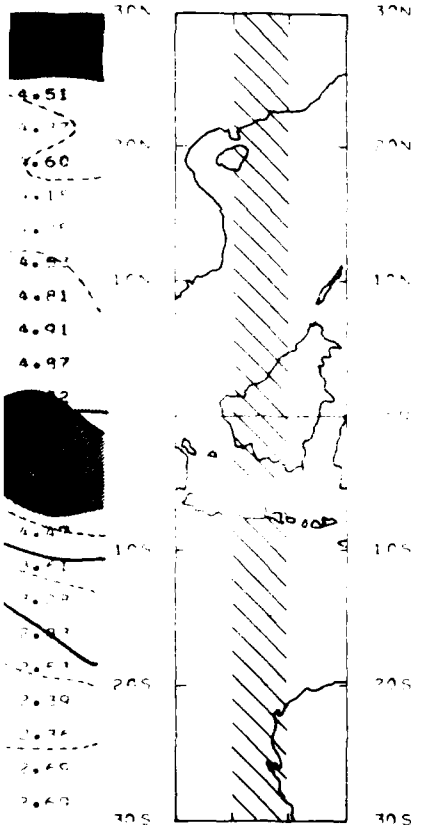

DEC 65-72 | JAN TO FEB 66-73 | FEB TO MAR 65-73 | MAR TO APR 65-73 | APR TO MAY 65-73 | MAY TO JUN 65-73 | JUN TO JUL 65-73 | JUL TO AUG 65-72 | AUG TO SEP 65-72 | SEP TO OCT 65-72 | OCT TO NOV 65-72 | NOV TO DEC 65-72 | DEC TO

DEC 65-72 | JAN TO FEB 66-73 | FEB TO MAR 65-73 | MAR TO APR 65-73 | APR TO MAY 65-73 | MAY TO JUN 65-73 | JUN TO JUL 65-73 | JUL TO AUG 65-72 | AUG TO SEP 65-72 | SEP TO OCT 65-72 | OCT TO NOV 65-72 | NOV TO DEC 65-72 | DEC TO

FROM MEAN FROM 110E TO 115E

JUL TO AUG 65-72 | AUG TO SEP 65-72 | SEP TO OCT 65-72 | OCT TO NOV 65-72 | NOV TO DEC 65-72 | DEC TO JAN 66-73

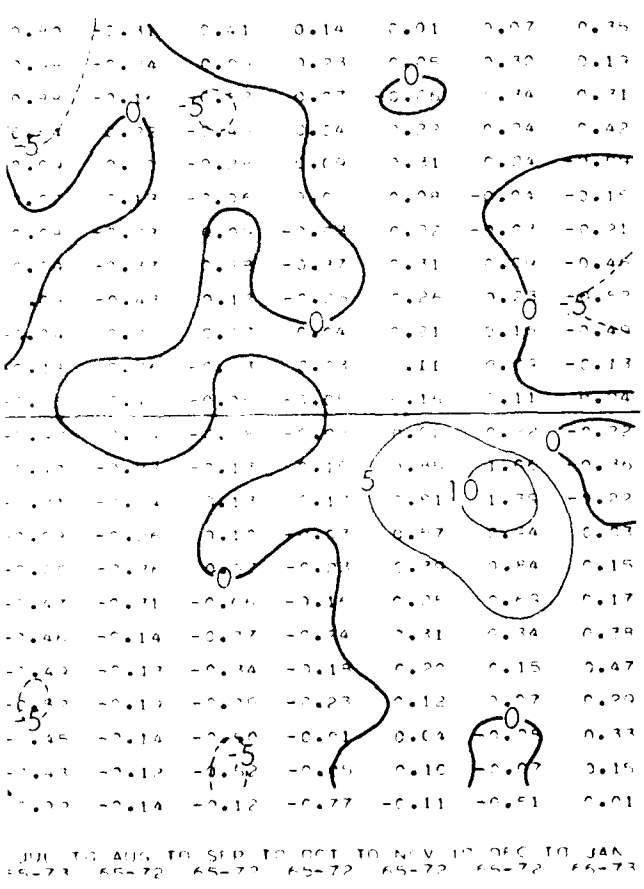

JUL TO AUG 65-72 | AUG TO SEP 65-72 | SEP TO OCT 65-72 | OCT TO NOV 65-72 | NOV TO DEC 65-72 | DEC TO JAN 66-73

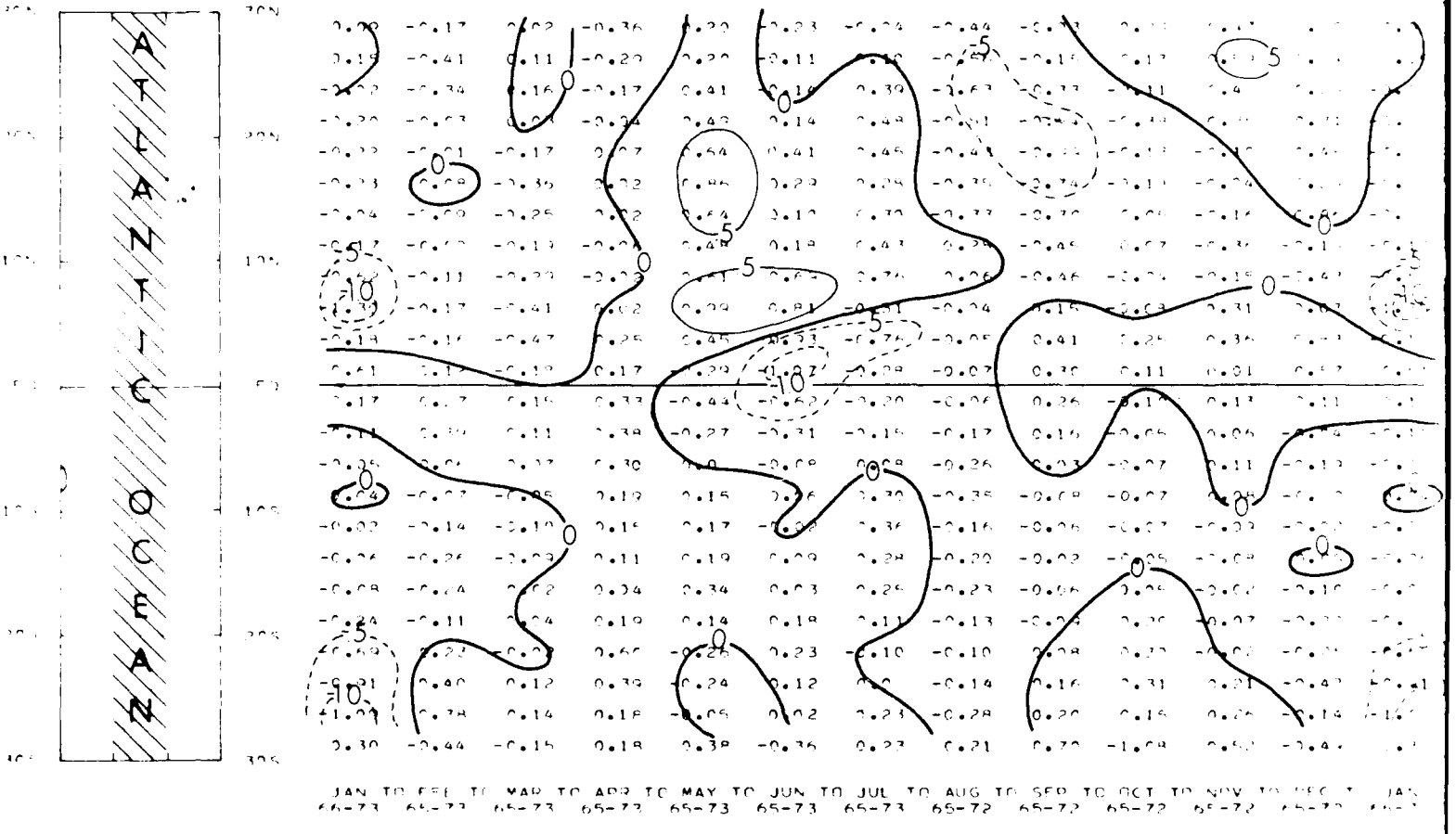
CLOUD COVER IN OCTAS
MONTH TO MONTH CHANGE IN LONG TERM MEAN FROM 30W
JAN TO FEB
FEB TO MAR
MAR TO APR
APR TO MAY
MAY TO JUN
JUN TO JUL
JUL TO AUG
AUG TO SEP
SEP TO OCT
OCT TO NOV
NOV TO DEC
DEC TO JAN
65-73
65-72
ATLANTIC OCEAN
30N
20N
10N
EQ
10S
20S
30S

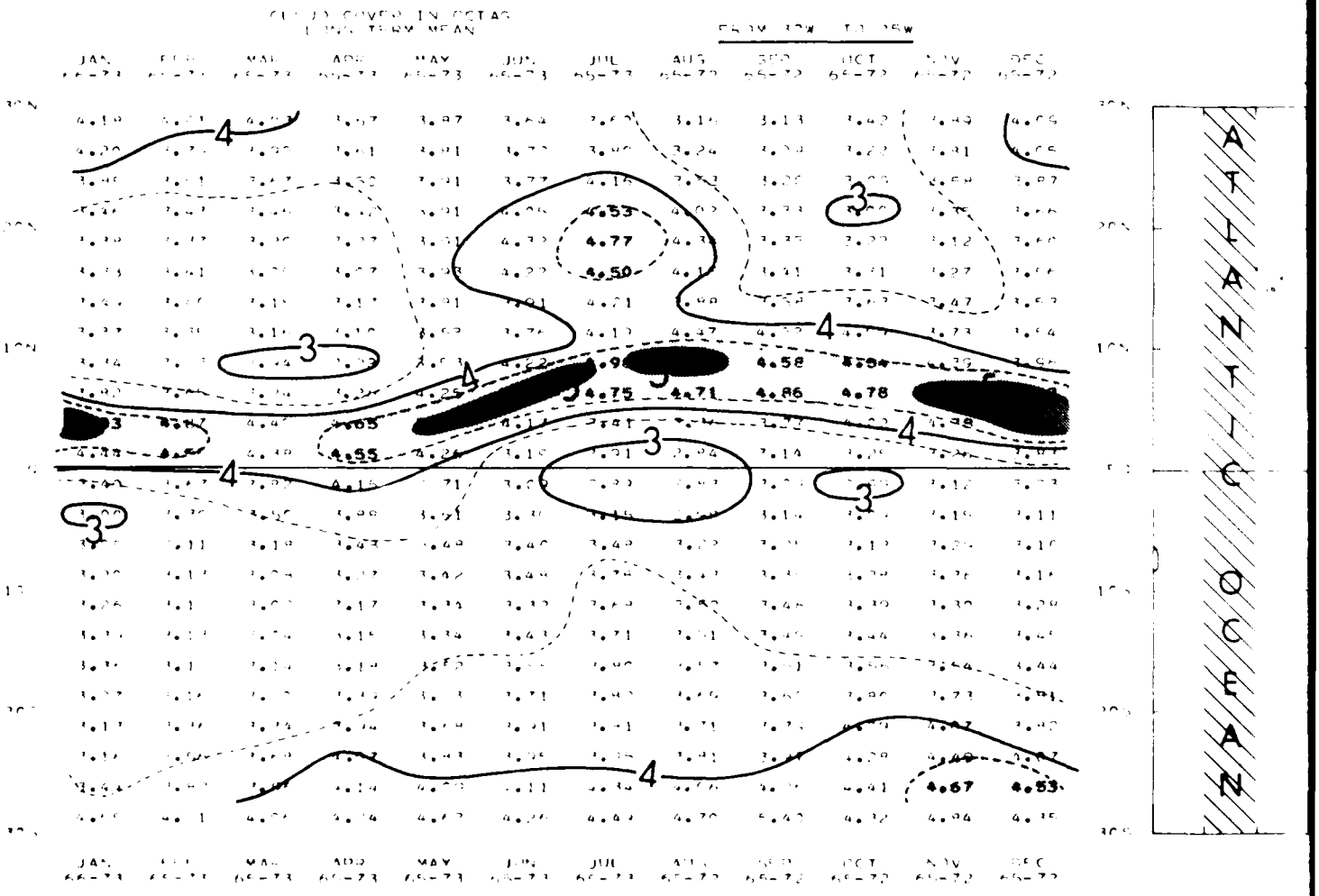

TERM MEAN FROM 60W TO 55W

JUL TO AUG 73	AUG TO SEP 65-72	SEP TO OCT 65-72	OCT TO NOV 65-72	NOV TO DEC 65-72	DEC TO JAN 66-73	
	0.16	0.48	0.41	0.32	-0.02	-0.14
	-0.02	0.40	0.52	0.07	0.0	-0.14
	-0.02	0.21	0.56	0.04	-0.05	-0.13
	-0.02	0.05	0.39	0.01	0.04	-0.16
	-0.03	0.07	0.17	-0.04	0.05	-0.14
	-0.09	-0.10	0.14	-0.09	-0.05	-0.12
	0.06	0.04	0.14	-0.27	-0.10	-0.01
	0.02	-0.28	0.28	-0.13	-0.15	-0.11
	-0.49	-0.35	0.15	0.26	0.08	-0.23
	-0.25	-0.61	0.11	0.41	0.23	0.18
	-0.18	-0.69	0.03	0.45	0.12	0.50
	-0.28	-0.57	-0.01	0.57	0.13	0.41
	-0.21	-0.43	0.19	0.59	0.0	0.52
		-0.19	0.42	0.53	0.17	0.43
	0.41	0.52	0.72	0.28	0.14	0.12
	0.42	1.17	0.78	0.15	0.16	0.0
	0.27	1.11	0.93	0.27	0.18	-0.10
	0.10	1.02	1.02	0.12	0.13	-0.05
	0.08	0.59	1.00	0.06	0.02	0.08
	0.03	0.27	0.86	0.06	0.13	0.03
	0.0	-0.13	0.49	-0.0	0.16	0.17
	-0.03	-0.23	0.60	-0.10	0.28	0.02
	0.02	-0.33	0.43	-0.03	0.02	0.27
	-0.53	0.06	-0.14	0.36	0.60	-0.63

JUL TO AUG 73	AUG TO SEP 65-72	SEP TO OCT 65-72	OCT TO NOV 65-72	NOV TO DEC 65-72	DEC TO JAN 66-73

30N
20N
10N
EQ
10S
20S
30S

CLOUD COVER IN OCTAS
MONTH TO MONTH CHANGE IN LONG TERM MEAN FROM 60W TO 55W

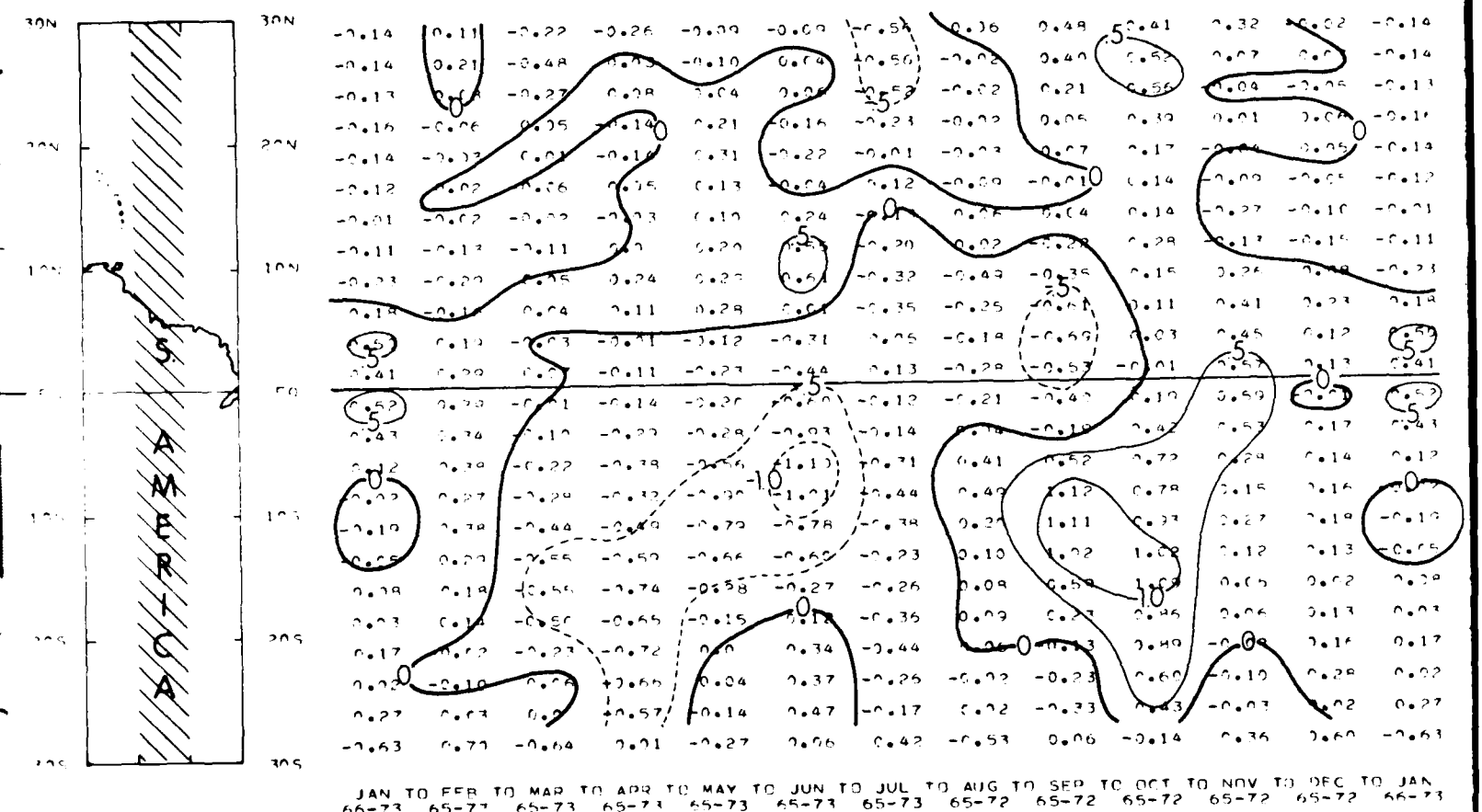

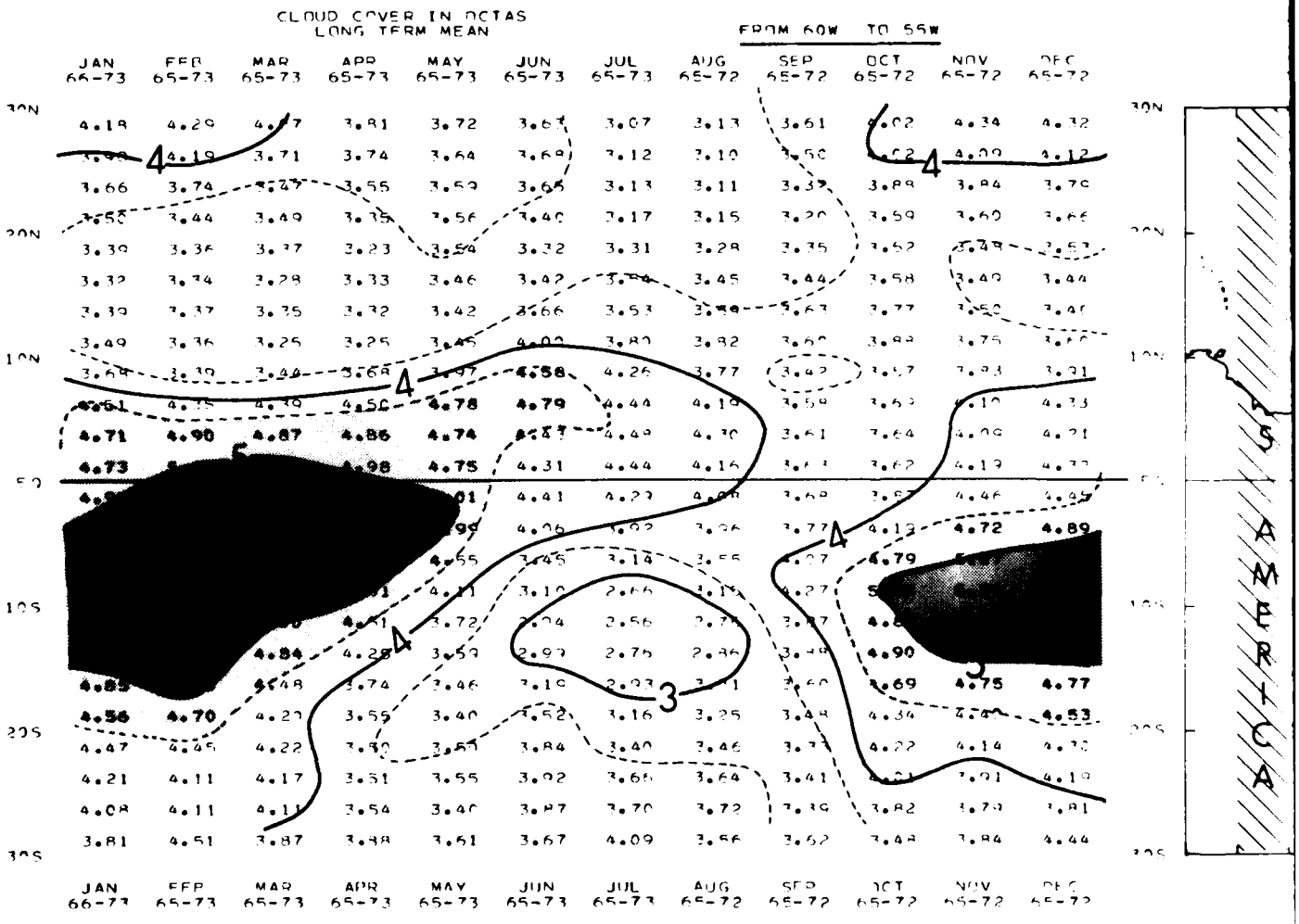

M MEAN FROM 105W TO 100W

TO AUG 65-72	TO SEP 65-72	TO OCT 65-72	TO NOV 65-72	TO DEC 65-72	TO JAN 66-73	
0.34	0.16	-0.24	0.36	0.17	0.37	30N
0.32	-0.06	-0.08	-0.04	0.87	-0.10	
0.23	-0.10	-0.08	-0.07	0.74	-0.27	
0.16	-0.12	-0.07	-0.72	0.47	-0.21	20N
0.37	-0.10	-0.02	-0.05	0.42	-0.23	
0.57	-0.21	-0.04	-0.06	0.30	-0.31	
0.58	-0.23	-0.01	-0.06	-0.03	-0.27	
0.35	-0.20	-0.51	-1.21	-0.20	-0.21	10N
-0.03	-0.28	-0.27	-1.05	-0.44	-0.21	
-0.05	-0.24	0.11	0.14	-0.31	-0.53	
0.37	-0.14	-0.24	0.24	-0.02	-0.36	
0.40	0.16	-0.10	-0.11	-0.27	-0.06	EQ
0.14	0.21	-0.06	-0.07	-0.15	-0.27	
0.33	0.08	-0.26	-0.12	-0.01	-0.19	
0.13	0.05	-0.40	-0.21	-0.17	-0.21	
0.13	-0.02	-0.42	-0.13	0.22	-0.29	10S
0.16	-0.03	-0.40	0.17	-0.07	-0.39	
0.04	0.08	-0.33	0.27	-0.14	-0.33	
-0.08	0.00	-0.24	0.22	-0.26	-0.09	
0.04	-0.07	-0.17	0.07	-0.23	0.02	
0.16	-0.20	-0.21	-0.04	-0.09	0.11	20S
0.26	-0.19	-0.09	-0.18	-0.07	-0.02	
-0.21	-0.08	-0.20	-0.10	-0.20	-0.02	
0.56	-0.17	-0.61	-0.36	0.26	-0.61	30S

TO AUG 65-72	TO SEP 65-72	TO OCT 65-72	TO NOV 65-72	TO DEC 65-72	TO JAN 66-73

CLOUD COVER IN OCTAS
MONTH TO MONTH CHANGE IN LONG TERM MEAN FROM 105W TO 100W

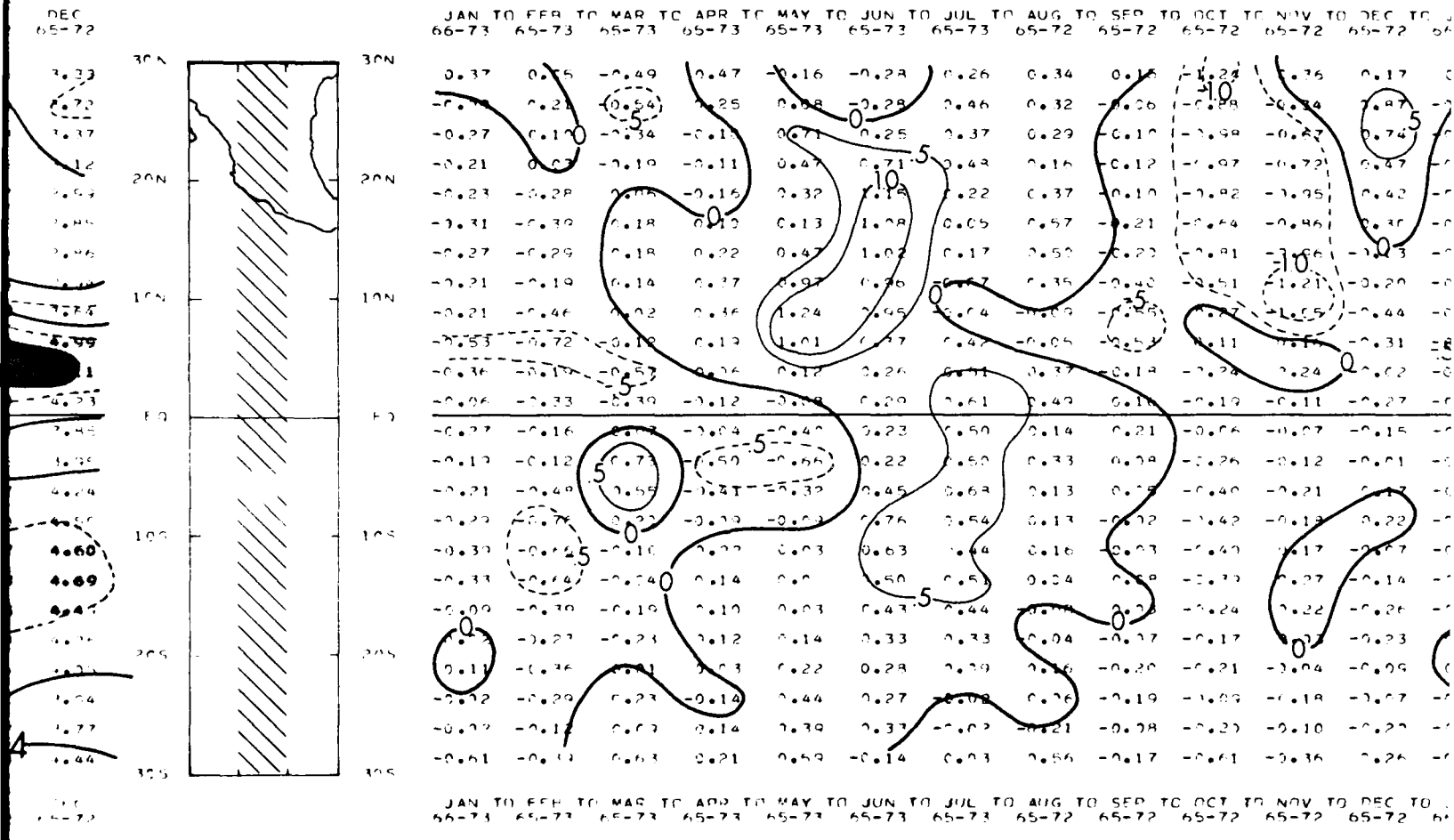

CLOUD COVER IN OCTAS
LONG TERM MEAN

FROM 105W TO 100W

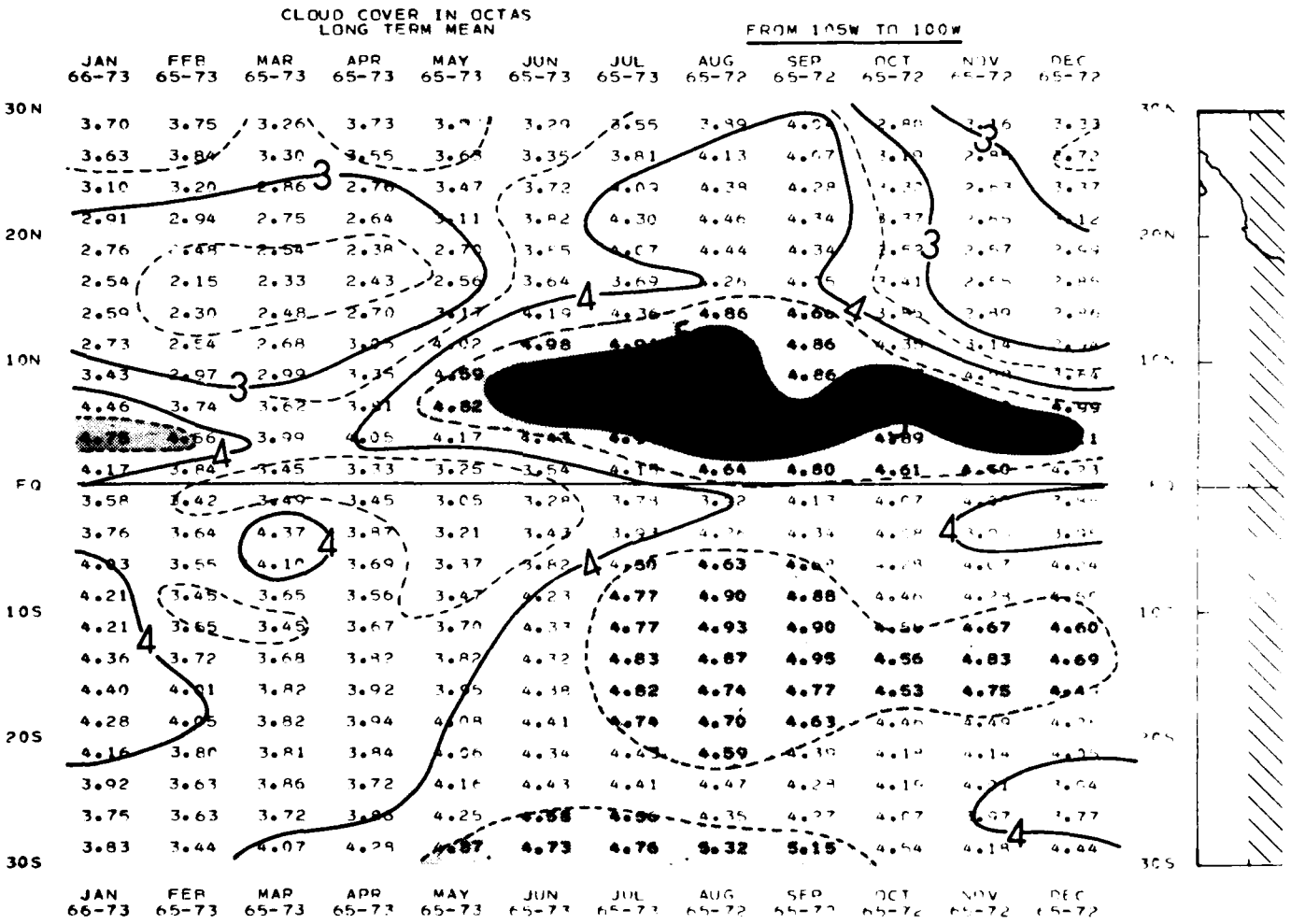

LONG TERM MEAN FROM 170W TO 155W

TO JUL 73	TO AUG 65-73	TO SEP 65-72	TO OCT 65-72	TO NOV 65-72	TO DEC 65-72	TO JAN 66-73	
[illegible]	0.12	-0.13	0.19	0.48	0.31	0.41	0.23
[illegible]	0.20	-0.13	0.10	0.58	0.28	0.26	0.17
[illegible]	0.17	-0.06	0.10	0.53	0.22	0.06	0.11
[illegible]	0.15	0.03	0.26	0.19	0.12	0.08	0.19
[illegible]	0.15	-0.13	0.26	0.15	0.03	0.12	-0.02
[illegible]	0.19	-0.14	0.19	0.11	-0.01	0.01	0.06
[illegible]	0.01	-0.16	0.30	0.18	-0.23	-0.14	0.11
[illegible]	0.11	-0.02	0.13	0.36	-0.37	-0.27	0.11
[illegible]	0.03	-0.08	-0.17	0.45	-0.19	-0.07	-0.21
[illegible]	-0.19	-0.20	-0.07	-0.01	0.31	0.12	-0.56
[illegible]	-0.21	-0.34	0.13	-0.11	0.14	0.20	-0.03
[illegible]	-0.05	-0.08	0.08	-0.09	0.07	-0.02	0.36
[illegible]	-0.01	-0.05	0.05	-0.10	0.09	0.05	0.24
[illegible]	-0.15	-0.10	0.15	-0.15	0.16	0.22	0.15
[illegible]	-0.31	-0.03	0.06	-0.15	0.28	0.32	0.24
[illegible]	-0.33	0.11	0.01	-0.12	0.51	0.28	-0.13
[illegible]	-0.07	0.37	0.31	0.22	0.50	0.17	-0.03
[illegible]	0.06	0.18	-0.22	0.41	0.17	0.42	-0.05
[illegible]	0.13	0.10	-0.13	0.41	-0.19	0.40	-0.14
[illegible]	0.13	0.03	0.05	0.22	-0.33	0.43	-0.05
[illegible]	0.34	-0.16	0.18	-0.01	-0.33	0.18	0.23
[illegible]	0.02	0.05	0.29	-0.39	-0.35	0.31	0.36
[illegible]	-0.21	-0.12	0.29	-0.43	0.0	0.10	0.52
[illegible]	-0.13	-0.35	0.53	-0.15	-0.87	0.24	0.33

ON TO JUL 73	TO AUG 65-73	TO SEP 65-72	TO OCT 65-72	TO NOV 65-72	TO DEC 65-72	TO JAN 66-73

30N
20N
10N
EQ
10S
20S
30S

CLOUD COVER IN OCTAS
MONTH TO MONTH CHANGE IN LONG TERM MEAN FROM 170W TO 165W

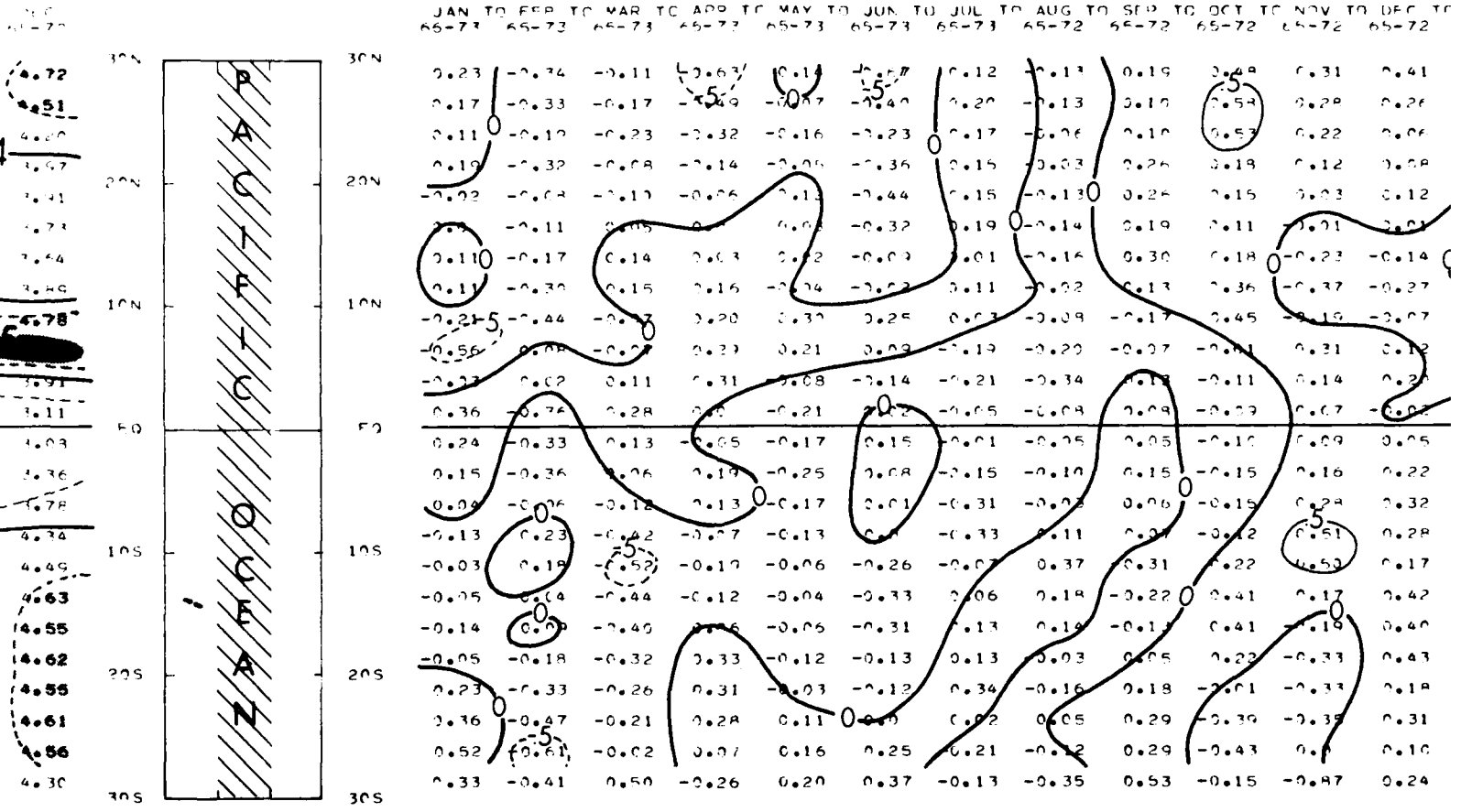

CLOUD COVER IN OCTAS
LONG TERM MEAN

FROM 170W TO 165W

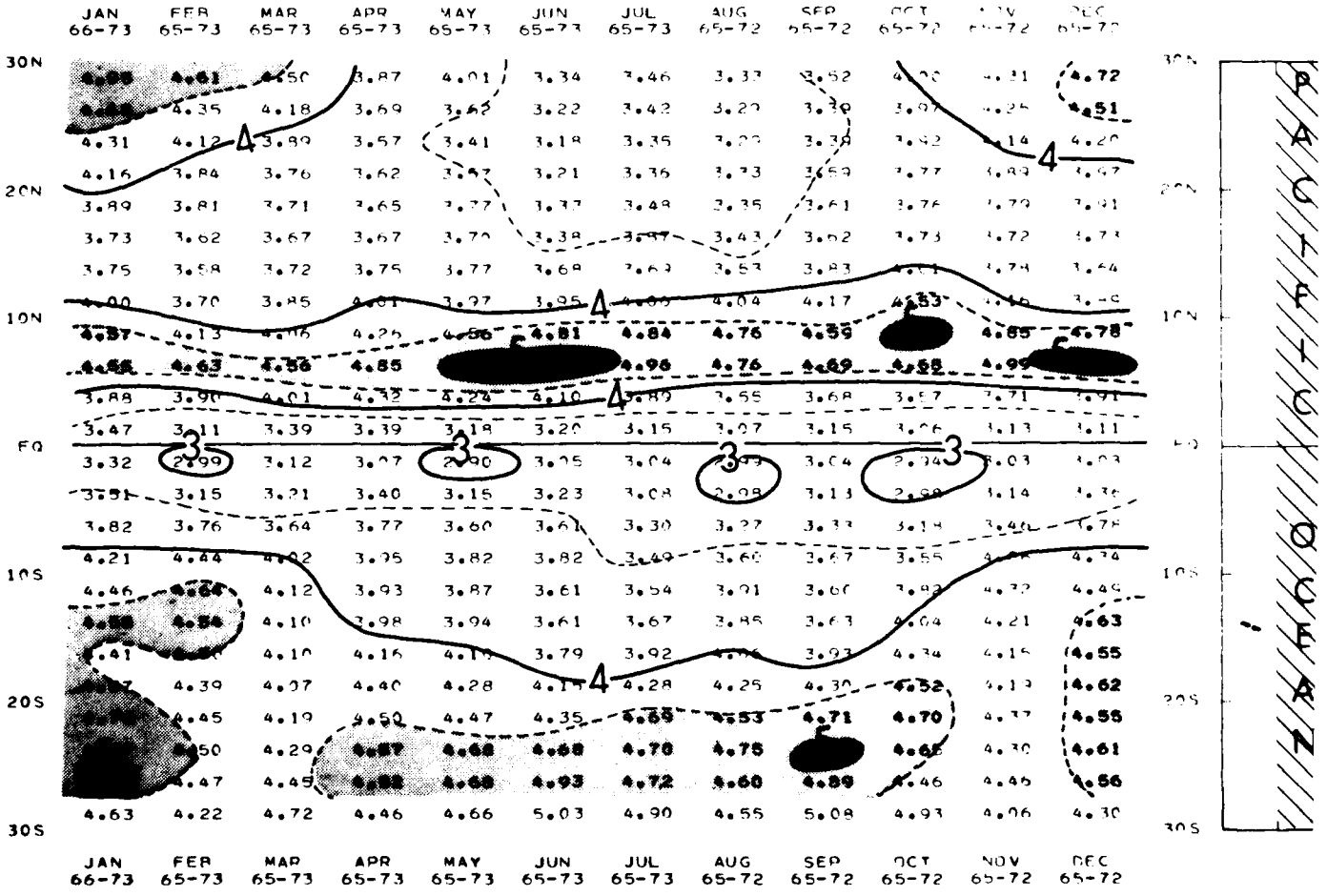

C TERM MEAN FROM 135E TO 140E

JUL TO AUG 65-73	JUL TO AUG 65-72	SEP TO OCT 65-72	OCT TO NOV 65-72	NOV TO DEC 65-72	DEC TO JAN 65-72	DEC TO JAN 66-73	
-1.37	-0.18	0.11	0.52	0.44	0.43	-0.01	30N
-0.84	0.06	0.06	0.23	0.54	0.40	-0.12	
0.12	0.10	0.03	-0.01	0.46	0.34	-0.13	
0.44	0.15	0.13	-0.39	0.51	0.23	-0.13	
0.89	0.14	-0.25	-0.59	0.22	0.10	0.20	20N
0.97	0.19	-0.17	-0.65	-0.01	-0.12	0.42	
0.86	0.11	0.06	-0.81	0.06	-0.37	0.35	
0.76	-0.08	0.02	-0.68	0.08	-0.25	0.07	
0.26	-0.32	0.15	-0.44	-0.06	0.09	-0.31	10N
-0.03	-0.27	0.01	-0.17	-0.01	0.19	-0.22	
0.03	-0.20	-0.17	-0.12	0.13	0.12	0.30	
0.05	-0.12	-0.14	-0.07	0.19	0.23	0.25	
0.14	-0.29	0.02	0.12	0.23	0.31	-0.07	EQ
0.04	-0.24	0.26	-0.14	0.06	-0.21	0.03	
-0.27	-0.12	-0.52	-0.05	-0.11	0.66	0.38	
-0.47	-0.16	-0.33	0.09	0.04	1.00	0.76	10S
-0.44	-0.17	-0.14	0.19	0.38	0.89	0.86	
-0.47	-0.13	0.09	0.26	0.64	0.77	0.63	
-0.30	-0.01	0.19	0.37	0.81	0.45	0.41	
-0.13	-0.14	0.31	0.49	0.81	0.45	-0.27	
-0.17	-0.24	0.28	0.23	0.65	0.32	-0.45	20S
-0.40	-0.07	0.03	0.15	0.51	0.22	-0.29	
-0.54	-0.15	0.02	0.09	0.39	-0.03	-0.07	
-1.00	0.81	-0.57	0.27	0.02	0.31	-0.21	30S

D JUL TO AUG 65-73 | JUL TO AUG 65-72 | SEP TO OCT 65-72 | OCT TO NOV 65-72 | NOV TO DEC 65-72 | DEC TO JAN 65-72 | DEC TO JAN 66-73

CLOUD COVER IN OCTAS
MONTH TO MONTH CHANGE IN LONG TERM MEAN FROM 135E TO 140E

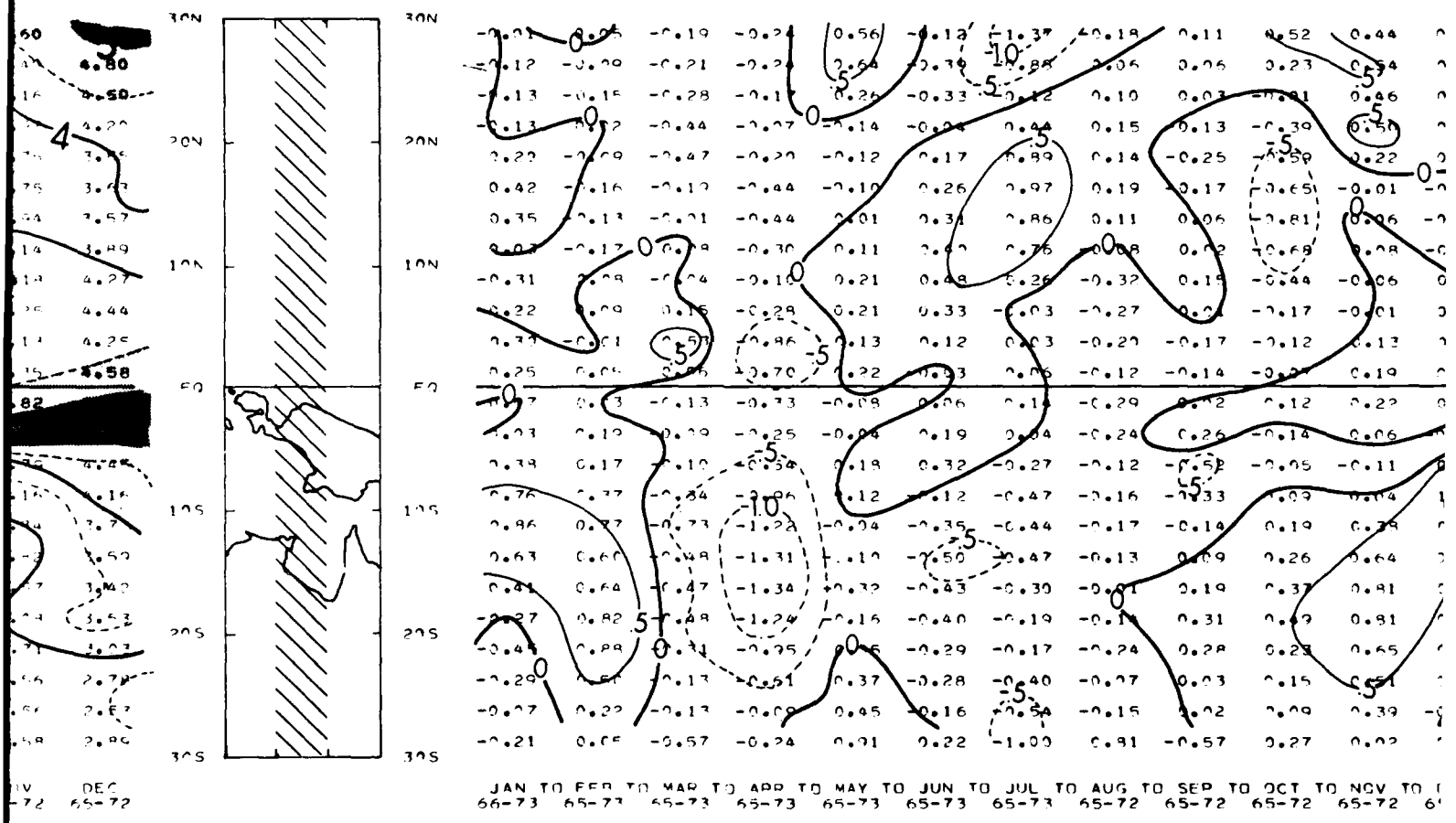

CLOUD COVER IN OCTAS
LONG TERM MEAN

FROM 135E TO 140E

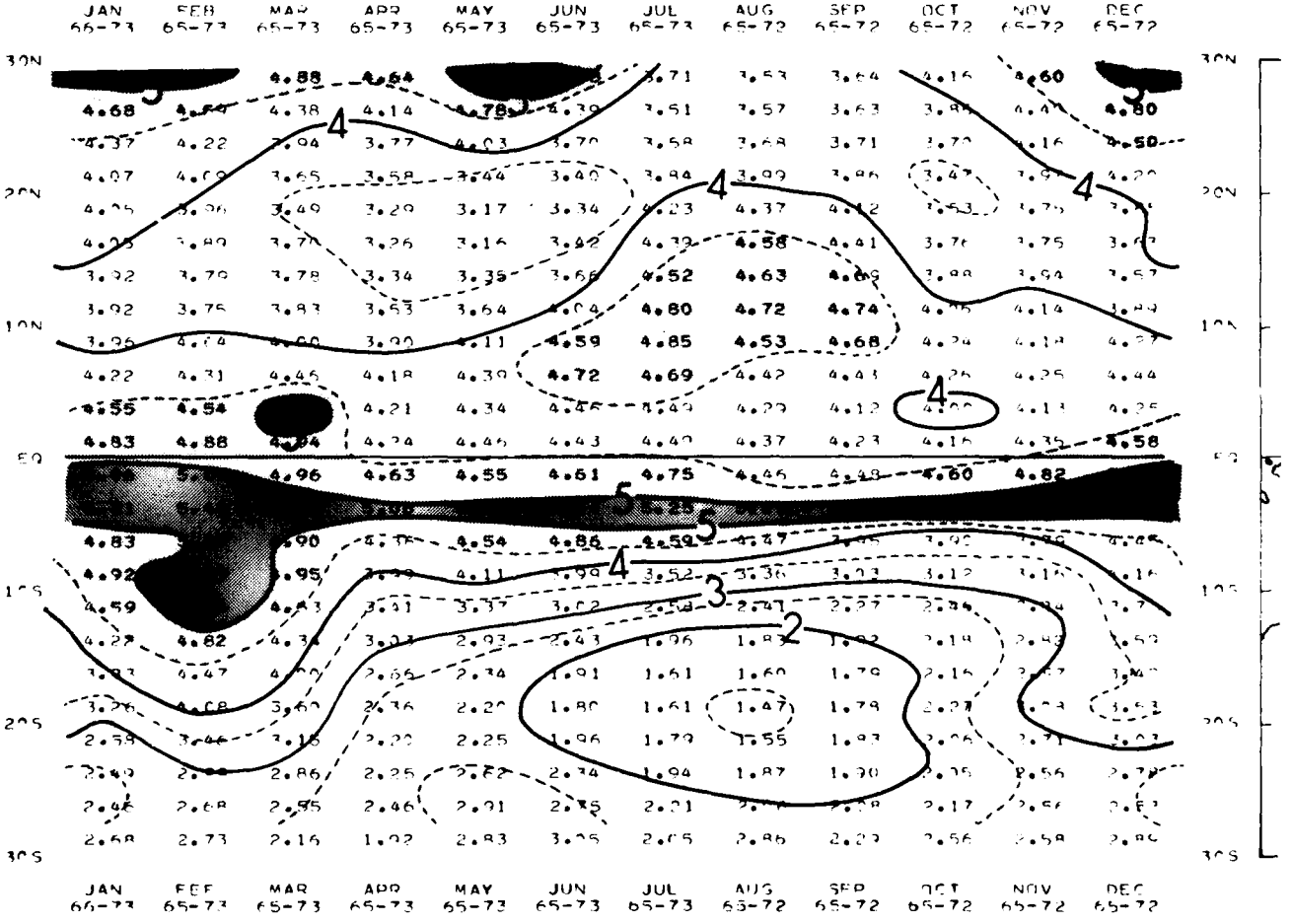

TERM MEAN FROM 30W TO 25W

JUL TO AUG 65-73	AUG TO SEP 65-72	SEP TO OCT 65-72	OCT TO NOV 65-72	NOV TO DEC 65-72	DEC TO JAN 65-72	JAN 66-73	
.24	-0.44	-0.03	0.29	0.47	0.20	0.06	30N
.10	-0.46	-0.15	0.13	0.55	0.24	0.15	
0.39	-0.63	-0.33	-0.11	0.49	0.29	-0.03	
.49	-0.61	-0.64	-0.38	0.35	0.31	-0.20	20N
.45	-0.43	-0.09	-0.13	-0.10	0.48	-0.22	
0.29	-0.35	-0.74	-0.19	-0.04	0.29	-0.23	
.39	-0.77	-0.30	0.05	-0.16	0.06	-0.04	
.43	0.38	-0.45	0.07	-0.36	-0.19	-0.17	
0.76	0.06	-0.46	-0.04	-0.15	-0.43	-0.62	10N
0.81	-0.04	0.15	-0.03	0.31	0.07	-1.34	
.76	-0.05	0.41	0.25	0.36	0.83	-0.19	
0.28	-0.07	0.30	0.11	0.01	0.57	0.61	
0.20	-0.06	0.26	-0.14	0.13	0.11	0.17	EQ
0.15	-0.17	0.16	-0.05	0.06	-0.04	-0.11	
0.08	-0.26	0.03	-0.07	0.11	-0.19	-0.05	
0.30	-0.35	-0.08	-0.07	0.28	-0.20	0.04	10S
0.36	-0.16	-0.06	-0.07	-0.09	-0.02	-0.02	
0.28	-0.20	-0.02	-0.05	-0.08	0.09	-0.06	
0.26	-0.23	-0.06	0.05	-0.02	-0.10	-0.08	
0.11	-0.13	-0.09	0.20	-0.07	-0.22	-0.24	
0.10	-0.10	0.08	0.30	-0.02	-0.26	-0.65	20S
0.0	-0.14	0.16	0.31	0.21	-0.42	-0.90	
0.23	-0.28	0.20	0.15	0.26	-0.14	-1.09	
0.27	0.21	0.70	-1.08	0.52	-0.49	0.30	30S

JUL TO AUG 65-73	AUG TO SEP 65-72	SEP TO OCT 65-72	OCT TO NOV 65-72	NOV TO DEC 65-72	DEC TO JAN 65-72	JAN 66-73

END

DATE
FILMED

8 -85

DTI